

**Republic of Iraq
Ministry of Higher Education & Scientific
Research
University of Babylon
College of Materials Engineering
Department of Polymer Engineering and
Petrochemical Industries**



Investigation of Residual Stresses in Polystyrene Products by Ultrasonic Technique

A Dissertation
Submitted to The Council of The
College of Materials Engineering/ University
of Babylon in Partial Fulfillment of The Requirements for
the Degree of Doctor of Philosophy in Materials Engineering/
Polymers

Lina Fadhil Kadhim
B.Sc. in Materials Engineering (2001)
M.Sc. in Materials Engineering (2006)

Supervised by

Prof.
Ali Abdul Amier Al-Zubiedy
(Ph.D.)

Prof.
Hanna Jawad Kadhim
(Ph.D.)

2023 A.D

1445 A.H.

بِسْمِ اللَّهِ الرَّحْمَنِ الرَّحِيمِ



صدق الله العظيم

سورة فاطر / الآية ٢٨

Supervisors Certificate

We certify that this thesis entitled "**Investigation of Residual Stresses in Polystyrene Products by Ultrasonic Technique**" is prepared by (**Lina Fadhil Kadhim**) under our supervision at the Department of Polymers and Petrochemical Industries / College of Materials Engineering/ University of Babylon in partial fulfillment of the requirements for the Degree of Philosophy-Doctorate in Materials Engineering / Polymer.

Prof.

Dr. Ali Abdul Amier Al-Zubiedy

(Ph.D.)

/ / 2023

Prof.

Dr. Hanna Jawad Kadhim

(Ph.D.)

/ / 2023

Examining Committee Approval

We certify that we have read this Dissertation entitled "**Investigation of Residual Stresses in Polystyrene Products by Ultrasonic Technique**" and as an examining committee, we have examined the student (**Lina Fadhil Kadhim**) in the contents and that is related to it and that in our opinion it meets the standard of a Dissertation for the Degree of the Doctor of Philosophy-Doctorate in Materials Engineering / polymers.

Signature

Prof. Dr. Bashar O. Bedaiwi

Committee Chair

Date: / / 2023

Signature

Prof. Dr. Mohsin A. Al-Shammari

Committee Member

Date: / / 2023

Signature

Prof. Dr. Ahmed F. Hamzah

Committee Member

Date: / / 2023

Signature

Prof. Dr. Zoalfokkar Kareem Mezaal

Committee Member

Date: / / 2023

Signature

Prof. Dr. Nawres H. Mostafa

Committee Member

Date: / / 2023

Signature

Prof.

Dr. Ali Abdul Amier Al-Zubiedy

Committee Member

Date: / / 2023

Signature

Prof.

Prof. Dr. Hanna Jawad Kadhim

Committee Member

Date: / / 2023

Approval of the Department of
Polymers and Petrochemical Industries
Head of Department

Approval of the College of Materials
Engineering
Dean of College

Signature

Prof. Dr. Zoalfokkar Kareem Mezaal

Date: / / 2023

Signature

Prof. Dr. Abdulraheem Kadhim AbidAli

Date: / / 2023

Dedication

To ...

The Widest Cave and Most Science

The Remnant of Allah in Earth

The Deliverance Ship

The Eye of Life

I dedicate my humble efforts

Lina Fadhil

2023

Acknowledgements

- ❖ First and foremost my sincere gratitude to the almighty Allah for granting me the opportunity and the capability to proceed this work.*
- ❖ I owe my deepest gratitude to the people who keep me on the right track my family for all their love, patience, support and encouragement.*
- ❖ I am very grateful to Prof. Dr. Ali A. A. Al-Zubiedy for his abundant help and Prof. Dr. Hanaa J. Kadhim.*
- ❖ I would like to thank everyone help me in performing this work from the staff of laboratories at Polymer Engineering & Petrochemical Industries department.*

ABSTRACT

Residual stresses are built up due to various processing operations and affect significantly on the materials performance. It is important to develop accurate and reliable methods for analysis of residual stresses in engineering components that causes catastrophic fracture without previous warning. Polymers are poor in the resistance to crack extension, so the residual stresses are influencing inevitably on the performance of polymeric products. The development of nondestructive techniques (NDT) is very important from technical and economical point of view. The ultrasonic technology is more extensively applied in the assessment of residual stresses in metals. In this work, the ultrasonic pulse-echo technique was applied on the first time in measuring residual stresses for polystyrene products.

According to the difference in morphology between polymeric components, through thickness residual stresses were determined twice in this work. Through thickness residual stresses in terms of acoustoelastic constant and through depending on the determined previously acoustoelastic constant for polystyrene sheets. The residual stresses were evaluated due to cooling from temperatures (180, 200)°C by air and water under various applied pressures (0, 45.714, 76.19, 106.667, 152.381)MPa. The ultrasonic velocity of reference (annealed) specimen (2260) m/s was approved in the evaluation of residual stresses due to ultrasonic test. The air and water cooling from (180, 200)°C were corresponded with increasing in ultrasonic velocity while tensile residual stresses were related with decreasing in ultrasonic velocity for evaluated residual stresses in terms of acoustoelastic constant.

SPSS software through (p-value) were showed that air and water cooling from (180, 200)°C resulted tensile residual stress without zero pressure. The optimum pressures against residual stresses from (HABCFFNN) were obtained under (106.667, 76.19)MPa pressures while the optimal through thickness residual stresses due to water cooling from (180, 200)°C were (-70.003,

10.579)MPa. The best temperature of preparing polystyrene specimens was 200°C because the high percent of beneficial compressive residual stresses that increase fatigue and creep strength. The evaluated through thickness residual stresses were resulted from (thermal stresses due to cooling type, over load applied pressures, restraining of polymeric sheets inside metal molds). The range of ultrasonic velocity produced from pulse-echo test were (2000-2500) m/s due to air and water cooling from (180, 200). From SPSS, the significant pressure on residual stresses due to water cooling from (200)°C was 152.714.

Table of Contents		
Subject		Page
Dedication		I
Acknowledgements		II
Abstract		III
Table of contents		V
List of figures		IX
List of tables		XIV
List of symbols & abbreviations		XV
Chapter One: Introduction		
No.	Subject	Page
1.1	Introduction	1
1.2	Residual stresses	1
1.3	The sources of residual stresses	1
1.4	Importance of measuring residual stresses	3
1.5	The effects of residual stresses on material properties	4
1.6	Aim of current work	4
1.7	Contribution of current work	5
Chapter Two: Theoretical Background and Literature Review		
No.	Subject	Page
2.1	Introduction	6
2.2	Destructive measurement techniques	6
2.2.1	Layer removal and curvature	6
2.2.2	Analytical contour method	11
2.2.3	Hole drilling method (ASTM E837)	15

2.2.4	Method of sectioning	22
2.2.5	Ring-core method semi destructive	23
2.2.6	The slitting (parting-out) method	24
2.2.7	Partial excision (splitting) method	25
2.2.8	Crack compliance method	27
2.3	Non-destructive measurement techniques	27
2.4	Chemical methods	49
2.5	Indentation Method	59
2.6	Ultrasonic technique	69
2.7	The principles of acoustoelasticity	71
2.8	Ultrasonic technique and residual stresses	72
2.9	Pulse Echo Method	74
2.10	Polymer overview	77
2.11	Polymers and ultrasonic waves	77
2.12	Glass transition in polymers	79
2.13	Glassy polymers and the amorphous structure	80
2.14	Applications of glassy polymers	81
2.15	Chemical structure of polystyrene(PS)	81
2.16	Properties of polystyrene(PS)	84
2.17	Types of polystyrene	85
2.18	Applications of polystyrene	88
2.19	Literature review	93
2.19.1	Literature review of polystyrene	93
2.19.2	Literature review of ultrasonic test	93

2.19.3	Literature review of optimization method	98
Chapter Three: Optimization and Statistical Solutions		
No.	Subject	Page
3.1	Introduction	100
3.2	The optimization method	100
3.3	Artificial bee colony Algorithm (ABC)	103
3.4	Artificial neural networks ANN	105
3.5	Statistical software (SS)	110
Chapter Four: Experimental part		
4.1	Introduction	112
4.2	Properties of PS	112
4.3	Preparation of specimens	113
4.4	Annealing treatment	117
4.5	Melt flow rate (MFR)	118
4.6	Differential Scanning Calorimeter (DSC)	118
4.7	Fourier transform infrared (FTIR)	119
4.8	Density test	119
4.9	Tensile test	120
4.10	Ultrasonic pulse-echo test	120
Chapter Five: Results and Discussion		
5.1	Introduction	123
5.2	Differential Scanning Calorimeter Test (DSC)	123
5.3	Fourier transformation infrared spectroscopy (FTIR)	124
5.4	Tensile test	126
5.5	Ultrasonic longitudinal velocity	127

5.6	Residual stresses in terms of acoustoelastic constant	131
5.6.1	Residual stresses along specimens length	131
5.6.2	Residual stresses due to various applied pressures	134
5.7	Evaluated residual stresses	140
5.7.1	Residual stresses along specimen length	141
5.7.2	Residual stresses according to various applied pressures	143
5.8	Statistical package for social science (SPSS)	148
5.9	Hybrid ABC and FFNN flowchart	150
5.10	Results of (HABCFNN) Algorithm	154
Chapter Six :Conclusions and Recommendations		
6.1	Conclusions	160
6.2	Recommendations	161
References		
	References	162

List of Figures		
No.	Subject	Page
1-1	Three main influences on the development of residual stresses	3
2-1	sample The forms of specimens investigated by layer removal and curvature technique: (a) flat plate sample (b) cylinder	7
2-2	Principle of layer removal technique	8
2-3	Experimental setup of layer removal method	9
2-4	The results of layer removal method	10
2-5	Three cuts of 7050-T7452 forging used to map 3D residual stresses	12
2-6	The peak to valley amplitude of the contour	14
2-7	The constituents of hole drilling and hole drilling apparatus	15
2-8	Schematic representation of strain gauge for measuring the residual stresses (top view)	17
2-9	Geometries of strain gauge rosette	18
2-10	Section from sectioning method	23
2-11	Slitting method	24
2-12	Measuring of residual stresses by slitting	25
2-13	Method of splitting (a) rods (b) wood (c) axial stresses of tubes (d) circumferential stresses of tubes	27
2-14	The radiation of diffraction through crystal structure	28
2-15	The various orientations that used to determine (ϵ_T), (ϵ_A) and (ϵ_N)	33
2-16	The electromagnetic spectrum	40
2-17	Ordinary light without control over light vector	41
2-18	Refractive index while passing from one medium to other	42

2-19	Polariscope with light source and polarizer	43
2-20	Plane of polarization	44
2-21	The pattern of birefringence for tensile specimens from polycarbonate	44
2-22	The compensator LWC-100 used to determine the retardation value	48
2-23	Polariscope for measurement of residual stresses	48
2-24	Sketch of the indentation device	61
2-25	The relation among residual stresses and load-depth curve	62
2-26	The loading-unloading indentation curves and the presence of residual	64
2-27	The geometry of cone indentation: (a) is the true contact radius and (h) is the depth of indentation	65
2-28	The geometry and size of spherical indenters	65
2-29	The maximum indentation of sharp conical indenter	67
2-30	The loading curve of elastic-plastic material and elastic unloading	69
2-31	Propagation of longitudinal wave in a medium	74
2-32	The transducer in contact ultrasonic method	76
2-33	The principle of pulse-echo method	76
2-34	Relationship between specific volume and temperature	79
2-35	The molecular chains of (a) amorphous (b) crystalline polymer	80
2-36	(a)The chemical structure of PS,(b) The addition polymerization of PS from styrene- monomer	82

2-37	(a):The addition polymerization of PS from styrene monomer The various configurations of polystyrene	83
2-38	PS in building: (a) in construction (b) in concrete as aggregate	86
2-39	Compound styrofoam into keyboard buttons	87
2-40	PS in medical devices	89
2-41	Use of PS in solar cells	90
2-42	Parts of automotive that fabricated from PS	91
2-43	Capacitors made from Polystyrene	91
3-1	A simple position update scheme	103
3-2	Flowchart of artificial bee colony ABC	105
3-3	ANN basic unit	107
3-4	Types of feed forward neural network FFNN input layer	108
3-5	Flow chart of SPSS analyzing data	111
4-1	Research methodology	113
4-2	(a) hydraulic press,(b)The metal mold	115
4-3	PS specimen (sheet)	116
4-4	Procedure of preparing PS specimens	117
4-5	Annealing treatment of PS	117
4-6	Tensile test specimen	120
4-7	The ultrasonic pulse echo device	121
5-1	The DSC of PS specimen	124
5-2	FTIR spectra of PS with standard and experimental bands	125
5-3	Stress-strain tensile curve of PS	126

5-4	Longitudinal velocity along specimen length cooled by air from 180°C under various pressures	128
5-5	Longitudinal velocity along specimen length cooled by water from 180°C under various pressures	129
5-6	Longitudinal velocity along specimen length cooled from 200°C by air under various pressures	130
5-7	Longitudinal velocity along specimen length cooled from 200°C by water under various pressures	130
5-8	Residual stresses in terms of K along air cooled specimen from 180°C under various pressures	132
5-9	Residual stresses in terms of K along water cooled specimen from 180°C under various pressures	133
5-10	Residual stresses in terms of K along air cooled specimen from 200°C under various pressures	133
5-11	Residual stresses in terms of K along water cooled specimen from 200°C under various pressures	134
5-12	Residual stresses in terms of K at 25mm for all specimens cooled from 180°C	135
5-13	Residual stresses in terms of K at 75mm for all specimens cooled from 180°C	136
5-14	Residual stresses in terms of K at 125mm for all specimens cooled from 180°C	136
5-15	Residual stresses in terms of K at 25mm for all specimens cooled from 200°C	138
5-16	Residual stresses in terms of K at 75mm for all specimens cooled from 200°C	139
5-17	Residual stresses in terms of K at 125mm for all specimens cooled from 200°C	139

5-18	Evaluated residual stresses along air cooled specimens from 180°C under various pressures	140
5-19	Evaluated residual stresses along water cooled specimens from 180°C under various pressures	141
5-20	Evaluated residual stresses along air cooled specimen from 200°C under various pressures	142
5-21	Evaluated residual stresses along water cooled specimen from 200°C under various pressures	142
5-22	Evaluated Residual stresses at 25mm for all specimens cooled from 180°C	143
5-23	Evaluated Residual stresses at 75mm for all specimens cooled from 180°C	144
5-24	Evaluated Residual stresses at 125 mm for all specimens cooled from 180°C	145
5-25	Evaluated Residual stresses at 25 mm for all specimens cooled from 200°C	146
5-26	Evaluated Residual stresses at 75 mm for all specimens cooled from 200°C	146
5-27	Evaluated Residual stresses at 125 mm for all specimens cooled from 200°C	147
5-28	Mean velocity for all specimens due to SPSS	149
5-29	Mean stress for all specimens due to SPSS	149
5-30	Flowchart of HABCFFNN	152
5-31	Types of functions in neural network	153
5-32	The related block between ABC-FFNN	153
5-33	Input included layers of FFNN	154
5-34	Hidden layers of FFNN	155

5-35	Representation of one training process at 180°C	156
5-36	Representation of one training process at 200°C	157
5-37	Performance of residual stresses of PS specimens prepared at 180°C	158
5-38	Performance of residual stresses for PS specimens prepared at 200°C	158
5-39	Regression plot of hybrid ABC-FFNN	159

List of Tables		
No.	Subject	Page
4-1	Basic Properties of PS	112
4-2	Transformation the hydrolytic pressure to mold pressure	114
5-1	Experimental and standard bands of PS	125
5-2	SPSS, p-value of ultrasonic velocities and residual stresses	150
5-3	The parameters of (HABCFNN	151

List of Abbreviation	
Abbreviation	Description
ABC	Artificial bee colony
FFNA	Feed Forward Neural Network
NDT	Non destructive test
PS	Polystyrene
XRD	X- ray diffraction

Symbols List of		
symbol	Description	Units
Tg	Glass transition temperature	°C
σ	stress	MPa
σ_{res}	Residual stress	MPa
V	velocity	m/sec
P	pressure	MPa

Chapter One
Introduction

Chapter One

Introduction

1.1 Introduction

Residual stress is a problem occurs in many components and manufactured structures, it has important influences on the behavior of the materials and structural components, particularly on their mechanical strength, distortion, dimensional stability, resistance to corrosion, fatigue life and brittle fracture. The residual stress analysis is unavoidable stage in the design of structural elements and estimation of the reliability under real conditions of service.

1.2 Residual Stresses

The residual stresses are internal stresses have remained within the material after manufacturing processes without application of external forces or temperature gradients as well as produced by non-homogeneous plastic deformation due to service loading of the part [1]. Residual stresses are present in materials or structures essentially due to the manufacturing processes, independently from any external load that applied on the structure or materials [2].

The combination of residual stresses and external loads causes useful or harmful stresses according to sign, distribution and magnitude of these stresses. Residual stresses are self-equilibrating where the summation of local tensile and compressive stresses have showed zero resultants of forces and moments through the entire volume of the material or structure [3].

1.3 Sources of Residual Stresses

The sources of residual stresses at any product have categorized into:

1. Mechanical: mechanical residual stresses have developed as a result of processes of manufacturing which change the material shape such as forming, rolling, extrusion, forging, drawing, machining and bending due to the production of non-uniform plastic deformation. These residual stresses also can be generated during service as in railway rails at the deformed surfaces. In some cases, deliberated mechanical residual stresses could be induced to develop a specific profile of stress (usually compressive) for a component as in: (toughening of glass, cold drawing (cold expansion of holes) and shot peening [3, 4]. Residual stresses can be presented in extruded shapes, molded parts and thermoformed products. These stresses may be a normal part of the manufacturing process due to thickness changes due to non-uniform flow rates or inclusions [5].

2. Thermal: thermal residual stresses have occurred during processes of manufacturing such as casting, welding and quenching according to the non-uniform operations of heating or cooling [3]. The subsequent thermal treatments have resulted distortion that include warpage, crazing and change the pattern of residual stresses [5]. The changes in volume that arising from solidification or solid state transformations [6]. The differences in the thermal expansion coefficient at pieces made from various materials led to induce residual stresses [6]. Residual stresses also have resulted from manufacturing conditions and influenced on the polymer products performance from mechanical properties to dimensional accuracy [7].

3. Chemical: chemical residual stresses in materials have developed due to (material phase transformation, density changes and precipitation). For example chemical surface treatments, coatings, hardening alloys by precipitation and polymerization process [3]. Moreover, the stress also has induced if the material thrown or soaked into chemical solutions [8].

1.4 Importance of Measuring Residual Stresses

The knowledge of residual stress state is very complex to be deduced from experimental measurements or predicted by modeling [3], so the identification of residual stress distribution is important to predict the part performance under various conditions [9]. Moreover, the knowledge of residual stresses in machined and molded polymer products is very important to understand various appearances like dimensional stability and susceptibility to chemically assisted cracking [5].

The existence of residual stresses may not obvious and ignored during engineering design due to their characteristic of self-equilibrium [3]. In any free body diagram, the equilibrium of stress must preserved, where the existence of tensile residual stresses into component must be balanced by the compressive stresses at another place of body. The residual stresses were useful during their operation in the same plane of applied load and when they are opposite to applied load direction, such as the a compressive residual stresses at a component subjected to an applied tensile load [10]. There are three fundamental parameters have influenced on the development of residual stresses as shown in Figure (1-1) [11].

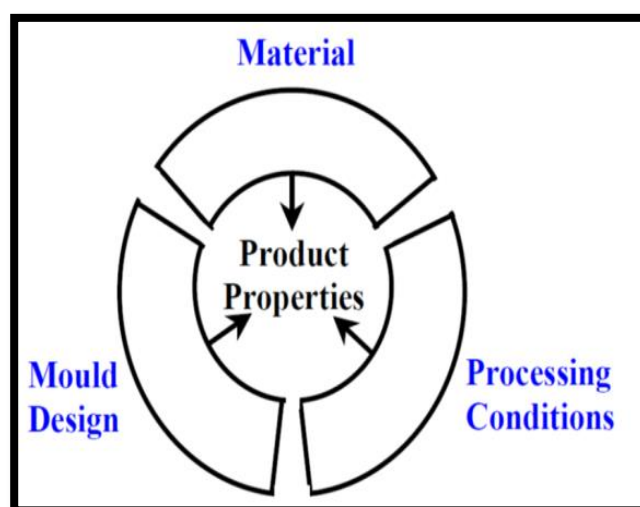


Figure (1-1): Three main influences on the development of residual stresses [11]

1.5 Effects of Residual Stresses on Material Properties

The magnitude and distribution of the residual stresses have taken into account through the manufacturing and design of various materials because they have limited the engineering properties of materials and welded structures [1, 10]. Residual stresses may be either detrimental or beneficial depending on the situation, sign and location where compressive residual stresses are useful because of the improvement in the following properties:

1. Fatigue strength due to preventing the fatigue crack initiation and propagation.
2. Wear resistance and bending strength of glass and brittle ceramics.
3. Stress-corrosion cracking resistance by preventing the initiation of surface cracks [1, 9, 10].

In general, the tensile residual stresses are considered as the failure reasons due to the cracks that produced from (quenching, fatigue and stress corrosion cracking), so they are undesirable [3,10]. There are other operations which produce detrimental tensile stresses such as welding, rod or wire drawing and grinding [1]. However, the compressive residual stresses could obstruct the growing of fatigue cracks where most cracks have occurred on the surface of the products [3].

1.6 Aim of Current Work

1-The measurement of through thickness residual stresses for sheets from polystyrene polymer that manufactured by melting granulates in closed molds at different temperatures (180, 200)°C, then pressed under various pressures (0, 45.714,76.19, 106.667, 152.381)MPa and two types of cooling in (air, water).

2-Applying at the first time non-destructive accurate pulse-echo ultrasonic technique on polystyrene sheets along specimen length in order to measure

through thickness residual stresses and overcome the problem of catastrophic fracture that produced from over loading because of the possibility of in-service measurements.

3-Built the algorithm hybrid artificial bee colony for training feed forward neural network (HABCFFNN) to obtain the optimal through thickness residual stresses with corresponding effective applied pressures that corresponding to less detriment residual stresses.

4-Estimation of maximum and minimum proportions of convergence and errors due to the utilization of statistical program SPSS.

1.7 Contribution of Current Work

In this work, the ultrasonic technique is used innovatively on polystyrene polymer for detecting residual stresses that induced from several sources. The sources of residual stresses are (thermal gradient, applying of pressures, restraining of sheets inside closed molds) due to the preparation of polystyrene specimens. The ultrasonic pulse-echo technique are utilized at the first time in evaluating through thickness residual stresses.

The optimization process is executed in order to obtain best values of applied pressures and cooling type at two temperatures (180, 200)°C. In addition, the corresponding less destruction through thickness residual stresses are determined. The optimization algorithm built with MATLAB is an innovative combination between (artificial bee colony, feed forward neural network, residual stresses, polystyrene polymer).

Chapter Two

Theoretical Background
and Literature Review

Chapter Two

Theoretical Background and Literature Review

2.1 Introduction

There are various efforts are made in order to evaluate the impact of residual stresses on characteristics of molded polymers. The introduction of residual stresses are carried out by all polymer processing techniques. There are destructive techniques(DT) and nondestructive techniques. The destructive techniques include destroying the engineering parts.The nondestructive techniques (NDT) are allowing for determining flaws, imperfections, non-uniformity and residual stresses without destroying the engineering part. The ultrasonic technique is considered as a nondestructive promising technique for evaluating residual stresses. Nondestructive techniques (NDT) also are applied in evaluating quality control on various constructions.

2.2 Destructive Measurement Techniques

2.2.1 Layer Removal and Curvature

A- Layer Removal Method

The method of layer removal has depended on Stoney's Method. It has involved noticing the resulted deformation due to the removal of series layers from material. This technique has suited to specimens of cylindrical shape and flat plates where the residual stresses have varied within depth [3]. Figure (2-1) depicts by diagram examples of the layer removal technique. This method includes the deformation measurements on one surface by the usage of strain gauges while paralleling layers have removed from the opposite surface of material. The method is general and applied on all materials such as paperboard [3].

Many methods have employed in order to measure the curvature of specimen, such as: (optical and laser scanning techniques, strain gauges, electron speckle pattern interferometry (ESPI)). The technique of layer removal method is only applicable on plates [3]. The layer removal & curvature techniques have employed for measuring the residual stresses within the test pieces of simple geometries [10].

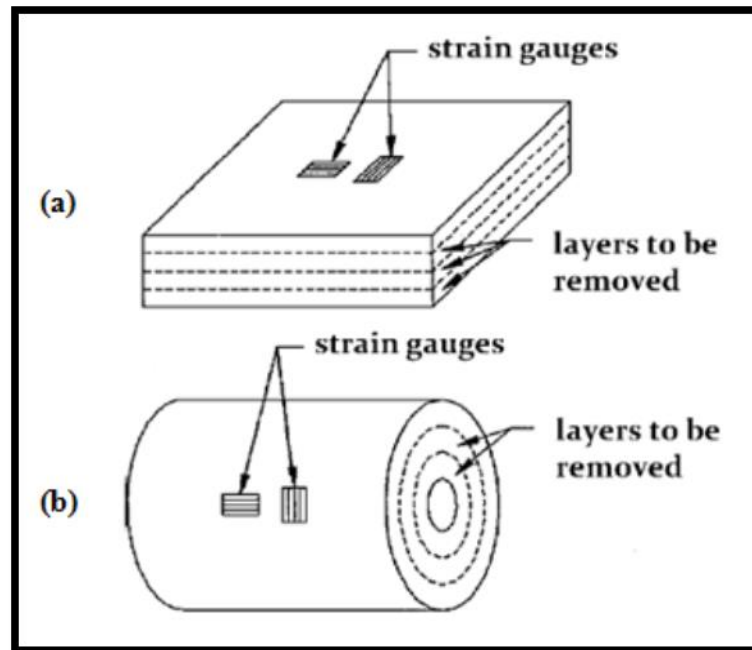


Figure (2-1): The forms of specimens investigated by layer removal & curvature technique (a) flat plate sample (b) cylinder sample [1]

The method of layer removal and curvature is appropriate only for a sample which is relatively long as compared to its thickness. The methods of layer removal and curvature are relatively easy technique that is often employed for the measurement of residual stresses in a specimen with simple geometries [12]. Layer-removal technique is the most accurate technique for measuring residual stresses in plastics and can be used with sheets and plates [13].

The technique of layer-removal has based on the curvature measurement of flat specimens following progressive mechanical removal of thin surface layers. According to layer removal, the specimen has restored the equilibrium by warpage to an arc of circular shape [14]. There are also some forms of layer

removal technique have combined with X-ray diffraction to generate the stress profile, so the method becomes destructive and the cutting have done carefully to ensure the steadiness of the stress state [1].

The layer removal method has liked the crack compliance method, it has depended on the removing of material from the specimen and measuring the resulted strain or distortion as shown into Figure (2-2). The layer removal from the sample removes the residual stress contained therein, the sample has distorted in order to obtain the equilibrium where this distortion has corresponded to the theory of Euler–Bernoulli beam [12].

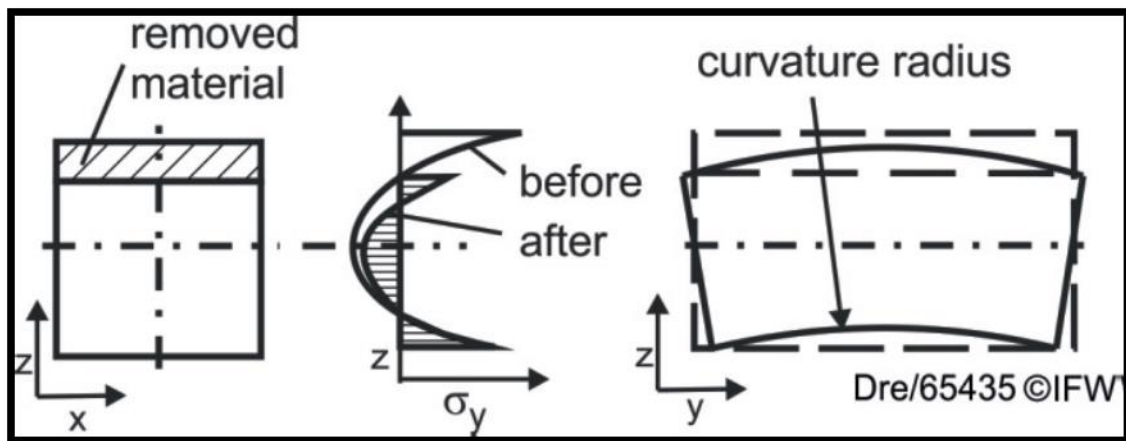


Figure (2-2): Principle of Layer Removal Technique [15]

The technique of layer-removal includes measuring the degree of curvature introduced into flat plate samples by removing thin layers from the specimen surface, it is possible to calculate the strain and consequently the residual stresses in the removed layer by measuring the specimen curvature [16]. According to the layers removed from one side of flat plate which contains residual stresses where the stresses have become unbalanced and the plate bended [10].

The curvature has depended on: the original stress distribution which existent in the removed layer and the elastic properties of the remainder plate. According to the series of curvature measurements with sequential removed layer, the distribution of stress in the original plate has concluded

[10]. The first point is difficult to obtain if the initial bars are not optimally flat where the first step of milling will not be uniform in thickness [17].

In the last step of milling, the bars are not stiff where the deformations depend slightly on the position of bars from the assembly of milling. Moreover, the thicker bars, the lower deformations [17], Figure (2-3) shows the principle of method by using an example of beam.

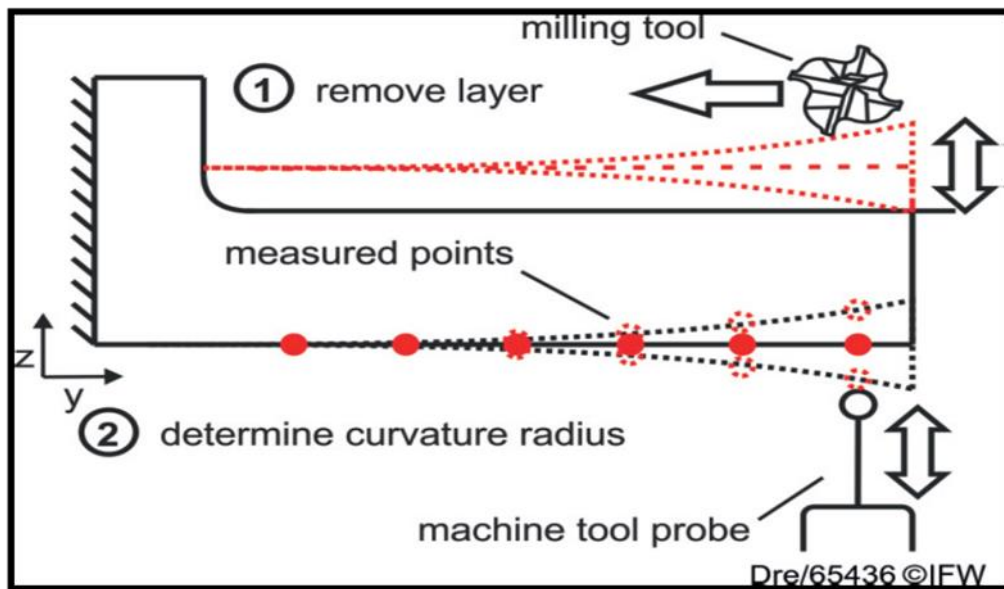


Figure (2-3): Experimental setup of layer removal method [12]

Some layers that have removed from a flat plate are involving residual stresses and the plate starts to bend due to the unbalanced stresses. Clearly, the curvature depends on the distribution of original residual stresses that present in the removed layers and from the elastic properties of the remained plate. The stresses distribution in the original plate has calculated after the removal of successive layers and the curvature has measured [12].

The layer removal technique is the most extensively employed method to measure the residual stresses. The rectangular sample has cut from the pipe interested area and the layers have removed from one side of the surfaces. The sample has undergone changes in dimensions after each removed of layer as

well as the average stress that has determined due to the change in dimensions in each layer.

The residual stress results have attained as an example shown in Figure (2-4), where the residual stresses determined through depth and the deflection changed against the specimen length. Moreover, the sectioning machine has introduced undesirable stresses such as surface residual stresses or overall yielding stresses to the test sample and reduced the measurement of accuracy [18].

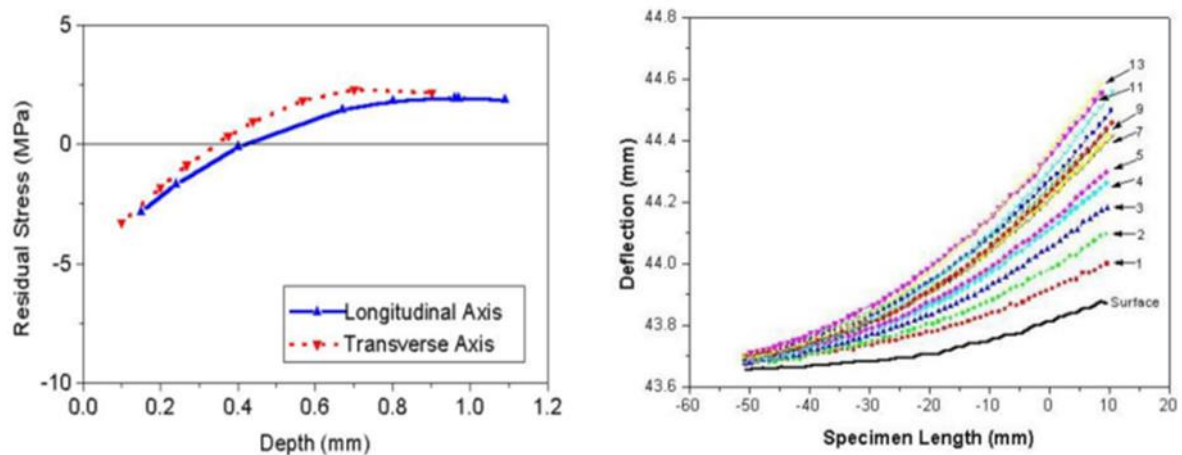


Figure (2-4): The results of layer removal method [13]

The frequent measurements of curvature have employed to calculate the stresses through the coatings and layers. The deposition layer has induced stresses that cause the curve of substrate, the resulted changes in curvature from deposition have determined the corresponding differences in residual stresses with respect to the thickness of deposition, the data from experiment have attained for different thicknesses from sputtering [19]. The specimen thickness has measured prior to layer removal and after each successive stage of removing layers, the thickness was determined by using a micrometer [20].

The calculation of residual stresses distribution in polymers by the layer-removal method requires the determination of modulus variation in the plane

specimen at different positions across the specimen thickness. Accordingly, measurements of modulus were made at different stages of layer removal using the method of layer removal considers the removed material in a large layer, it has supposed that the residual stresses are constant through the layer [12].

B- Layer Removal by Electrochemical Machining

This technique of layer removal has applied by the usage of electrochemical machining (ECM) for measuring the residual stresses in metals, the electro chemical machining (ECM) is able for machining of any electrical conductive material associated with high rate of removal as well as the ignorance of mechanical properties because it is a process of metal removal that is non-mechanical. The rate of removal in the ECM machining is independent on the hardness and toughness of material [1]. This technique does not required strain gauges and hence the samples does not require special preparation such as the gauges gluing [12].

2.2.2 Analytical Contour Method

The contour method is a recently invented relaxation method, it has proposed firstly in 2000 which evaluated a residual stress 2D map on the plane of interest [1]. This method has applied in several cases such as: Tee-joint welded carbon steel, quenched thick plates, cold-expanded hole, forgings of AL alloy, all types of materials [1]. In the analytical contour method, the sample has cut carefully in two halves causing the relaxation of residual stresses of normal direction on the cut plane.

The deviation of surface contours has associated with the elastic relaxation of residual stresses and employed to determine the original residual stresses. One of the exceptional strengths of the analytical contour method is that it affords a complete cross-sectional chart in compared to 1D depth profile from the component of residual stresses that is normal to the cross section as shown in Figure (2-5). This method has applied in several cases such as: Tee-joint welded

carbon steel, quenched thick plates, cold-expanded hole as well as forgings of AL alloy [1].

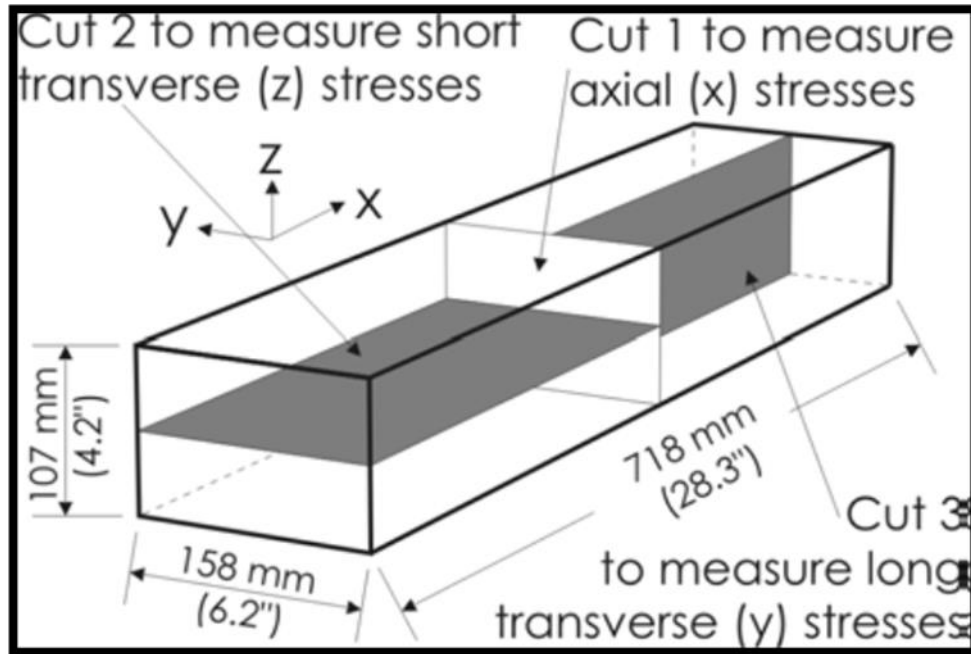


Figure (2-5): Three cuts of 7050-T7452 forging used to map 3D residual stresses [21]

The cuts have executed with wire electric discharge machining (EDM) by the usage of wire diameter ($150\ \mu\text{m}$) made from brass. The part has immersed in deionized water under controlled temperature through the cutting process [22]. The cut have deviate from the original plane of cutting that has led to errors in the measurement of stresses, the part must be restricted by fixing it to a supported plate on two sides of the cut [22].

All the clamps, specimen and backing plate have permitted to come into state of thermal equilibrium at the tank of water before clamping to prevent any thermal stresses [21]. The analytical contour method has improvements in measuring the residual stresses as compared to conventional relaxation methods, it depends on the difference in the principle of elastic superposition [1]. The specimen must be suitable constrained essentially to avoid its movement during the cutting.

The specimen cutting is the important step in implementation of the contour method because the next procedures (reduction of data and stress analysis) have based on the cutting quality. The appropriate method of cutting is the Wire Electrical Discharge Machining (WEDM) because it uses the electrical discharges or sparks to remove material instead of tools with hard cutting [1].

The constant cut width has related strongly to the (type of cutting wire, type of material under cutting, specimen geometry and operating parameters of WEDM). The wire of cutting must be as thin as possible for the removing of minimum amount of material that is particularly significant for the cases of high gradient in stress [1].

The relief of residual stresses that needed to measure on the two surfaces of cut. A Coordinate Measuring Machine (CMM) is sufficiently precise for measurement of surface profile. A (CMM) has designed to measure the intricate shapes with high accuracy and especially employed for determining the satisfaction of the tolerance specifications to the manufactured parts. A CMM has employed a ruby tipped stylus as a sensor for discovering the specimen surface, the mechanical assemblage has moved the sensor device (stylus) to contact with the measured surface, the stylus deflection has triggered a computer to prerecord the location of each point of contact [1].

According to this analytical method, the contours of the two cutting surfaces have measured by the usage of coordinate measuring machine (CMM) after each cut. A (CMM) records the mechanical contact with a probe has touch trigger and an optical-electrical system has employed glass scales which give the positioned probe as well as has combined with the machine coordinates for siting the surface, a spherical tip of ruby of 1mm diameter has employed on the probe. The surfaces of cut have measured on 1 mm grid spaced for the

smaller surfaces and up to 2 mm for the largest surfaces as well as have given the points on each cut surface in the range (13,000-17,000) [21].

The peak-to-valley amplitude of the contour was approximately 60 μm and resolved readily due to the (CMM) that have shown from figure (2-6) where the contour was measured for cut 3 from Figure (2-5). In the following contour where the regions of compressive residual stress have represented by high spots in the contour while tensile regions by low spots. The periodicity of the contour refers to the multiple cold compressions that has applied on the forging [21].

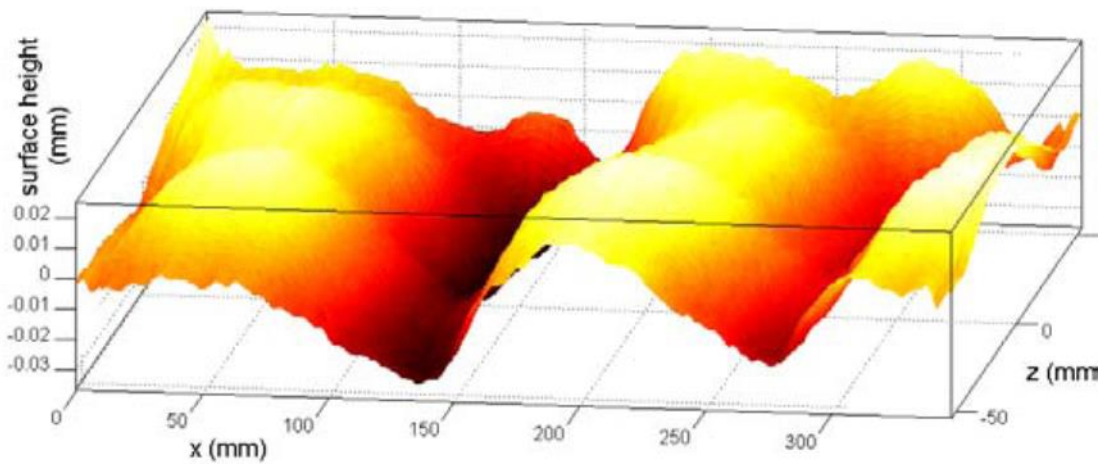


Figure (2-6): the peak to valley amplitude of the contour [21]

The original present stresses on the cut plane has determined numerically by the elastic deformation of the cut surface into the counteractive contour shape which has gauged on the same surface, so this has achieved by the usage of 3D finite element elastic model. The model has built-up of one half of the part but the surface of cut has formalized as flat rather than slightly deformed shape that measured by the contours of surface [21].

According to the stress determination, the counteractive of the measured surface contour has applied as displacement boundary conditions on the corresponding surface to cut [21]. The results have compared with the stress prediction by finite element method [21]. In the application of residual stresses

measurement which a challenge for another methods, the analytical contour method is capable to draw the residual stresses quite accurately. The measurements of contour method were relatively simple either experimentally or analytically even by comparing with another methods that do not have capable for measuring the same stresses [21].

2.2.3. Hole Drilling Method (ASTM E837)

The hole drilling is semi-destructive method has included the drilling of a small hole through a specimen, the released surface strains have measured by using a special rosette of strain gauge for measuring residual stresses [10]. The typical hole drilling device and its constituents have shown in Figure (3-8). It is significant to select an appropriate method of drilling because any residual stress that established by the process of drilling has unfavorably influenced on the results, this involves the usage of conventional drilling method, abrasive jet machining and air turbines of high speed [1, 10].

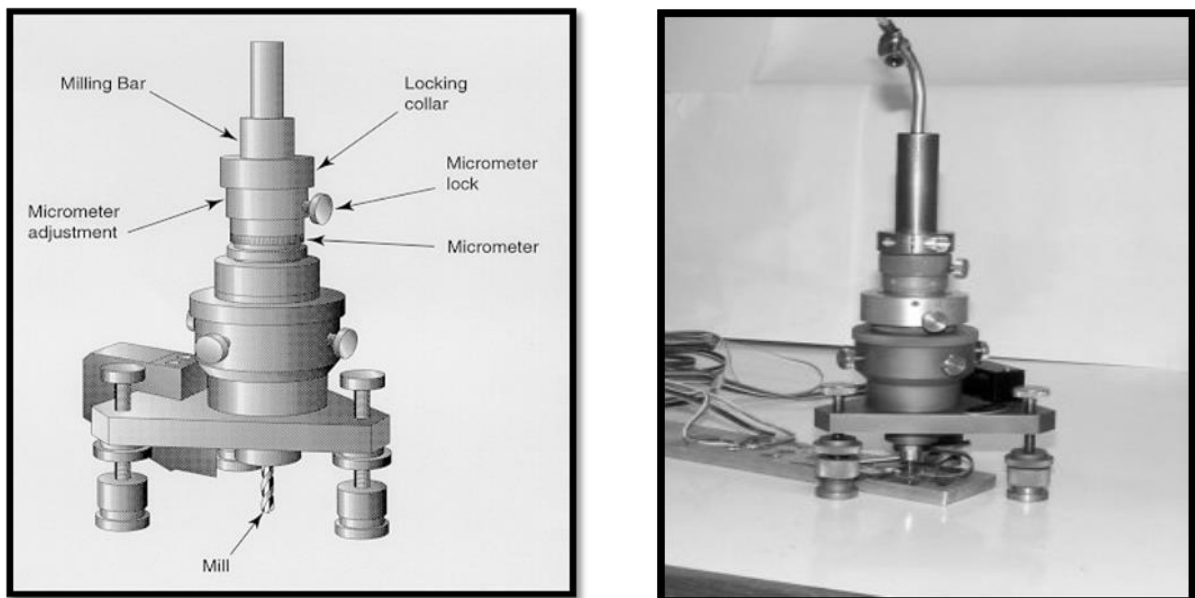


Figure (2-7): The constituents of hole drilling rig and hole drilling apparatus [23]

This technique includes drilling of a hole through material and measuring of the surface strains in the neighbor of a hole through the drilling process. The electrical resistance strain gauges have applied usually to calculate quantitatively the strains near the drilled hole. The strains have employed to determine the biaxial stresses and their distribution at and near the surface of part [23]. The standard of hole drilling method is (ASTM E837-99) [8] and the most utilized technique hole drilling method is according to ASTM standard E837-13a [24].

The release of strain near the hole is approximately comprehensive but this method has suffered from the limited sensitivity of strain and potential errors as well as uncertainties associated to the hole dimensions with respect to (diameter, concentricity, profile, depth, roughness of surface, flatness, preparation of specimen), Figure (2-8) depicts the geometry of strain gauge for measuring the residual stresses [10].

In the method of hole drilling, the accomplishment of good bonding between specimen and strain gauges has required some surface preparation, if the near surface residual stresses are significant, it must not remove too much material. The choosing of an appropriate strain gauge and size of drill are important as well as the two are directly connected because this has determined the maximum depth of measurement. The gauge size is significant and has related to the present type of stresses [10].

The small gauges have given a more localized measurement but more difficult to handle, it only gives information of limited depth because of the conforming small drill size and probably predisposed to larger errors which related with misalignment or anomalies on surface [10]. The application of this method has limited by the basic measurements where the field of stress is fundamentally uniform. The another methods of analysis such as Integral and Power series techniques have improved for determining the residual stress

distributions in non-uniform stress fields where the ASTM E837 standard does not apply severely [10].

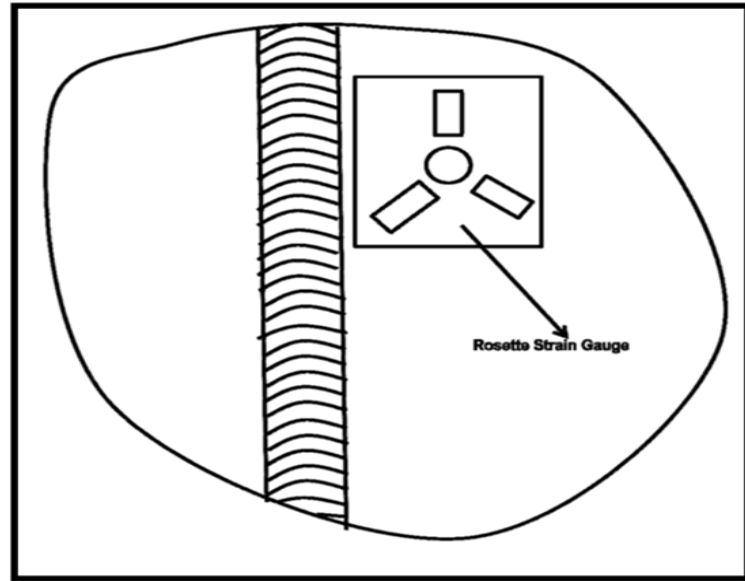


Figure (2-8): Schematic representation of strain gauge for measuring the residual stresses (top view) [1]

Although some drawbacks, the hole drilling method remains a popular method for the residual stresses measurement, there are latter developments involve the induction of new rosette designs and the developments of carrying out full field measurements such as laser speckle interferometry, Moire interferometry and holography. There are other improvements include the application of this method on (thick coatings, materials of non-uniform and severe gradients of stress) and novel drilling methods to increase the sensitivity of strain and confidence in measurements [10].

According to the hole drilling, the locked up residual stresses have released and the corresponding strains of surface have measured by usage of appropriate strain gauges that glued round the hole [1]. The range of resolution in the hole diameter region where the minimum analyzed hole depth does not exceed $0.5 \times d_0$ where d_0 is the diameter of hole [1].

There are several geometries of strain gauge that present for determining the residual stresses and have shown in Figure (2-9):

-Type A strain gauge is the most commonly employed and recommended design for measurements of general purpose.

-Type B strain gauge is beneficial if the needed measurements were near (obstacle, fillet, radius).

-Type C strain gauge has used 6 grids induced newly to give improved sensitivity of strain [10].

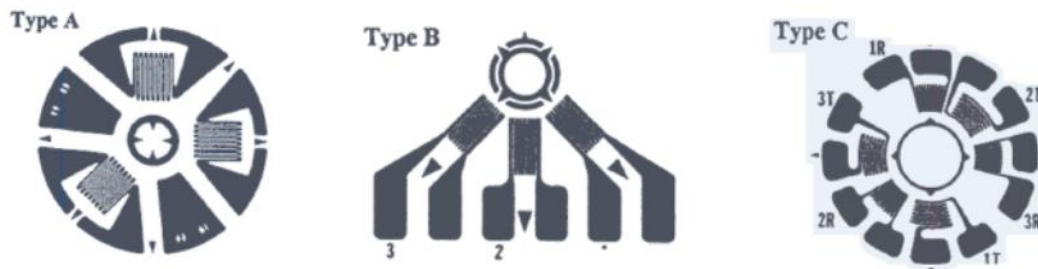


Figure (2-9): Geometries of strain gauge rosette [10]

The principle of determining residual stresses due to the hole drilling method is the material removal from a stressed surface that permitting relax the surface slightly and consequently the relaxation of residual stresses [10]. The principle of hole drilling method has included the induction of a small hole into a part involving residual stresses and consequent measurement of the locally released surface strains [10].

Effectively, the hole has drilled in the center of the component by a special rosette of strain gauge [10]. The method of hole drilling is inexpensive, quick and common semi destructive technique. It has applied on isotropic and machinable materials with known elastic parameters [1]. The hole-drilling method as compared to another techniques of residual stresses measurement is applicable on all groups of materials, this method has determined macro residual stresses [1]. The hole drilling for measuring residual stresses has done with important carefulness to avoid the induction of errors.

There are three main causes of error: introduction of stresses from machining have added to the measured residual stresses, non-cylindrical hole shape, and eccentricity but it is the unique method for the residual stresses measurement with accepted standard ASTM [1]. The modification for the technique of hole drilling by usage of a bit drill to minimize the heat and pressure created during the process of drilling which demonstrates that the technique of hole drilling has successfully utilized with plastics [16].

The hole drilling methods have categorized into the following:

1- High Speed hole drilling (HS)

The extra stress that has induced by the technique of high speed hole drilling is comparatively lesser than the produced stresses by another techniques of hole-drilling, the method of high speed hole drilling has several advantages involved: the experimental setup is simple, the operation is straightforward and the precision is improved. The main problem of the hole drilling technique considers the induction of stresses of machining while the HS hole drilling method has allowed to resolve the problem of introducing lower extra stress [1].

High speed hole drilling has suggested for measuring the residual stresses of specimens with high toughness and hardness, furthermore, the tool wear has caused the introduced stresses to rise and therefore cause significant errors of measurement. In extreme cases, the wear of tool may be very sharp where the tool has failed catastrophically, high speed hole-drilling has unsuccessful for using in the method of strain gauge. Moreover, the wear of tool makes the introduced stress increased and ; thus, led to substantial errors in measurement [1], the magnitude of extra induced stresses has depended on the used method of drilling and working parameters [10].

2- Hole Drilling Electrical Discharge Machining (EDM)

The electrical discharge machining hole-drilling (EDM) method affords as an alternate method for measuring the residual stresses [1], the method of hole drilling electrical discharge machining (EDM) has employed for measuring the residual stresses of component, the discovered portion of strain that released by strain gauge not originates from the original component but from the introduced residual stresses at the layer of conversion through the hole-drilling process, this extra strain imperatively induces an error in the measurement unless it is taken account in some manner [1].

The technique of electrical discharge machining (EDM) as the high-speed hole drilling method affords the same degree of reliability and constancy in measurement with respect to the experimental results. Moreover, they also have found that the error in measurement which introduced by the (EDM) is dependent on the working parameters and independent on the magnitude of residual stresses through the original component [1].

There are several preparations for assessing the residual stresses due to the subsequent stages: preparation of surface and installation of strain gauge, the strain gauges have bonded to the sample at the points of calculating residual stresses, each rosette grid element has related to an indicator of strain with recorded of zero readings, the milling guide has located over the gauge center and attached with a safe manner to the part of sample by the usage of a particular type of cement [1].

Lastly, the magnitudes of principal residual stresses and their directions have determined by the usage of suitable equations [1]. The advantages of this method are that no restraint on the mechanical properties of ferrous materials and its ability of drilling holes on different metals with high accuracy [1].

3- The Incremental hole drilling method

The incremental hole drilling method is an enhancement on the fundamental method of hole drilling that includes execution of the drilling in a sequence of small steps, it enhances the method versatility and enables the measurement of stress profiles and gradients where the residual stresses are not uniform within depth [1]. A pneumatic drill of high speed runs exceeding (200,000) rpm has employed to drill hole without introducing any additional machining stresses and modifying the existing system of stress.

The strain data at pre-determined depths are accurately gained. On the other hand, the accuracy of method depends on the number of increments and their corresponding depths. The more representative profile of residual stresses, The larger number of drilling increments for the same thickness of laminate [1]. According to the effect of increment depth, the choosing of an increment is very important (one increment per ply) and has led to little over-estimated stress, the drilled increment per ply has produced by the relaxation of stresses during and after the process of drilling [1].

The incremental hole-drilling method has suggested if the residual stresses within depth are not identical. It needs the suitable trade-off with respect to both the number of drilling increments and the depth of every increment [1]. The method of incremental hole drilling has improved the technique versatility and enabled the measurement of stress gradients and profiles. There is no point for making measurements beyond the depth that equal to the diameter of drill because no measured extra strain [10].

4-Deep Hole drilling Method

The method of deep hole drilling is semi destructive, it is a different method combines the elements of hole drilling and ring core methods, it is a standard method for the residual stresses measurement into isotropic materials and especially suitable to thick components, it gives the deep internal stresses

measurement for quite huge specimens such as castings of steel and aluminum with several tons weight. In the method of deep-hole drilling, a hole has first drilled over the thickness of component, the hole diameter has measured precisely and the core of material round the hole has trepanned out, the core trepanning has carried out by using a wire electrical discharge machining (WEDM) operation to relax the residual stresses into the core, the diameter of hole has re-measured to determine the residual stresses from the difference in the hole diameter [1].

The method of deep hole drilling is semi destructive employed for measuring the residual stresses because although the hole has left in the component, the hole diameter is quite small and accord with the hole which needs to successive machining. The main advantage of this technique is enabling the measurement of deep internal stresses. The methods of hole drilling and deep hole drilling are easy, fast, semi destructive, used for wide range of materials that have limited sensitivity of strain and resolution [1].

2.2.4 Method of Sectioning

The sectioning method is destructive depends on the measurement of deformation according to the relief of residual stresses upon the removal of material from sample. The sectioning technique includes generating a cut on the plate to relief the residual stresses that presented on the cutting line, the employed cutting process must not induce heat or plasticity, so that the original residual stresses have measured without the effect of plasticity on the planes of cutting surfaces. Figure (2-10) depicts the method of sectioning where a series of cuts has made to assess the residual stresses into section of I-beam, the released strains through the process of cutting have measured by the usage of electrical or mechanical strain gauges [1].

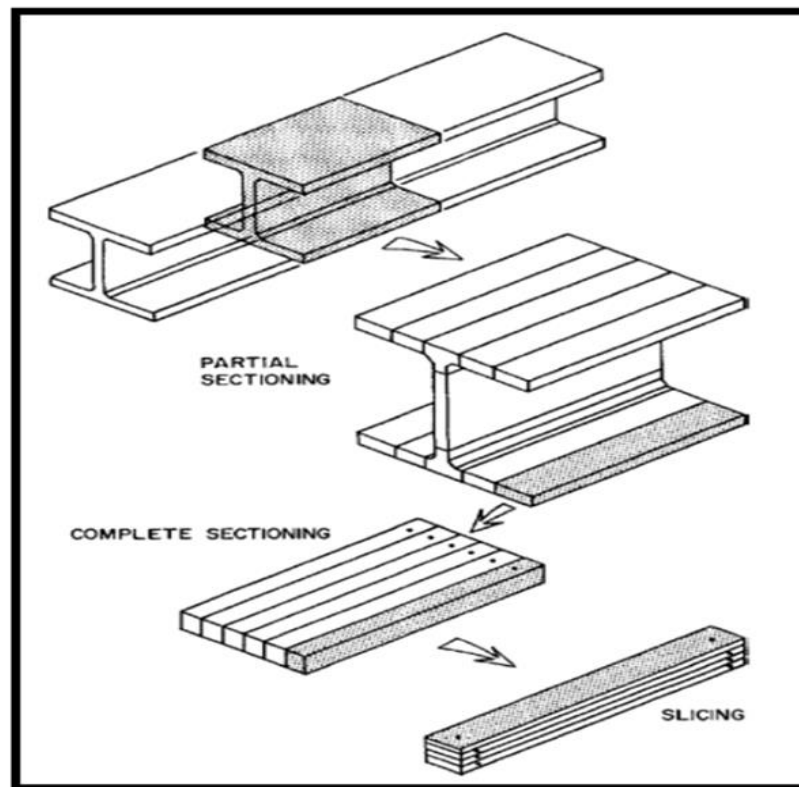


Figure (2-10) Section from sectioning method [1]

2.2.5 Ring-Core Method semi destructive

Ring-core method is a semi-destructive method, it is variant of the hole-drilling method because the hole drilling method includes the drilling of a central hole, the ring core method includes the measurement of deformation into a central region has produced by the annular slot cutting into surrounding material. and measuring the resulting deformation of the surrounding surface

The ring-core method as the hole-drilling method, has a fundamental execution to assess the stresses in-plane and an incremental execution to calculate the profile of stress. The ring-core method has an advantage over the hole-drilling method is that it provides larger surface strains, it generates greater specimen damage and is less easy to implement practically [1].

2.2.6 The Slitting (Parting-out) Method

The method of slitting is very similar to the method of hole-drilling but it uses a long slit rather than a hole as shown in Figure (2-11) that illustrates the geometry of slitting method. Strain gauges have attached either on the front or back surfaces or both of them and the released strains have measured while the slit has incrementally increased in depth. The slit has produced by a thin saw, milling cutter or wire electrical discharge machining (WEDM) [1].

The perpendicular residual stresses on the cut have calculated from the measured strains by the usage of determined finite element calibration constants. The method of slitting has an advantage over the method of hole drilling where it has assessed the profile of stress over the entire specimen depth, the front strain gauge provides with near surface stresses while the back strain gauge provides with deeper stresses [1].

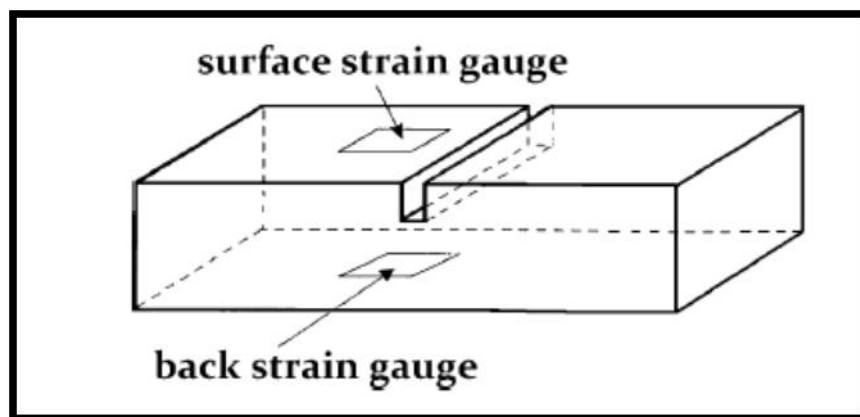


Figure (2-11): Slitting method [1]

The method of slitting provides only the normal residual stresses on the cut surface while the method of hole drilling provides with three in-plane stresses, the extra cuts have made to find another components of stress where the overall procedure is similar to the sectioning method. The slitting method has also applied to estimate the stress intensity factor produced by residual stresses that is very beneficial for studying the fracture and fatigue [1].

For measuring the residual stresses of pipe in the circumferential direction have depicted by Figure (2-12), a ring sample has removed from the pipe of (one-inch) width and the ring then is slit open, when the pipe has tensile stresses on the inside wall and the ring tends to reduce the diameter and close, the maximum residual stresses have determined by measuring the difference in diameter over time [18].

In order to measure the longitudinal residual stresses, a small section with rectangular shape has cut from the pipe end, the displacement has monitored with time at the end of removed section [18]. The residual stresses have created in pipes during the process of manufacturing, the magnitude is too important and cannot be ignored, for example the measured residual stresses in pipes of HDPE are generally between (470-1200) psi, thus; the influence of residual stresses on the properties of material has assessed [18].

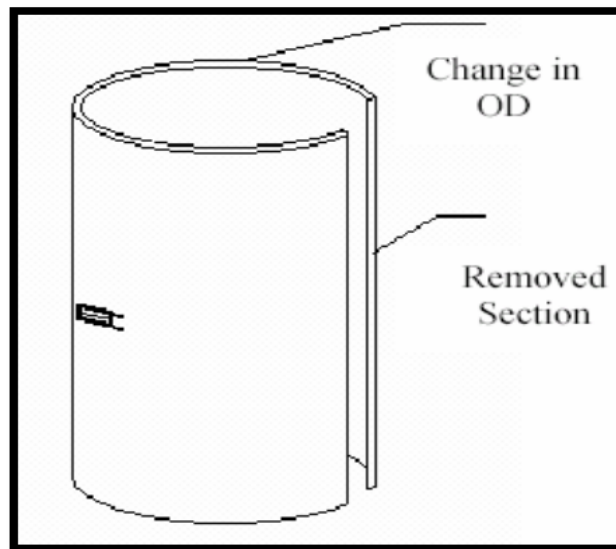


Figure (2-12): Measuring of residual stresses by slitting [25]

2.2.7 Partial Excision (Splitting) method

The method of splitting includes the measurement of the curvature or deflection for a thin plate due to the material adding or removing that involving residual stresses where partial excision is a procedure carried out by cutting deep slots at each end of the strain gauge as shown in figure (2-13). This technique

has firstly developed for the stresses assessment in electroplated materials and is beneficial for evaluating the stresses introduced by shot-peening [1].

Figure (2-13) illustrates a deep cut has been made through the sample as well as the opening or closing of the neighboring material refers the signal and approximate size of the present residual stresses. This technique is utilized extensively as a fast test for the purpose of quality control through the production of material.

The “prong” test has shown in Figure (2-13-b), it is a different method for evaluating stresses in dried lumber. The splitting method of thin-wall tube has depicted through Figures (2-13-c,d) which are examples on method of Stoney and sometimes called the method of curvature [1]. Figure (2-13-c) has usually utilized to evaluate the residual stresses in thin-walled tubes by assessing the longitudinal stresses while figure (2-13-d) has evaluated of the residual stresses through circumferential stresses. The last arrangement has applied commonly for tubes of heat exchangers and specified by standard ASTM (E1928) [1].

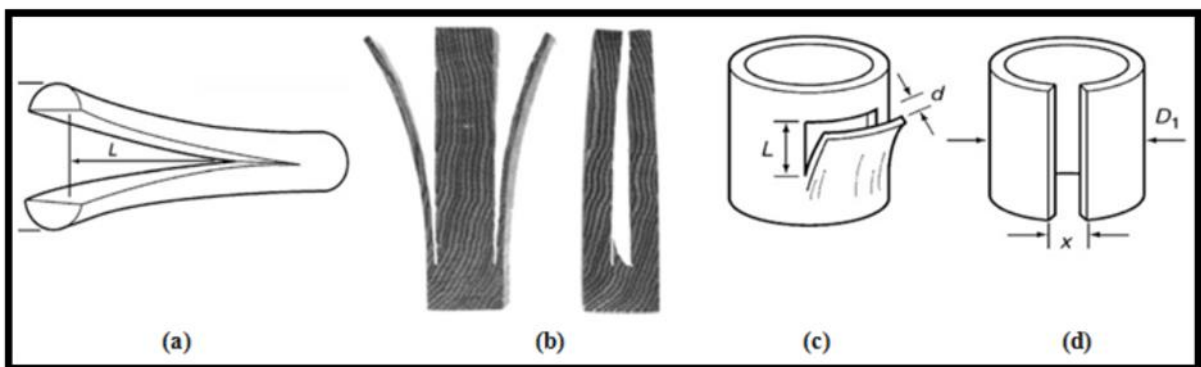


Figure (2-13): Method of splitting (a) rods (b) wood (c) axial stresses of tubes (d) circumferential stresses of tubes [1].

2.2.8 Crack Compliance Method

The method of crack compliance has based on cutting a small slot to see the stress relaxation in the neighborhood of a slot by applying strain gauge interferometry, the depth of increment for slot has allowed for stress resolving in field normal to the crack as a function of depth for comparatively simple stress distribution. There are different removal techniques have reported. Another method depends on cutting a section with the electrical discharge machining (EDM) and deducing the prior normal stresses [19] where the crack compliance method determines the material residual stresses which has removed in a small crack [12].

2.3 Non-Destructive Measurement Techniques:

There are many techniques non-destructive as diffraction method, photoelastic method, and ultrasonic method

1-Diffraction Methods

A- X-Ray Diffraction

there are several diffraction methods included: traditional XRD method, synchrotron X-ray method and method of neutron diffraction, they have applied for various materials involved: materials have polycrystals, materials with fine grains, metals and ceramics [1].The principle of X-ray diffraction method is shown at Figure (2-14).

Bragg's equation of diffraction has used the in inter planar spacing changes d to discover the elastic strain ϵ due to knowing of the incident wavelength. The results of strain have converted into stress by usage of appropriate magnitude of stiffness [19]. X-ray method is sensitive to the direction of detection and detrimental to human health [20].

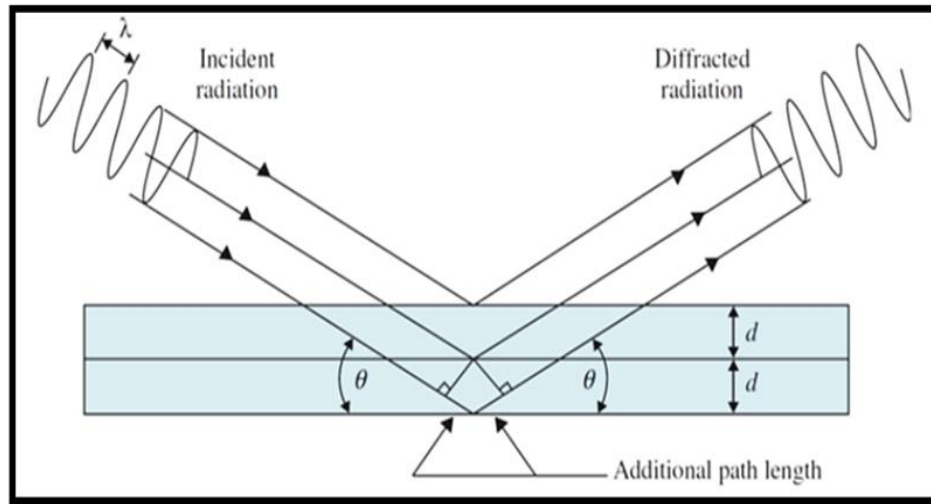


Figure (2-14): The radiation of diffraction through crystal structure [3]

The main limitation imposed in XRD is the size and geometry of test piece, the entire part size must fit with the diffractometer, the geometry of XRD can both hit the detector and the measurement area without hitting obstructions [3], the diffractometer can be seen in Figure (2-15) [3].

In XRD, the strain is measured in the lattice of crystal and then determines the kinked residual stresses that has calculated from the elastic constants by the assumption of a linear elastic distortion of the suitable plane of crystal lattice.

XRD occurs when the radiation interacts with regularly arranged atoms, the radiation has absorbed and then reradiated under the same frequency where the strong emissions have occurred at specific orientations and few emissions at another orientations. The angles of strong emissions have described by law of Bragg [3]. It is necessary to obtain accurate measurement of spacing at stress free state (d_0). The results of strain have converted into stress by usage of appropriate magnitude of stiffness [19].

1. Traditional X-ray Method

XRD method is a laboratory method and does not employed for big welds because the available limited space on most lines of beam. It also cannot be applied on nanostructured materials according to the difficulty in analyzing the

diffraction of peaks for nanomaterial [1]. It is hard to determine the accurate position of peak or to calculate the shift in peak for studying the macroscopic stress according to intense plastic deformation for several materials, thus; the best methods are mechanical methods for the residual stresses measurement at all types of nanomaterial without the influence of nanostructure [1]. It has utilized when the metal is subjected to either applied or residual stress, the planes of atoms in the crystal structure of metal have changed their spacing according to the resulting elastic strains [1].

The total stress of metal has attained by direct measuring of the inter-planar atomic spacing by XRD method, metals are consist of a 3D regular array of atoms for the formation of a crystal, most components of metal have composed of many small crystallites called grains which have oriented randomly due to their crystalline configuration and melted together to form a whole solid, if a polycrystalline metal has subjected to stress, the elastic strains have resulted in the crystal lattice of the individual crystallites [1].

The method of X ray diffraction for measuring residual stresses has applied on crystalline materials, comparatively fine grained, and diffraction has produced at any direction of the sample surface [1]. XRD samples are metals or ceramic, provided the peak of diffraction has appropriate intensity and free of interference from neighboring peaks as well as has resulted in the area of high back-reflection with the affordable of radiations [1].

Few inquisitors have applied method of XRD to assess the residual stresses distribution in the welds of dissimilar metals and measure the residual stresses in both longitudinal and transversal directions of the butt welding with double-electrode of steel plates [1]. According to this small depth of penetration, the normal stress on the surface has assumed to be zero, the investigated volume has considered in the plane stress state. This case allows of the stereotyping for

stress-strain equations and there is no fixture for accurate determination of the lattice plane dimensions in unstressed state [3].

According to the existent of residual stresses, elongations and contractions have produced through the crystal lattice and the inter-planar spacing has changed. These changes in (d) can be measured as a shift in the pattern of diffraction, by measuring the shift in the pattern of diffraction, it can be evaluated the altering of the inter-planar spacing and consequently calculated the strain within the material [3].

In another words X ray diffraction method obligate samples to be cut-down for measuring the residual stresses. X-ray has hit the measurement region and diffract by the reagent without hitting any obstacles. The portable devices of X-ray diffractions are now available on several structures such as pipelines, bridges and welds. The speed of measurements with XRD method depends on several factors such as the material type, X-ray source and the degree of accuracy.

The speed of measurement can be curtailed due to the precise choice of X-ray source and set-up test. There is a reciprocating between the need to spatial resolution with field of strain and time of data collection as well as the reduction of measurement time [1]. For measuring internal stresses in polycrystalline material, XRD depends on the elastic deformations. These deformations have led to differences in the space lattice planes from stress free value to the magnitude of applied stress, the measurement is comparatively simple and the equipment is available [10].

The main limitation of XRD is the size and geometry of test piece where the entire part size must fit with the diffractometer [3]. X-ray method is sensitive to the direction of detection and detrimental to human health [11]. the limitation of XRD technique in the residual stresses measurement through the welded structure thickness [1].

2. X-Ray Synchrotron Diffraction (Hard X-ray)

High energy X-ray synchrotron technique is a tool used for measuring locked-in residual strains in semi-crystalline polymers, it attains the difference in diffraction angle through a volume gauge with a spatial measurement in the range of 1mm, the strain of lattice has determined from angles of diffraction [26], The strain has calculated by subtraction of the lattice parameter in unstressed state from the lattice parameter in the actual stressed state and the lattice parameter in unstressed state must be known accurately and this requirement introduces important uncertainty into the measurement of strain because the unstressed lattice parameter has influenced by many material parameters such as alloy content, phase composition and others [3].

The distribution of strain by 3D maps have depths in millimeters for engineering components, the spatial resolutions have limited by the crystallite size of the sample and not by the device [19]. The sources of synchrotron generation have provided the entrance to X-ray with high energy. At X ray synchrotron with high energy, the length of attenuation increases remarkably.

According to very high intensities of X-ray, they have produced path lengths in centimeters even for steel [1]. X-ray synchrotron has applied for measuring the field of internal elastic residual strain in polymers and other types of materials, for example it is employed successfully to measure the residual strains in a commercial system of gas pipeline from HDPE polymer [26].

The main advantages of X-ray synchrotron diffraction are the high intensity and The method also is appropriate to: the collection of obtained maps from 2D or 3D strain field, monitor the phase transformations [1]. X-ray synchrotron have higher depth of penetration into materials than conventional XRD where X-ray synchrotron (hard X-ray) provides beams with high intensity of energy and capable to provide high spatial resolution. The increased penetration depth has regarded as one of the important advantages of

synchrotron X-ray diffraction as compared to the conventional X-ray diffraction as well as the synchrotron diffraction is much quicker than conventional X-ray diffraction and the time of measurements are of a fraction of second, the possible size of intense narrow beams is (1mm-10 μ m) [19].

The full 3D stress condition must be considered and the stress condition cannot be considered under plane stress as in XRD because the higher energy radiation penetrates into tens or hundreds of millimeters into a material, it is possible to obtain detailed maps of strain for the components with few hours of beam time [3].

B-Neutron Diffraction Method

The method of neutron diffraction is too similar to the method of X-ray diffraction since it depends on the elastic deformations through a polycrystalline material which has led to differences in the lattice spacing of the planes at the stress-free state. The neutron diffraction has applied over the two past decades in solving engineering problems [1]. Neutron diffraction (ND) is one of the diffraction methods that uses penetrating radiation where neutrons have a very large depths of penetration.

Neutron diffraction is non-destructive method allows capability of measuring residual stresses inside the compounds without sectioning or layer removal. The accuracy of neutron diffraction (ND) technique requires measuring accurately the lattice space at unstressed state of the crystallographic planes because the state of deep stress is triaxial. In neutron diffraction method as X-ray synchrotron method, the lattice space in unstressed state should be known but the measurement is difficult.

Neutron diffraction requires several minutes to one hour for each measurement of strain, the measurements are very expensive, a single determination of stress in each (1mm³) from the gauge volume of component that requires at least three strain measurements as well as it is especially

beneficial technique for the validity between theoretical and numerical models and its measurements are made over the whole surface and depth of samples [3, 20].

According to each point of measurement, strain has measured in three orthogonal directions: (1) axial strain (ϵ_A) along the sample axis (2) transverse strain (ϵ_T) that is transverse to the sample axis (3) normal strain (ϵ_N) through the wall thickness. The neutron diffraction method has accomplished by installing each sample in three various orientations as shown in Figure (2-15), the direction of measured strain has split the directions of incident and diffracted beam fifty-fifty [1].

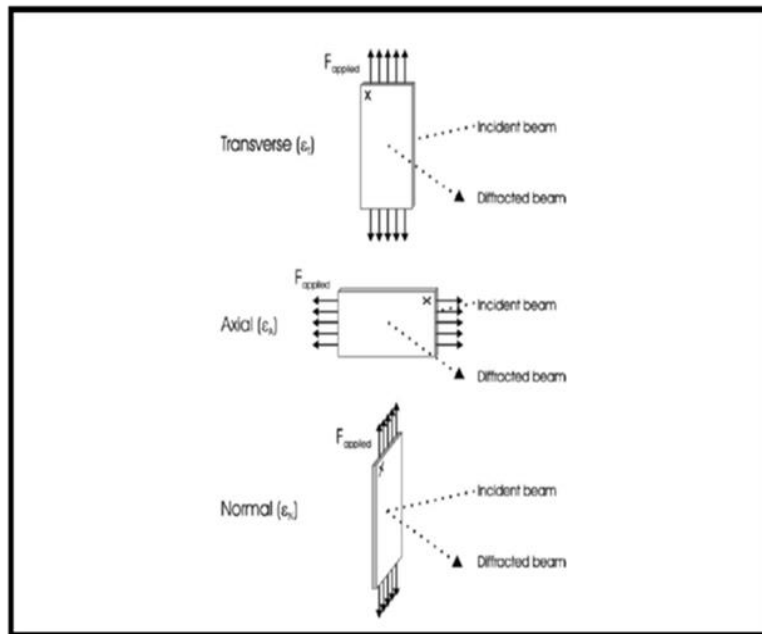


Figure (2-15): The various orientations that used to determine (ϵ_T), (ϵ_A) and (ϵ_N) [1]

Neutron diffraction ND is more suitable for composite or multiphase materials including elements of high and low atomic numbers. Recently, neutrons have studied the induced stresses due to welding process. The device of neutron diffraction method provides information interested with the activating of smart transformations with respect to material, it delivers information concerned family of phase or grain for the alloys and composites optimization

performance [1]. Neutron diffraction as a method for stress assessment with the collection capacity to large amounts of data across the sensitive detectors of location over the whole depth and surface by relying on the sample thickness [10].

Neutron diffraction method has determined the residual stresses in crystalline materials, it determines the elastic strain components paralleled to the scattering vector that can be converted to stress, the components of strain can be computed according to the differences in the lattice spacing of crystal [19]. If the crystalline materials have exposed to the radiation of (0.5-3) Å wavelength (close to inter planar spacing), these materials have strained elastically and scattered this radiation coherently as distinctive peaks of Bragg that imaged usually by a sensitive detector of position. The occurring angle of any given peak has determined by the usage of Bragg's law as follows:

$$2d_{hkl} \sin \theta_{hkl} = \lambda \quad \text{Eq.(2-1)}$$

Where λ is the radiation wavelength, d_{hkl} is the spacing lattice plane from the planes of crystallography (hkl) which responsible for peak of Bragg, θ_{hkl} is the angular position for this peak of diffraction. This peak has noticed at an angle $2\theta_{hkl}$ from the incident beam.

If a sample has strained elastically, the differences in space lattice; thus, any elastic strain will be apparent as a $2\theta_{hkl}$ shift magnitude for a specific plane of reflection that illuminated by a fixed wavelength. By differentiation of Bragg equation [19],

$$\Delta\theta_{hkl} = \left(-\frac{\Delta d}{d_o}\right) \tan\theta \quad \text{Eq.(2-2)}$$

Where Δd is the difference in lattice space. The strain in the planes hkl has determined in the direction of measuring strain which is along the scattering vector and perpendicular on the planes of diffraction planes [19].

$$\epsilon = \frac{\Delta d}{d_o} = -\Delta \cot \theta_o \quad \text{Eq.(2-3)}$$

The method of neutron diffraction has large penetration depth as compared with diffraction of X-ray, X-ray diffraction method has several limitations in the residual stresses measurement for a welded structure through the thickness while a neutron is capable of penetration into little centimeters, so it has applied widely for evaluation of internal residual stresses in materials. ND is particularly beneficial for alloys that have high atomic number because X-ray penetration falls off quickly in this protocol [1]. The method of neutron diffraction provides complete 3D charts of the residual stresses with high spatial resolution of the engineered components through translational and rotational movements [1, 10].

The relative cost of neutron diffraction application as compared to another methods of diffraction such as X-ray is much higher basely due to the cost of equipment. Neutron diffraction method is very expensive for using in the quality control routine process at the engineering applications [1]. On the other hand, the measurements of neutron diffraction are slow as compared with synchrotron X-ray diffraction [1] but the measurements have carried out in the same procedure of XRD where the detector has moved around the specimen and localized the positions of diffracted beams with high intensity [10].

The greatest neutrons advantage is obtaining very large depths of penetration that makes them able to measure depths from 0.2 mm near surface reaching to 25 mm in steel and to 100 mm in Al. The neutron diffraction method availability is very much lower as compared to another techniques of diffraction such as X-ray diffraction method [10].

B- Magnetic Methods

The magnetic methods are non-destructive methods applied only for measuring residual stresses of ferromagnetic materials [20]. the primary

advantages of these methods are: cheap, simple and very rapid where the measurements in seconds. the equipment is portable and the depth of measuring biaxial stresses is (6-10) mm [10]. The drawback of the magnetic methods is the limited range of materials which has inspected and the inherent sensitivity according to different microstructural features [10]. Magnetic methods can be classified into:

1.Magnetostriction

The ferromagnetic characteristics of steel and other ferromagnetic materials are sensitive to the state of internal stresses according to magnetostriction and the subsequent influence of magnetoelastic. Magnetostriction is a procedure where the strain in each magnetic domain is along its direction of magnetization. At minimum energy, the magnetization has aligned with the directions of crystalline via the easy axes of magnetization.

The difference in the level of stress has resulted a difference in the number of domains that aligned along each one of the easy axes that has led to a reduction in the magnetoelastic energy [10]. the combination of magnetic methods has required to eliminate the influence of other variables The dependence of the magnetic parameters on stress is strong, there are many another variables which also have influenced on the measurement such as (grain size, texture, hardness) [10].

2.Magnetic Barkhausen Noise (MBN)

The most widely known and applied magnetics method for measuring the residual stresses is the Magnetic Barkhausen Noise (MBN), the MBN method has associated with the state of residual stresses because the ferromagnetic properties of steels and other ferromagnetic materials are sensitive to the state of internal stresses [3]. The magnetic Barkhausen noise method (MBN) has special significance due to its possibility as a non-destructive industrial device to

measure the surface residual stresses (SRS) and other microstructural parameters [1].

The analysis of MBN method includes the measurement of number and magnitude of magnetic reorientations that have carried out by the magnetic domains in a ferromagnetic material through the reversal of magnetization. These reorientations have noticed as random pulses with respect to (duration, temporal separation, amplitude) as well as these pulses (reorientations) are roughly similar to noise [3].

The MBN method has applied on ferromagnetic materials that have composed of magnetic regions with small order that called magnetic domains. Each domain is magnetized spontaneously along the easy axes of the crystallographic direction of magnetization. Moreover, the magnetization vector inside the oriented domains where the total material magnetization is zero with the exception of the natural magnets [1].

Although most steels and several ceramics are ferromagnetic materials and have produced the Magnetic Barkhausen Noise (MBN), there are many non-ferromagnetic engineering materials where the Magnetic Barkhausen Noise (MBN) does not applicable to them. Moreover, the MBN method has a limited area of stress sensitivity (roughly ± 300 MPa) as well as the depth of measurement is few millimeters. The MBN is sensitive to the differences in magnitudes of applied stresses [1], The sensitivity of this technique to other properties of metallic materials has consequently needed to calibration with a nearly identical specimen [3].

The "magneto-elastic interaction" is the interaction phenomenon among (elastic properties, structure of domain, magnetic properties) of material. As a result of magneto-elastic interaction, in positive magnetic anisotropic materials such as (iron, most steels and cobalt), the compressive stresses have decreased Barkhausen noise intensity while tensile stresses increased it, so that the residual

stresses amount can be computed by measuring of the Barkhausen noise intensity .

Barkhausen noise has also influenced by the material microstructure and sensitive to the stress state for ferromagnetic materials. The stress dependence of Barkhausen signal has differed from one material to another. Moreover, different materials must be calibrated individually for the effectiveness of MBN in calculating residual or applied stresses [1]. There are several advantages of MBN method: appropriate for the circular shapes like rings, rapid, does not require direct contact to the sample and the penetration of this method is greater than X-ray diffraction by 100 times.

The depth of measurement depends basely on the material permeability (typically over 0.2 mm) for components with hardened surface, the method of Barkhausen noise is able to determine subsurface stresses without the surface layer removal [1]. One of the limitations of this method is the saturation of the MBN energy signal in either tension or compression, the stress cannot alter the energy level of MBN by arising minimum or maximum energy values, so this has limited the connection between stress and energy of MBN to the values of maximum tensile and compressive stress [1].

3. Eddy Current Technique

Eddy current techniques are introducing eddy currents in the material understudy and discovering of the changes in the electrical conductivity or magnetic permeability as a result of residual stresses through changes in the test coil impedance. The depth of penetration has changed by altering the excitation frequency, the penetration depth is around 1mm at practical frequencies and the probe cannot identify the direction of applied stress. Although the methods of eddy current are not well suited to basic measurements of residual stresses due to the sensitivity of eddy current monitoring to plastic work and microstructural changes, they can provide a quick and cheap inspection method [1].

C- Photo elastic Technique

Photo elastic stress analysis has become a technique of outstanding importance to engineers over the years and it is vital to understand stress and strain definition in a body [25, 27]. Photo elasticity is an experimental nondestructive analysis technique depends on the photo elastic influence that represents a variation in the optical indication due to the mechanical stress [15]. The discovery of photo elasticity effect is accredited by Sir David Brewster who published the write up of his finding in 1816 through the examination of clear stressed glass with polarized light which exhibited color patterns [27, 22]. This method is cheap, fast and very simple [15].

The photoelastic method has investigated the surface and internal stresses of the material and provides us with (distribution of general stress, sites of stress concentrations and areas of flow stress) as well as the designs have modified after obtaining these results [15]. On the other hand, this method has used to give qualitative assessment of the stress state in the molded products where the colors have generated and the spaces for various contours of color have characterized the regions of high stress [1].

The amorphous mediums are isotropic when unstressed and become anisotropic when stressed [25, 27]. The isotropic materials have contained the same physical and mechanical properties throughout its volume in every direction [28]. In anisotropic materials the properties have changed with direction [22, 27], this anisotropic behavior is calculated due to the chemical configuration and chain conformation, the anisotropic behavior has canceled out on a macroscopic scale if the macromolecules are randomly coiled [14]. There are main points in this method as the following:

a-Light and Electromagnetic Spectrum

A source of light is needed to perform photo elastic stress analysis, the light is electromagnetic radiation whereas the waves of light have gone in all

directions through propagation [15]. The light transfers in a vacuum or air at speed ($C=3.00 \times 10^8 \text{ m/s}$), the speed is lower in transparent bodies [15]. The chart of electromagnetic spectrum of various zones is shown in Figure (2-16) [22].

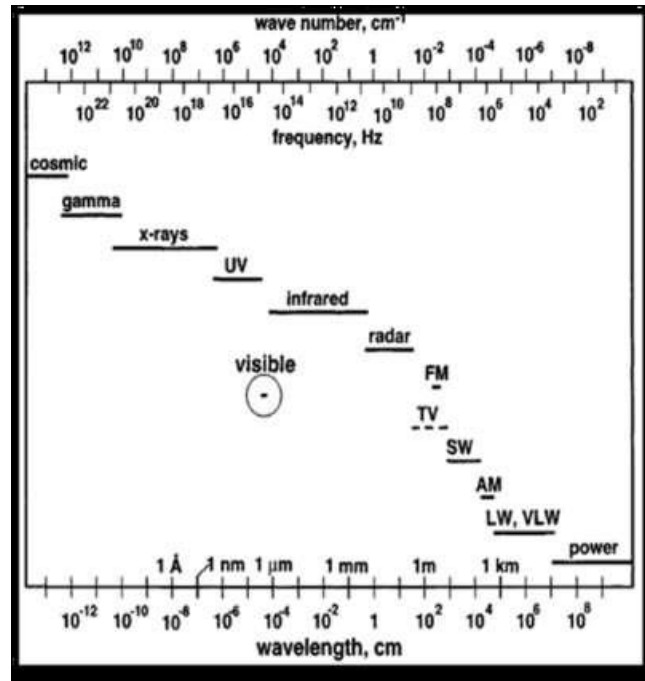


Figure (2-16): The electromagnetic spectrum [6]

The electromagnetic spectrum covers very wide range from radio to X-ray waves with wavelengths between (1m or more - less than billionth of meter). The optical radiation on the electromagnetic spectrum between radio waves and X-rays have exhibited unique combination of (ray, wave and quantum properties). At shorter wavelengths of X ray, the electromagnetic radiation behaves as particle like while at the other end with longer wavelengths behaves mostly as wavelike, the visible portion has occupied an intermediate position which exhibiting properties of wave like and particle like with different degrees [22].

Monochromatic and polychromatic represent two fundamental series of light. Laser light is an symbol of a monochromatic light which characterized by only one frequency. Sources of monochromatic are chosen when quantitative

photoelastic measurements are necessary. The white light is an example of polychromatic light which had many various frequencies [15]. These individual wave lengths or monochromatic lines may be polarized as plane, circularly, elliptically. The white or polychromatic light includes a combination of lights with various wave lengths, the intensity of light is proportional to the square amplitude of vibration [22].

The frequency of light is related to its color [15]. In photo elasticity, the range of band color usually called monochromatic lines which having various frequencies and have distinguished from one another through the color sense, for visible light the entire range of colors frequency in the spectrum approximately between 90 nm (deep red) to 700 nm (deep violet) [22]. There are two convenient ways to describe the propagation of the light and its interaction with materials: electromagnetic wave model and quantum model.

The light comprehensives (infrared, ultraviolet, and radio) waves. It is treated in the form of electromagnetic waves. Whenever, the wave of trains of radiation can be depicted perfectly by two vectors that vertical to the direction of ray travel and perpendicular to each other. The electric and magnetic are these vectors. They exist at the same time at right angle planes such that the intersection line of planes is parallel to the direction of ray light. The term polarization commonly used to denote several kinds of control over the existence of light vector, the ordinary light without any polarizer has the behavior shown in Figure (2-17) [22].

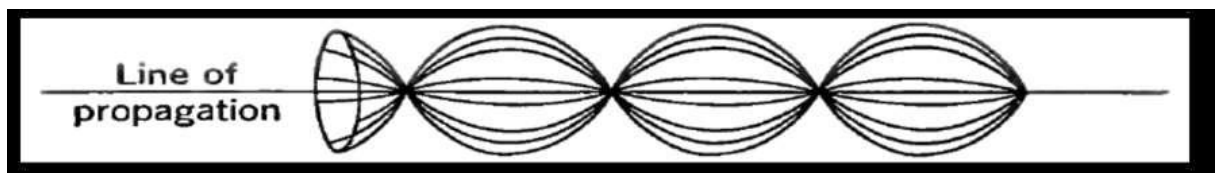


Figure (2-17): Ordinary light without control over light vector [22]

b- The Index of Refraction

The change in direction of a wave passing from one medium to another and caused by its change in speed is known as the refraction in physics [15]. Figure (2-18) shows the refractive index when light passes from one medium to another [29]. There is a change in velocity according to the passing of light from one medium of certain density to the other medium with different density, the index of refraction is the ratio of these velocities [22]:

$$\text{Index of Refraction} = \frac{\text{velocity in 1st medium}}{\text{velocity in 2nd medium}} \quad \text{Eq. (2 - 4)}$$

The index of refraction changes with the level of stress and this optical property is making the basis of photo elasticity technique [15]. Isotropic polymers have exhibited a temporary double refractive index when they are stressed [22].

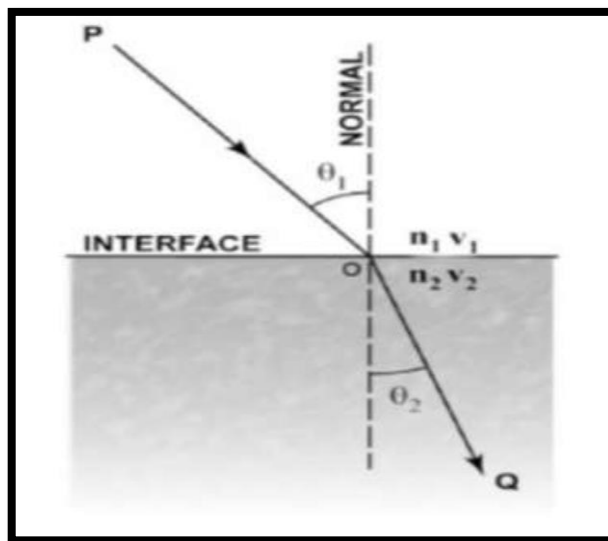


Figure (2.18):Refractive index while passing from one medium to other [29]

c-The Polariscopes Instrument

The polariscope is a device has used for performing the analysis of photo elasticity [15], The manufactured polariscope has shown in Figure (2-19) which consists of light source (L) and polarizator (P) [22]. Polarimeter is developable

segment of device where polarimeter and identification of material are necessary to characterize the constant of material, this material constant is unique for each material and requires non trivial identification proceeding [30].



Figure (2-19): Polariscope with light source and polarizator [22]

d-Polarized Light

The polarized light method is a typical nondestructive measurement method has used for polymer analysis [8]. The qualitative evaluation of stress in a molded or extruded part can be performed inexpensively using polarized light [5]. When a beam of polarized light passes through an elastically stressed specimen which consists of transparent isotropic material . The decomposing of beam into two rays polarized in the planes of principles stresses [31]. The light is plane-polarized when the vector of light is confined to a single plane, the plane that contains vector of light has called as the vibration plane while the plane at right angles has called the polarization plane as shown in Figure (2-21) [22].

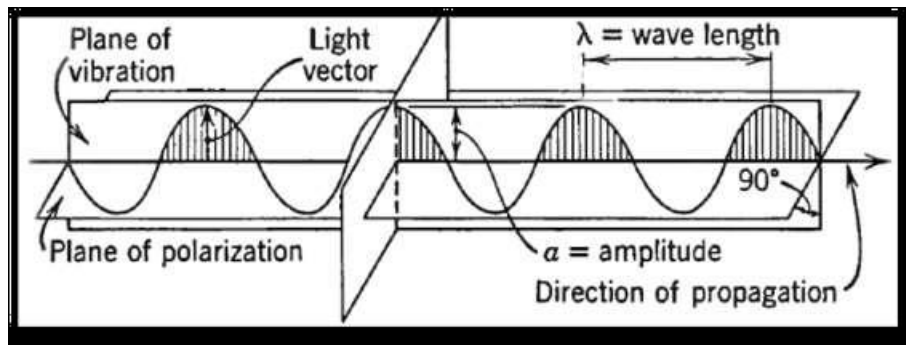


Figure (2-20): Plane of polarization [22]

The optical polarization of a polymer chain is anisotropic where the polymer backbone has various polarization in the longitudinal and transverse orientations [14]. The fringe patterns have formed when polarized light passes through a stressed transparent model and offered immediate qualitative information [15]. This pattern of birefringence generates a contour of color that related to the amount of present stress through the part cross-section as shown in Figure (2-21) [30].



**Figure (2-21): The pattern of birefringence for tensile specimens
from polycarbonate [30]**

e-Fundamental Optical Laws of Photo Elasticity

Photo elasticity depends on the birefringence phenomenon which denotes to the anisotropy of transparent strained material and consequently the refraction index (n) which has become directional. In this technique, the transmission light through strained materials has obeyed the two subsequent laws that have formed the principle of calculating photo elastic stress:

1. The direction of polarizing light is the principal-stress axes and has transmitted only on the principal stress planes.

2. The transmission of velocity on each principal plane has depended on the intensities of principal stresses in these two planes, while the variation in the refraction index has given due to the subsequent equations [22] (2-5, 2-6)

$$\delta_1 = n_1 - n_0 = A\sigma_1 + B\sigma_2 \quad \text{Eq.(2-5)}$$

$$\delta_2 = n_2 - n_0 = A\sigma_1 + B\sigma_2 \quad \text{Eq.(2-6)}$$

Where

δ_i =The difference in index of refraction on i axis

n_0 = The refractive index of material free of stress

n_1 =The refractive index on the principal plane 1

n_2 =The refractive index on the principal plane 2

σ_1 & σ_2 = The principal stresses

A & B =The material photoelastic constants

In this technique, the variation between the refractive indices on the principal planes has given due to [22]:

$$\delta_1 - \delta_2 = n_1 - n_2 = (A - B)(\sigma_1 - \sigma_2) = CB(\sigma_1 - \sigma_2) \quad \text{Eq.(2-7)}$$

Where CB is the constant of differential-optical stress

The stress-optical equation has established that the double refraction is proportional directly to the variation in principal stresses that is equal to the variation between two indices of refraction which revealed by the material under stress. Due to the differences between the refraction indices and the stress-optical constant or (Brewster's) constant, it is possible to determine the principal stresses variation. The variation between the indices of refraction has calculated

by dividing the retardation value on the material thickness [22]. According to the difference in velocity, the vibrating waves along two principal planes have emerged out of phase, the relative distance or retardation (δ) has given by:

$$\delta = (n_1 - n_2)t = CBt(\sigma_1 - \sigma_2) \quad \text{Eq.(2-8)}$$

or

$$n = \delta / \lambda = CBt(\sigma_1 - \sigma_2) / \lambda \quad \text{Eq.(2-9)}$$

Where:

t = The thickness of material for passing the light through it

λ = The light wavelength that is 570 nm for polymer due to the ASTM standard while the equation has represented the stress-optical law [22].

The retardation (δ_{nm}) due to the light source can be calculated by multiplying the value of compensator (R) and correction constant ($b_{nm}/\text{division}$) according to this relation ($\delta_{nm} = R \times b_{nm}/\text{division}$). The residual stress (σ) can be calculated by dividing the retardation value (δ_{nm}) of material which is accounted from the previous relation on the result of multiplication between thickness (t) and stress constant (CB_{Brewster}) according to each temperature due to the following relation: ($\sigma = \delta_{nm} / (t \times CB_{\text{Brewster}})$) [22].

f-The Procedure of Measuring Residual Stresses

Photoelasticity differs from other procedures because it gives us information of the stress already existent on the surface and within the material. Residual stresses are related to errors in processing and could also originate failure of the material [15]. The measurements of photoelasticity have carried out by the sample insertion into the polariscope, lighting it with a source of white light, arresting the image and saving it in format file of JPEG and conversion of JPEG file by using a software into text format and lastly analyzing the extracted numbers from digital images by the data extraction from photos,

the stress analysis is possible by noticing the intensity of average light with pixels.

The load and thermal healing analysis has shown that the intensity difference has depended on the stress magnitude, also the thermal healing is effectual during the relieving of internal stress as well as it is possible to notice the location of stress acting [15]. The digital images have captured from the samples when performing stress analysis by a photo elastic method where the digital photo is an assembly of numbers where these numbers have stored, modified, transmitted and converted into something to see. Every part has captured in the digital image form that is a pattern of light and dark areas, these areas have divided into pixels which are very small squares.

Every digital photo has numbers described the image, these numbers have represented the average brightness or intensity at each pixel for example the darkest part of the image is zero and the lightest is 255 [15]. The essential benefit is concentrated on the value of retardation (δ) or reading (r), for which maximal and minimal value of n are get.

If $\delta/\lambda=n$, where $n=0,1,2,\dots$, the interaction between two waves is called constructive interference. On the other hand, if it takes its minimum value, zero in this ideal case, for $\delta/\lambda=1/2,3/2,\dots$, this situation is called destructive interference and causes dark fringes, the regions of the highest concentration from isochromatic lines have represented the locations of residual stresses [22].

Figure (2-22) shows a single-wedge model LWC-100 equipment (also called quartz wedge or babinet compensator) has used to determine the retardation value and made of synthetic crystal materials. This compensator exhibits a linearly-variable retardation and when observed in polarized light will show equidistant fringes [22].

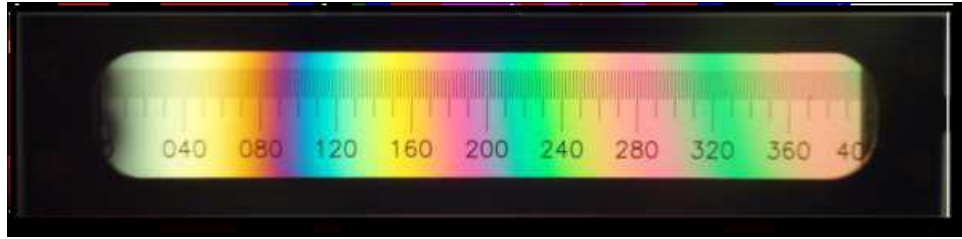


Figure (2-22): The compensator LWC-100 used to determine the retardation value [22]

Residual stresses are related to errors in processing and could also originate failure of the material [15]. The analysis of residual stresses is complex by the induced molecular orientation during processing. The birefringence technique measures the changing in optical properties of a polymer due to the presence of residual stresses, birefringence has several limitations for opaque materials [16]. However, the residual stresses have resulted distortion and induced anisotropy of polarization that has calculated due to the measurement of birefringence [14]. The resulting birefringence patterns are a qualitative indication of residual stress in the sample [5]. Figure (2.23) shows the principal of birefringence polariscope that utilized in determining the residual stresses from transparent components of polymer where polarizer & analyzer is set up $\pm 45^\circ$ direction [8, 24].

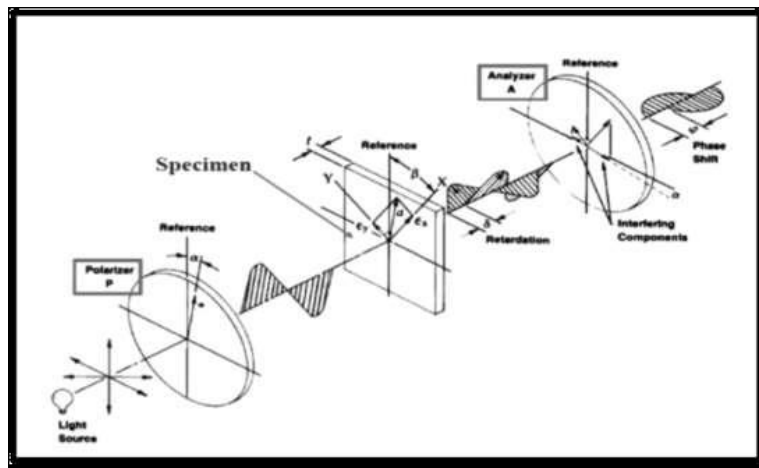


Figure (2.23): Polariscope for measurement of residual stresses [24]

2.4 Chemical Methods

One of the results of manufacturing procedures for plastics is the residual stress, which occurs during the cooling and shaping of melted polymer. The molding process of thermoplastics tends to induce residual or molded-in stresses within molded products. The presence of residual stresses do not always appear through visual signs on the plastic part. Regardless of the reason that causes the stress, if the molecules of polymer do not have a desirable orientation through the cycle of molding, an attempts is made on relieving these stresses so as to transfer them to the desired state after ejection [30].

In case of enough chain movements, the occurring of cracking and crazing weakens the part [30]. The cracking under normal load conditions is usually an index of excessive residual stress, where the crazing is the emergence of many fine micro cracks. The exposure of polymers to chemicals has aggravated these conditions which may not be apparent through the production and inspection of quality control [32]. In addition, these stresses have taken the dissipation time and are superimposed upon all operational stresses that are experienced during the service. Thus, the performance of long-term creep and the chemical resistance of the product has an inversed influence [30].

The chemical method test has been selected because it provides a sufficient level of accuracy for measuring the residual stresses. There is no need for finding the precise levels of residual stress or calculating their distributions. The chemical testing is considered to be a simple and quick method that depends on the environmental stress cracking caused by the residual stresses. Tensile residual stress significantly increases the likelihood of failure in plastics due to ESC [33, 24]. ESC is a type of fractures that is caused by tensile stress (whether applied or residual) in the presence of a chemical environment. It is necessary to point out that most stresses in injection-moldings are of a compressive nature

[18]. There are some precepts, health and safety considerations must be applied by researchers with chemical testing method:

A- All chemical tests should be conducted in a ventilated laboratory hood, or in a well-ventilated area because the reagents are flammable organic chemicals.

B- Chemical reagents should be stored in closed containers away from open flames, sparks, or locations where elevated temperatures may be expected.

C- Disposal of these materials must be in accordance with applicable federal or local regulations.

D- The researcher must consult the supplier's Safety Data Sheet before handling the specific reagents selected for testing and follow the manufacturer's instructions for handling precautions.

E- The determination of the acceptable molded-in stress level for an individual part should be made from its end use application, in particular, the chemical environment to which the part will be exposed [34]. There are many manners were presented in this method as the following:

1- Chemical Probe Technique

It is a typical destructive method used for plastics, the aim of this method is to accelerate the destruction at a concentrated point of stress by using a proper solvent for each material with an ideal concentration. It must be cautiously applied with a chemical solution and inevitably require trial and error to identify a proper concentration and soaking time for visualizing the destruction due to residual stress. The residual stress can be checked by generating cracks at a concentrated point of stress determined according to the solution concentration and soaking time that can be considered as influencing factors [8]. This technique is also known as solvent crazing [35] or solution soaking method [36].

This technique involves placing the polymer inside the chemical reagent and measuring the time taken for the polymer surface to fracture. The higher the residual stresses in the polymer the quicker it will fracture due to environmental stress cracking (ESC) [16]. The chemical probe technique can be used in principle to distinguish between well processed and poorly-processed polymeric moldings, the technique is not recommended as a substitute for other tests but for example does yield valuable information as the ESC susceptibility of complex molded components [37].

The chemical probe technique is a more speculative approach based on exposing the stressed part or product for a specific period of time to several environments of varying aggressiveness [35] in a progressive manner to estimate the magnitude of the residual tensile stress. The range of environments is selected according to the accuracy of measurement required [37].

There are reference data exist for the relationship between stress and time to crazing for different polymer–environment combinations with the polymers in the annealed state. The observation of the crazing and size of the cracks will indicate the level of stresses at the external surface of the part [35].

The chemical probe technique is based on establishing reference ESC data for the relationship between stress and time to fracture of a polymer in a specific chemical environment. When a plastic with unknown residual stress is exposed to the same environment, the time required for cracks or crazes to develop can be used to predict the magnitude of the unknown residual stresses in the plastic [16].

The normative reference ASTM D1939-84 provides useful background for conducting this test procedure where this standard determines residual stress in extruded or molded acrylonitrile-butadiene-styrene (ABS) parts by immersion in glacial acetic acid. Two sets of moldings were prepared one set under conditions known to produce “well-processed” moldings and the other under

conditions known to produce a “poorly-processed” product. The size and shape of the moldings should be the same for the test [37].

A range of chemical environments were selected and graded according to aggressiveness; care should be taken to ensure that the chemicals do not chemically attack the polymer where analytical reagent grade chemicals should be used in all the tests, the temperature of the testing shall normally be 23 ± 2 °C. Initially a chemical of moderate ESC aggressiveness was selected. A test cell was attached to the surface of one of the moldings and added the test environment to the cell [37].

The surface of the molding under investigation was attached to the test cell and the chemical environment that will cause crazing in a poorly-processed molding was added to the cell. The surface of the material was inspected for crazing and note its condition after 10 minutes. If crazing is observed the procedure should be repeated on identical moldings with less aggressive chemicals until crazing is not observed, If no crazing is observed the procedure should be repeated on identical moldings with more aggressive chemicals until crazing is observed [37].

This procedure was repeated for both sets of moldings to produce a table contains of the phrase (pass) or (fail) with respect to molded part and chemical solution. By using these results, it can be identified a chemical environment that will cause crazing in a poorly-processed moldings but not in well-processed moldings [37].

If no crazing is observed, the quality of the molding may be considered as “well-processed” (i.e. there are no significant surface or near surface tensile residual stresses). If crazing is observed, the molding may be considered as “poorly-processed”. This technique gives a full description of the moldings with respect to (their processing histories, elapsed time and storage conditions after

processing, location on the molding where the test cell was attached, environments tested, test temperature) [37]. Advantages of this manner:

1-The chemical probe technique is suitable for use in quality control applications (through the service) [16].

2-The chemical probe technique was shown to be effective in determining surface and near-surface residual tensile stresses in simple injection molded components [37].

3-the chemical probe method can still be used to identify regions of potential susceptibility to ESC, whether due to residual stress, microstructural sensitivity or a combination of both them [37].

Disadvantages of this manner are

1- This technique has implicit constraint to materials which are micro structurally homogeneous. Hence, there is potential uncertainty in its applicability to welded material and also to complex moldings [37].

2- The chemical probe technique has potential but uncertainty in the quantification of residual stress can arise if significant environment-enhanced relaxation occurs.

3- No information about stress distribution is obtained [14] and this method is difficult to digitize [36].

4- In injection-molded products, residual stresses can be of a magnitude sufficient to induce dimensional and shape changes and, in the presence of specific environments, can result in environment stress cracking (ESC) of the product [14].

In the case of POM, the hydrochloric acid is used to estimate residual stress, test method instructions are: the concentration of the hydrochloric acid aqueous solution must be defined according to the detected stress, the

temperature of the solution was maintained at 20C. If a molded part is contaminated by foreign materials like oil, it must be cleaned by methanol and then rinsed with water. The POM part was soaked slowly in the hydrochloric acid aqueous solution and leaved for 60 minutes (cracks generally occur within 50 minutes), finally the part was removed and rinsed with water and the cracks were checked [8].

2- ASTM D7474-17 METHOD

The method of ASTM D7474-17 is based on exposing the finished plastic parts to a series of chemical reagents which cause cracking and/or crazing of plastics. Cracking and crazing are analyzed visually without the help of optical devices (excluding glasses) from the surface of the sample.

Color changes in the part surface are not considered as crazing or cracking. In the case of controlled study and due to practicality and comparability of the results it is recommended to perform the conditioning of 24 hours before testing. The conditioning is not compulsory where samples were collected and conditioned in room temperature for minimum of 4 hours.

The samples are rinsed with isopropyl alcohol and dried in air. Dry and clean samples are soaked in to the solvent mixture which indicates the highest level of residual stresses for one minute and then rinsed with water. The sample is dried and visually inspected. If cracking or crazing is detected, the test is not continued, but the level of residual stresses is stated to be higher than the limit value. If no crazing is detected in the sample, it is soaked to the next solvent mixture for one minute, rinsed with water and examined for crazing.

This procedure is continued until cracking or crazing is detected, and the level of residual stresses is determined. The one minute time is measured with a stopwatch from when the sample is totally recessed into the solvent to the moment when the sample is removed from the solvent. The sample is rinsed

with clean water immediately after it is taken out from the solvent. This procedure is repeated for all the tested samples [24, 36].

3-Solvay Method for Poly Sulfonic Polymers

A Solvay method has been developed for measuring the residual stress level in parts molded from PSU (Poly sulfone) and PPSU (poly phenyl sulfone) resins. It involves the exposure of finished parts to chemical reagents which are known to produce cracking or crazing of the material at specific stress levels. The exposure of parts to these reagents under no load conditions allows the quantification of the residual stress levels.

Residual stress levels depend on numerous molding parameters. For this reason, individual samples may exhibit variations in stress levels. Therefore, testing multiple parts is recommended. The determining of stress levels through the use of reagent exposure is approximate in nature where small differences in the test conditions (ambient temperature, exposure time, or reagent concentration, etc) may cause slight variations in the test results that should be within 20 % of the actual stress level.

PSU parts and components are amorphous thermoplastics considered to have good chemical resistance, if residual stress levels are below 800 psi (5 MPa) they may typically be considered well molded.

The polymeric part at room temperature is rinsed with isopropyl alcohol, the part is exposed to reagent for one minute, then rinse with water and drying the part by blowing low-pressure compressed air on it. The exposure time required for these reagents to produce cracking at the noted stress level is one minute. This exposure time was employed to facilitate rapid testing and to limit the possibility of errors due to over or under exposure. Exposure for longer time periods produces cracking at stress levels lower than those specified. The part is inspected for cracked or crazed regions under strong light while hairline fractures may be difficult to see.

If the part has no cracks or crazes, the residual stress level is lower than the stress level for that reagent. Proceed to the next reagent and repeat the previous steps. The stress level in the part lies between the stress level shown for the reagent which induces cracking and the one directly above it. To maintain accurate stress readings, the reagents must be fresh, the reagents may absorb water, evaporate, or become contaminated, which can lead to erroneous stress indications. Although reagents can be calibrated by using samples with known stress levels, It may be more practical to replace reagents with fresh solvent from the sealed container periodically [34, 38].

4- MEK Test

There are another chemical techniques can be developed by some companies or factories for the quality control on the daily products due to the importance of their production such as MEK-test for PPSU products. MEK (methyl ethyl ketone) test is a simplified test has been utilized daily at the target company's production unit in everyday testing assurance to verify the affectivity of the batch annealing as a quality control method in everyday testing in the production quality assurance. The difference in this method is that only pure MEK-solvent is utilized.

The level of residual stresses is determined via the time of the exposure to the chemical (30s / 1min / 2min / 3min). Pure methyl ethyl ketone does not change its composition as time passes even though it vaporizes, the solution may lose its efficiency if it absorbs water from air. For this reason the methyl ethyl ketone is renewed weekly for production quality assurance testing. This method is developed according to ASTM D7474-17 and information received from Solvay (PSU & PPSU manufacturer) where long time experience is justified to utilize of MEK-testing.

This test also showed that 100% MEK does not give reliable result with testing time less than 1 minute. The residual stress level of as molded samples is between (8-10) MPa [24].

In order to select a suitable product utilized in the testing, the residual stress level of the selected moldings was verified. Samples were collected randomly from normal production. The approximate residual stress level of the as molded samples is performed with following procedure:

The molded samples are rinsed with isopropyl alcohol and dried by air, then they are soaked into acetone for 3 minutes, rinsed with water, dried and visually checked for cracks (10 MPa level). The undamaged samples are soaked into MEK for 1 minute and visually checked (8 MPa level). Color changes are not considered as cracking/crazing). The result is stated OK if no cracks can be detected on the surface of the fitting in visual inspection. Flash light is utilized to improve the visibility of the possible cracks. In unclear cases the possible cracking is verified in microscope examination or with endoscope [24].

5- Solvent Stress Test

This method is economical focused on measuring the residual stress at the surface of the part for molded specimens. This test takes the molded specimens and submerges them into different concentrations of solvent mixtures that are known to cause surface cracking at different stress levels, The exact solvent and concentrations levels are specific to each polymer and can be extended to polymer blends. The development of these tests require extensive knowledge of the material at known stress states. However, this test allows for more complex shapes to be tested and can provide an indication of stresses developed at thickness transitions, ribs and bosses as in (Figure 4-1). It can also be an effective method at quantifying stresses where processing may influence the localized stress in these areas [30]. Disadvantages of this process are:

1- This test has not been developed for every resin or polymer family, and most of the tests are used only for amorphous resins because the amorphous resins are more likely to exhibit sensitivity to solvents, as compared to semi-crystalline resins and it is easier to notice the crazing on transparent resins from a practical standpoint. Therefore, the ability to distinguish crazing at the different solvent concentrations is enhanced.

2-This method can only provide indications of the stress state at the surface of the part. It cannot directly measure the stress in the core of thick areas that may not be adequately packed out, and may be subjected to high tensile stresses [30].

5- Immersion Test:

A- Acetic Acid Immersion Test

This test is applicable for distinguishing between specimens that are highly stressed and specimens that are not provided with same conditions. Standard test method is according to ASTM D1939 (Determining residual stresses in extruded or molded Acrylonitrile- Butadiene-Styrene (ABS) parts by immersion in Glacial Acetic Acid).

Specimen are either complete molds or cut pieces of the molding of sufficient size without influencing the observed stress. Specimen is kept in an oven for 24 hour at 50 ± 30 °C, cooled in desiccators and immediately weighed to the nearest 0.001g. The equipment is sensitive balance up to 0.001g precision and micrometer flat ended up to 0.025 mm precision, the chemical agent is Glacial Acetic Acid of 99.7% assay. The important influencing factors are: (thickness of the specimen, test conditions (temperature and time), concentration of chemical solution) [39].

The acetic acid is placed in a container to ensure complete immersion of the specimen, the test specimen is placed into the acetic acid for 30 s; at the end of time, the specimen is removed and rinsed at once in running water, wiped

dry, and then carefully observed the cracking. If there is no crack another specimen is tested at interval of 90s, 2min with the same way. The results can be expressed in terms of no cracking, slight cracking, moderate cracking and extensive cracking [39].

B- Acetone Immersion Test (Chemical Attack)

This test method is applicable only for distinguishing between inadequately fused and adequately fused PVC. The adequacy of fusion of extruded poly (vinyl chloride) PVC pipe and molded fittings by acetone immersion can be verified according to ASTM D2152. Specimen shall be of a size that is convenient with immersion in the test container but not less than 13 mm in height.

Specimen shall be kept in an oven for 24 h at $50 \pm 30^{\circ}\text{C}$, cooled in desiccators and immediately weigh to the nearest 0.001. The equipment is sensitive balance up to 0.001 g precision and micrometer flat ended up to 0.025 mm precision. Solution is Acetone of maximum density of 0.7857 g /ml at 25°C . Important influencing factors are: (thickness of the specimen, test conditions (temperature and time), concentration of chemical solution) [40].

A sufficient amount of acetone is placed into sealed container without agitation to ensure complete immersion of the specimen is allowed to stay immersed for 20 min. After 20 min, The specimen is removed from the container and subjected for sign of attack. The swelling surface of test specimen is not considered an attack. The results of attack can be expressed in terms of lifting, raising or removing of any material outside surface or inside surface or mid wall of the specimen [40].

2.5 Indentation method

The indentation method is proposed as a simple technique for measuring the residual stresses [41]. The indentation method is applied for determining the

mechanical features, including elastic modulus, hardness, Poisson ratio, as well as the residual stresses [42, 43] and the hardness of metals and polymers [8]. It can also be determined to the relative contact area as a feature of evaluating residual stress [44].

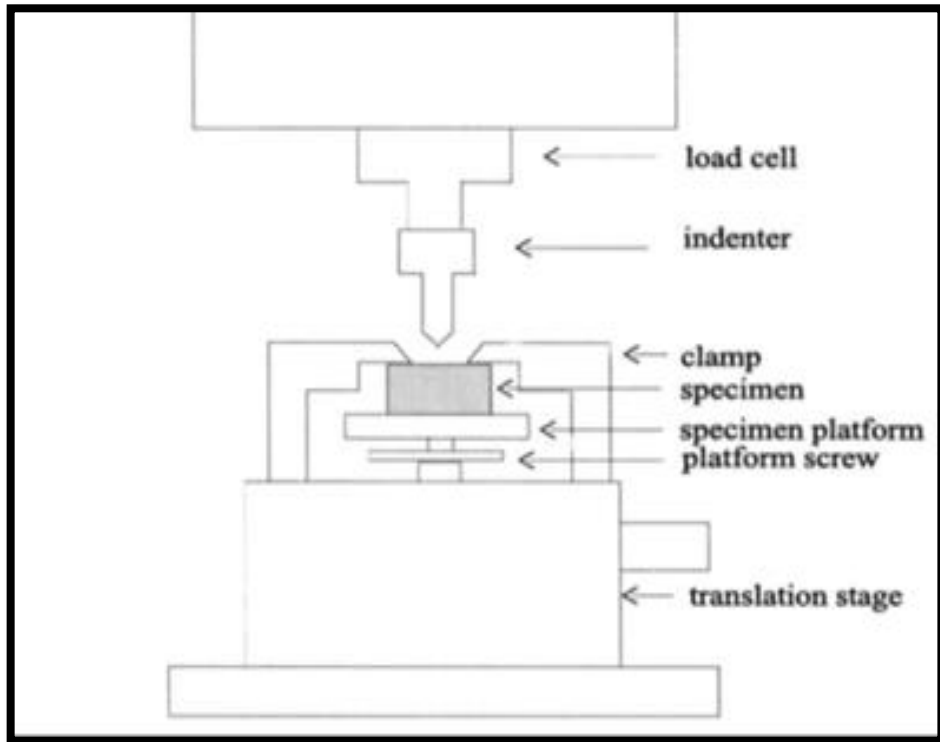
Indentation can be applied to obtain the localized averaged properties of flat specimens, being a simple and fast technique for measuring the mechanical properties and surface stresses of various materials [45]. Since there are differences in the properties of global indentation based on the existence of residual stress, this may help guide the direction and size of these stress [46].

The experimental setup of indentation technique is simple as compared with the uniaxial tensile test [45]. The indentation instrument needs to be fixed, and the pretreatment of surface is necessary [8]. The experimental setup of indentation technique is simple as compared with the uniaxial tensile test. On the other hand, the main disadvantage of the indentation technique is the complicated mechanical problem which arise from the non-homogeneous and/or inelastic deformation in the materials under indentation. Figure (2-24) illustrates the indentation device [45].

There are several physical features that characterize the indentation method:

- The indentation test has high resolution for three dimensional properties and exists in many size scales.
- In case the material properties are provided, the indentation can simplify quenching and thermal stresses in some cases [45].
- The indentation method can assess the properties of material with the conservation of structural integrity.
- It can be applied in studying the mechanical characteristics of materials like hardness and elastic modulus, over a wide range of size scales [47].

- The indentation techniques depend on semi-empirical formulae [47].
- The indentation test must be carried out within all the studying area avoiding the regions of porosity or micro cracks to probe the residual stresses [45].



Figure(2-24): Sketch of the indentation device [45]

The measurement of residual stresses via the indentation method is originally adopted from the traditional Rockwell and Vickers hardness tests. The residual stresses affect the indentation experiments and could be applied in measuring the local elastic and plastic material properties [45]. The load variation with distance can agree with the examining of local properties (on the size of micro-indentation) or the averaged properties (on the size of macro-indentation) [45].

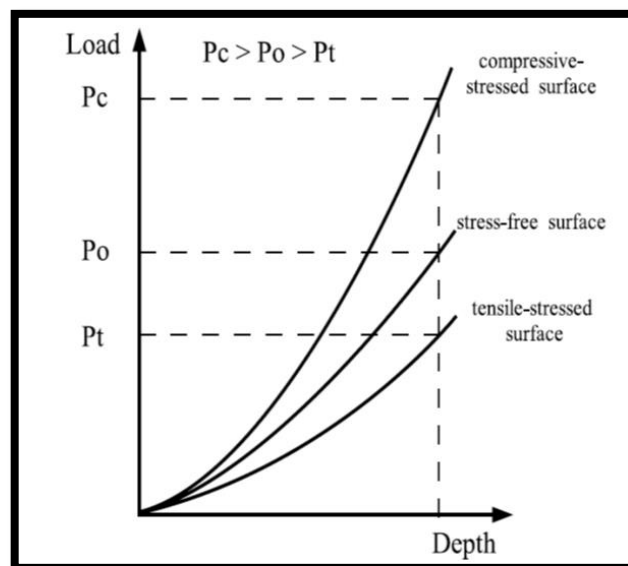
According to the correlations that exist between residual stress and the size of contact area under sharp cone indentation of elastic–perfectly plastic materials. In case of elastic and plastic deformations having equal magnitude,

the hardness is invariant of residual stresses under the dominance of plastic deformations around the contact region for most metals and alloys [48, 49].

The indentation test is advantageous for determining the residual stresses. It is beneficial in measuring residual stresses according to depth-sensing indentation. Figure(2-25) shows the load-depth curves according to the presence of residual stress and the types of stress [50]. Curves of (P-h) are plotted based on Kick's law which is applied on the loading part of the curve:

$$P = Ch^2 \quad \text{Eq.(2-9)}$$

C is a constant which relies on (the elastic-plastic properties of material, residual stresses and the indenter geometry) [45].



Figure(2-25):The relation among residual stresses and load-depth curve [50]

The load and depth of penetration were continuously registered during both loading and unloading through each test of indentation. The indentations are made at a distance of (5 to 7) times around the indentation contact radius, and it is inspected with an optical microscope [45]. Figure (2-26) presents the load-depth curves of indentation for the surfaces that have residual stresses and those who do not. To compute the residual stress, the indentation with energy method could be applied based on the loading and unloading curves of the

surface under stress, as well as the loading curve of the surface free of stress [50].

The initial elastic part of the unloading curve has a slope proportional to the material modulus of elasticity. In addition to the computation of material elastic properties, the residual plastic strain, yield stress, and the exponent of strain hardening can be calculated through the utilization of load-depth curves with indentation regions that are measured empirically [45].

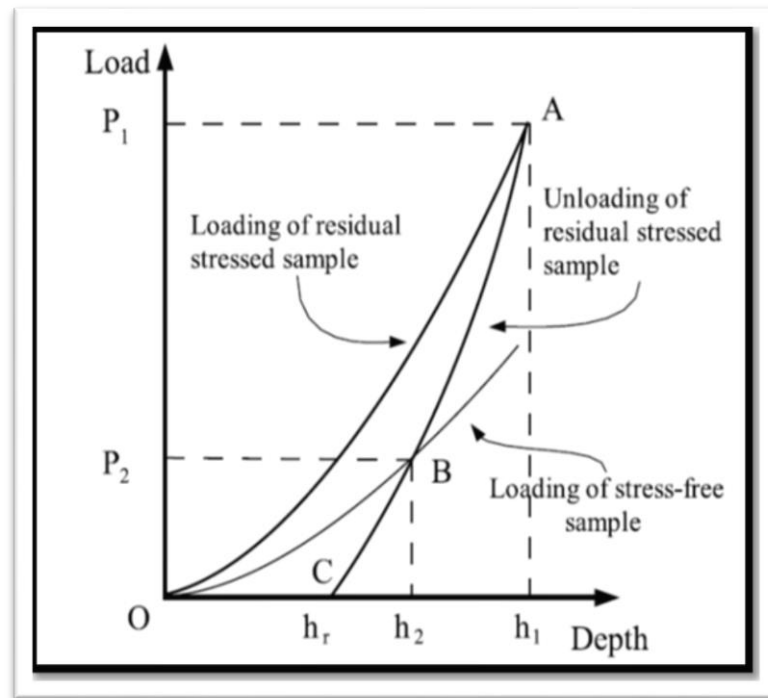
There are various forms of load-depth indentation curves with respect to the presence of residual stress: If the applied peak load is the same, the curves of indentation are shifted to higher peaks and lower depths that corresponded to tensile and compressive, applied or residual stresses, respectively.

If the depth of indentation is fixed, the indentation (load–depth) curves are shifted upwards and downwards with respect to compressive and tensile, applied or residual stresses, respectively [51]. The type of residual stress (either tension or compression) can be specified by the comparison between the load-depth curves of residual stressed material and stress free material, whereas the residual stresses magnitude of equi-biaxial type can be quantified for any material.

In case of compressive residual stresses, the indenter penetration into the material depth will be more difficult, causing the indentation compliance to decrease. As for tensile residual stress, the performance of indentation will be easier, causing the effective indentation compliance to increase consequently [45].

The determination of local material properties can be carried out on different size scales by utilizing various loads and sizes of indenter in order to obtain different contact radii and depths of indentation. The size of scales has ranged from nano to micro to macro levels. The examination of several (P-h)

indentation curves at a constant load has produced cracking into the penetration depth [45].



Figure(2-26):The loading-unloading indentation curves and the presence of residual stresses [50]

There are a number of configurations of the indenters, as follows:

1. Sharp or pointed indenters, including conical and Vickers indenters
2. Spherical indenters such as the ball indenter.

The sharp indentation tests can initiate and control fracture in brittle materials [42]. The sharp indentation could be applied for determining the residual stresses state in elastic-plastic materials if its state is uniform over material depth, as the plastic deformations tend to dominate the behavior of most metals and alloys [45, 51].

A shortcoming of applying the sharp indentation in extracting the residual stresses is its small effect on load-depth sensing indentation [52]. On the other hand, both the spherical and sharp indenters could be applied for measuring the

elastic characteristics of materials [45]. Figures (2-27, 2-28) show the geometry and size of cone and spherical indenters, respectively.

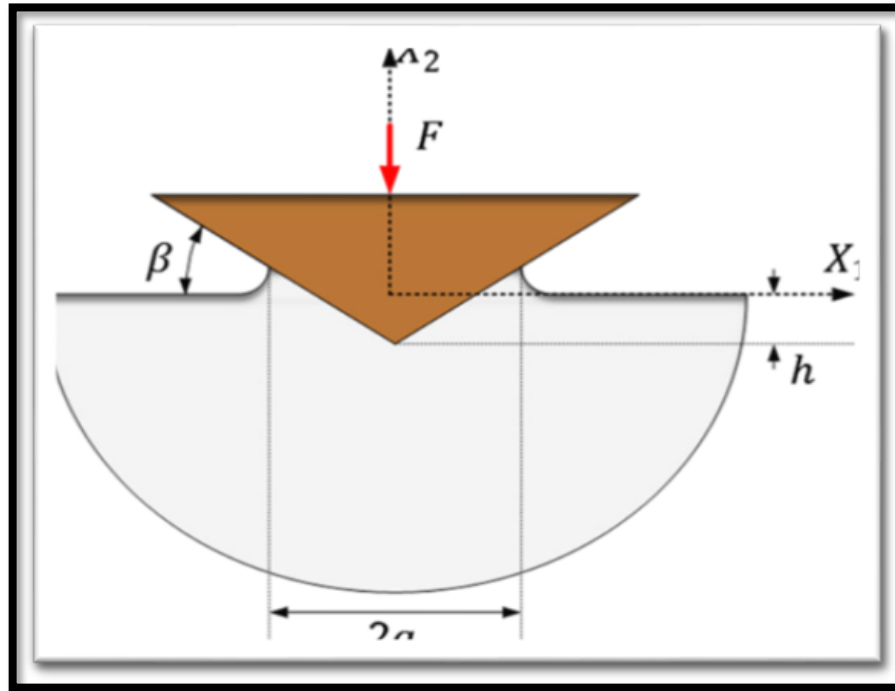


Figure (2-27):The geometry of cone indentation: (a) is the true contact radius and (h) is the depth of indentation [51]

For sharp indenter, the angle β represents the inclination of the indenter with the surface, and this angle is equal to:

$(\beta) = 22^\circ$ for four-sided pyramidal Vickers indenters and 19.7° for equivalent conical indenters [51, 53].

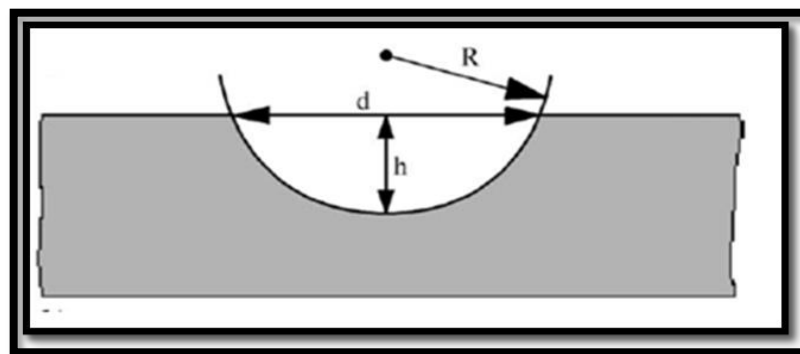


Figure (2-28): The geometry and size of spherical indenters [54]

For spherical indenter:

(d) is the diameter of the contact area

(R) represents the radius of the tip

(h) represents the depth of penetration, and they are connected by the following non-linear relation [55]:

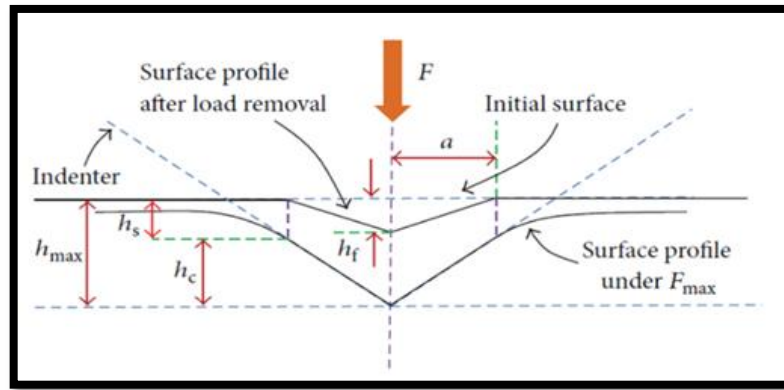
$$d = 2 \times \sqrt{h(2R - h)} \quad (2-10)$$

It can be noticed from the variety of indentation techniques that the force of indentation increases with the increase in the radius of tip, according to the increased contact area at the same depth of indentation. For example, the spherical indentation has greater tip radius (R) as compared (2a) to the sharp indenter [56].

The impression of sharp conical indenter is illustrated in Figure (2-28) where: (hc) is the depth of contact that is related to the deforming behavior of material (hs) is the elastic displacement, also referred to as sink-in of the surface at the contact perimeter (hmax) is the depth of indentation at maximum applied force (F_{max}) before the unloading part, the relationship due to Figure(2-29) is [57, 58]:

$$h_c = h_{max} - h_s \quad \text{Eq.(2-11)}$$

According to the application of sharp cone indentation on many ceramics and polymers, the elastic and plastic deformations are found to have comparable magnitudes, in addition to the fact that the invariance of hardness is lost [49, 45].



Figure(2-29): The maximum indentation of sharp conical indenter [58]

The models of indentation method are:

The residual stresses have an influence on the indentation hardness, loading and unloading curves, material pile-ups, and contact areas which led to the derivation of different models that have focused on applying various parameters and indenters to determine the residual stresses. Each indentation model has its own assumptions, limitations, materials and results [53, 59]. The developed indentation models that correlate with residual stresses are briefly discussed below.

A- Energy Method Model

This model depends on what residual stresses perform through the indentation technique. The reversal analysis is performed on material with known state of stress, so the error rate between the method output and well-known magnitude is below 9%. The results of this technique is put into comparison with XRD measurements, and the results turned out to be consistent [60, 61].

B- Sharp Indentation model

The sharp indentation test with sharp indenters as in Figure (2-27) is applied for determining the average residual stresses from the equi-biaxial state which exist proximally at the surface of elastic-plastic material over a depth of

(5-7) times the indentation depth used to discover and compute material properties and stress state. The used sharp indentation has carried out the microscopic determinations [45]. It must be noted that the sharp indentation and spherical indentation models have no easy application with thin film/layer structures [62].

Xu model is sharp indentation model that depends upon the correlation between the coefficient of elastic restitution and residual stresses [63]. This model requires precise measurement for the coefficient of elastic restitution. When the roughness of sample surface is great, the error in the coefficient of elastic restitution is also great, leading to a consequent decrease in the precision of measuring residual stresses [60, 61].

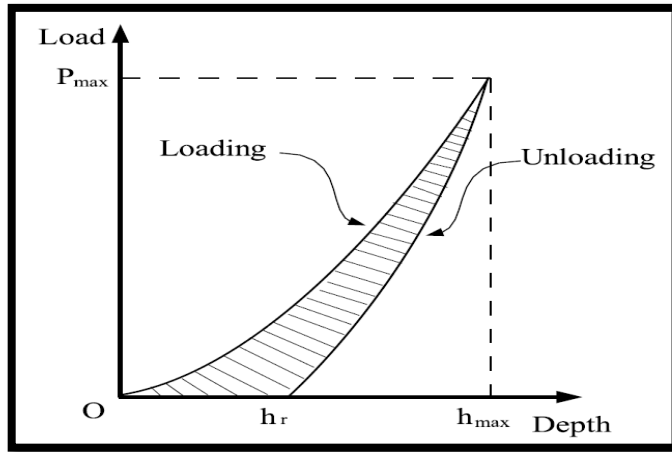
Figure (2-29) shows the depth of indentation at maximal applied load (loading curve) (h_{max}), with the depth of indentation at the state of total removed load (residual) or (unloading curve) (h_r). The ratio (h_r/h_{max}) could be an appropriate quantity for determining because it is more sensitive to the existence of residual stress. This ratio (h_r/h_{max}) is smaller for in-plane tensile residual stresses than for compressive stresses [64].

C- Spherical Indentation Model

The spherical indentation test is carried out by spherical indenters, as illustrated in Figure (2-28). For ceramics and composite coating materials, the determinations of 3D property could be performed by spherical indentation [45]. The following Swadener model is one of the spherical indentation models.

The Swadener Model is considered a spherical indenter because it tends to be of more sensitivity towards the impact of stress, like changes in area. The model is based on the assumption of biaxial stress and could demand a large indenter radius (R) for achieving results of higher accuracy [53, 59]. The Swadener model has applied the contact pressure as a replacement of contact area as an indication of stress [50]. For example, it is applied to determine the

residual stresses of Al alloy by the usage of Hertz contact theory as well as the correlations among hardness and yield strength. The precision of this model was between (10-20) % of the yield strength [65].



**Figure(2-30):The loading curve of elastic-plastic material
and elastic unloading**

2. 6 Ultrasonic Technique

In the past few years, there is a progress in improving the traditional techniques and developing novel methods for measuring residual stresses [66]. The nondestructive measurement is essential in optimizing the design of structures and improving their mechanical strengths [67, 68]. The development of ultrasonic method has happened before a half century and encouraged many researchers to study the acoustoelastic theory that applied basically to discover the stress of mechanical components where the velocity of wave has a close relation with stress [69]. In other words, the acoustoelasticity effect denotes to the differences in feature of propagating the acoustic waves in solids according to the residual or applied stresses [70].

The application of vibrating sound waves at frequencies more than 20 KHz beyond the human hearing is called ultrasonic waves that used in the fields of defense, medicine and industries [68]. The ultrasonic instrument is quick, appropriate to the operations of routine examination and able to measure internal

residual stresses for whole material [3]. The ultrasonic tool is portable, cheap and safe to operators [20]. The ultrasonic technique is a good candidate to measure thickness, give information on physical properties through the processing of polymer or composite materials [71], the piezoelectric transducers in ultrasonic techniques have used to discover internal flaws in engineering parts [67], measure structural dimensions [72] as well as detect and identify damage in complex structures [73].

This method has applied successfully for determining residual stresses in nuclear reactors, shipbuilding, oil and gas engineering, highway and rail way bridges, construction industry, aerospace industry as well as in repairing of welded structures and service inspection through manufacturing [66]. The properties of ultrasonic waves have affected with various parameters including texture of material, crystal structure, environmental temperature, water content, size of particles and coupling conditions [74]. The most important advantage of the ultrasonic equipment is the possibility to measure applied and residual stresses for both real structures and samples [1] as well as in surface/subsurface layers of a material [66], this technique have gained a great interest due to the accuracy and ease of application [75].

Ultrasonic waves could be described as mechanical waves which propagate at a frequency over than 20 KHz. This means that such waves tend to begin at the highest audible limit for human beings. In general, ultrasonic waves are generated and sensed using piezoelectric elements (transducers). The transducer converts the electrical energy into acoustical energy and vice-versa, thereby functioning as both transmitter and receiver. Various test conditions and materials demand different types of transducers. Higher frequency transducers (i.e. from 15 MHz to 25 MHz) have limited depth of penetration and high sensitivity to material discontinuities. On the contrary, lower frequency transducers (i.e. from 0.5 MHz to 2.25MHz) have a larger energy and penetration depth but less sensitive to material discontinuities [76].

Advantages of the ultrasonic technique are: the ultrasonic technique has considered as a promising non-destructive technique for residual stress evaluation [73]. The measurements are laboratory or on site, it is suitable for measuring applied and residual stresses [67], the implementation of test is quick [10], safe [74] easy to apply [77] and flexible [73]. The ultrasonic technique measures macro stresses over material bulk volume, suitable for routine inspection and industrial study of big components such as discs of steam turbine [78].

The ultrasonic device is suitable for quick installing and easy carrying, the depth of measurement and penetration are larger as compared to X-ray diffraction method [74, 79], the ultrasonic instrument is convenient to use and free of radiation hazards [2]. The ultrasonic device is not hurtful to operators [2], provides a gradient in stress [2, 74]. The ultrasonic stress measurement technique is portable provides through-thickness stress measurements for various materials [67].

Disadvantages of the ultrasonic technique are the ultrasonic test gives average measurements of stress over a bulk volume, the measurements through-thickness have required parallel surfaces and good surface finish of the component, it is not appropriate to the components of complex shape [67]. The ultrasonic test is very sensitive to the effects of microstructure (size of grain, amount of carbon, texture and structure) and to the service conditions as temperature [77]. The calibration of stress measurement necessitates a reference sample that is free of stress to give absolute measurements of stress [67]. In ultrasonic test, the velocities of waves have depended on microstructural inhomogeneity [1].

2.7 The Principle of Acoustoelasticity

The ultrasonic technique exploits the acoustoelastic property of materials by measuring the velocity of ultrasonic waves travelling through a component

[80]. Ultrasonic waves are sensitive to stress [67], the ultrasonic technique for stress measurement has depended on the linear relationship between speed of propagating ultrasonic wave through the sample and mechanical stress of material that is called principle of acoustoelasticity [81].

Acoustoelasticity is the subject of research for half a century [68]. In another words, the acoustic elasticity has described the influence of material residual stresses on the wave velocity [69]. In the field of residual stresses, the acoustic elastic effect has expressed of stress variation with flight time of the ultrasonic wave propagating into a fixed acoustic path through the elastic region [74, 81]. The sensitivity of acoustoelastic effect against stress increased when both directions of ultrasonic wave propagation and particle motion are parallel to the measured direction of stress in order to obtain absolute stress, so if all three directions coincide then the acoustoelastic effect is most strong [67].

Acoustoelasticity is the hypothesis of a linear relation between the speed of acoustic wave and the material elastic strain, it represents the basic of all ultrasonic techniques of measuring stress [75]. In some alloys, this linear relation between acoustic velocity and strain continues beyond the point of material yielding [75].

2.8 Ultrasonic Technique and Residual Stresses

The stress analysis by ultrasonic is used to find the levels of stress where the determination of stress is relied on the ultrasonic wave velocity [74], this dependence is a valuable tool in determining the material stress by determining the variation in velocity [82]. On the other hand, the velocity of ultrasonic wave has also affected by the microstructure and defects in material [74]. Ultrasonic evaluation for residual stress measurement has been an effective method owing to its easy implementation, low cost and intrinsically being nondestructive. The velocity variations of acoustic waves in materials can be related to the stress state in the deformed medium by the acoustoelastic effects [83].

The ultrasonic technology for measuring residual stresses has applied more widely in the residual stress inspection of members with regular shapes such as pipes, hubs, rails and gears due to its reliability, accuracy, and convenience, there is a severe requirement on the transducer angles of incidence and reception [84]. The ultrasonic test utilized the ultrasonic waves that contain very little energy and propagate within the stressed material [75]. As for the majority of materials, the relative differences in wave velocity are linear functions of strain and stress. (V) is the wave propagation velocity, the acoustoelastic constant or stress constant (K) is a parameter of material and its determination leads to directly assessment of material residual stresses [19, 2] as shown in Eq. (2-12):

$$\frac{\Delta V}{V^0} = K\Delta\sigma \quad \text{Eq. (2 - 12)}$$

where :

(V^0) is the ultrasonic wave velocity in a stressed free medium, σ is the applied or residual stress [19], the constant (K) describes the relative variation of velocity or travel time with stress [71]. The acoustoelastic constant have relied on: type of material, direction of wave propagation and polarization direction [7]. The measured stress is average stress acting between emitter and receiver [67], the stress (σ) could be applied or residual [19]

Ultrasonic test could be done for longitudinal and transverse (shear) waves. The longitudinal waves are known for having their displacement oscillations alongside the direction of propagations. As for transverse or shear waves, the displacement oscillations seems to occur at a right (transverse) angle to the wave propagating direction. Both types of waves are supported in solids, whereas only longitudinal waves are supported in fluids. The transmission of shear values is rather difficult in fluids [76].

Longitudinal (compressive) waves are often adopted in practical aspects. They are propagating in solid, liquid and gas medium, The longitudinally propagating wave is the most sensitive to stress variation [19]. It must be noted that longitudinal residual stress occurred in the direction of wave propagation [85] as shown in Figure (2-31).

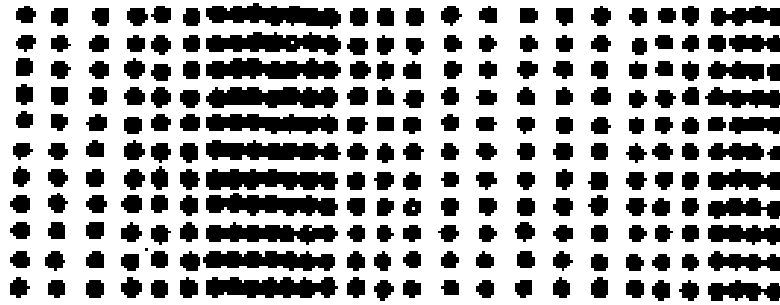


Figure (2-31): Propagation of longitudinal wave in a medium [86]

The ultrasonic measurement of stress provides an average condition over the path of waves propagation. The longitudinal wave has propagated in the direction of thickness employed to identify the average residual stress on the whole thickness of the sample [7]. The longitudinal residual stress that occurred in the direction of wave propagation could be determined as[85]:

$$\frac{V_L}{V_{L_0}} - 1 = K \cdot \sigma_{res} \quad \text{Eq. (2 - 13)}$$

It must be noted that longitudinal residual stress occurred in the direction of wave propagation [85], the longitudinally propagating wave is the most sensitive to stress variation [19].

2.9 Pulse-Echo Method

Echo method is applied for revealing defects in members made from various materials. The dual transmitter-receiver transducer has recorded the impulse after its reflection due to heterogeneous structure of material or limiting

surface. According to the defect in material, portion of ultrasonic wave is reflected and received by dual transducer.

There is a portion of ultrasonic wave passes through the defect and reaches to opposite wall of inspected material, this portion is reflected and returned to the dual transmitter-receiver with some delay as the bottom echo. The traveling time of the impulse, as well as the velocity of the ultrasonic waves are used for evaluating the depth of defect or reflected surface [86]. In order to obtain an efficient echo test, the grain size of tested material must be smaller than inspected defects. If this condition does not satisfied, the formed echoes by grain boundaries are overlapped any echo of defect.

The principle of defect inspection by echo test is applied by spreading of ultrasonic wave with short pulse; the evaluated time of travelling ultrasonic waves to the boundaries which separating materials of various elastic properties and densities. The knowledge of wave velocity lead to detect the distance to the reflected interface.

There are various fields for applying the echo test such as: detecting of small cracks, discontinuities in material structure, delamination between layers, measuring the thickness of slab, monitoring the curing in polymer adhesives. The important limitations of echo test are included: the need to use coupling agent (couplant), the inspected material of heterogeneous nature lead to crowd of echoes, elucidation of results is difficult [86].

Another name of pulse-echo test is contact ultrasonic method where the transducer is put within direct contact to the considered samples in order to transmits the ultrasound pulse inside the sample and detects the reflected signal from interface (edges or flaws) using the transducer itself that depicted in Figure (2-32) [76].

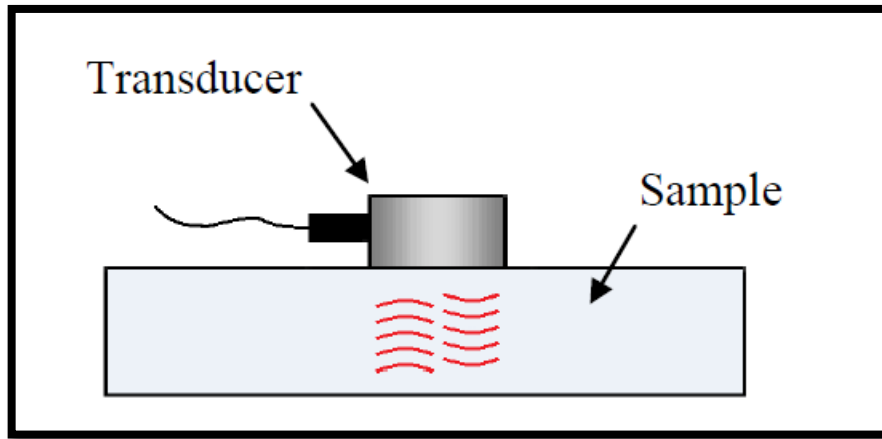


Figure (2-32): The transducer in contact ultrasonic method [76]

The principle of measurement by echo test is represented in Figure (2-33) where the reflected strength of signal is revealed against time for the generated signal and received echo via an oscilloscope. The distance of traveled signal is directly related with signal travel time in order to reveal the information as flaw sizes and location.

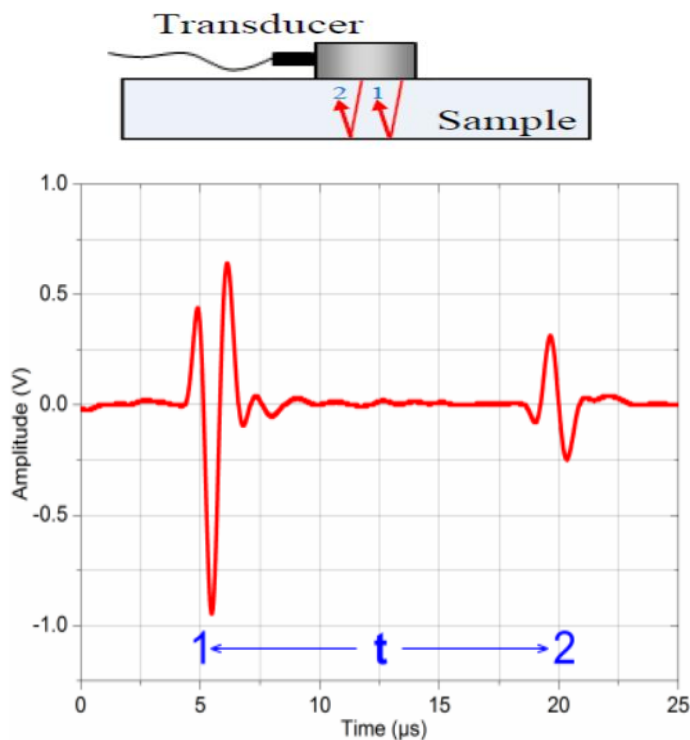


Figure (2-33):The principle of pulse-echo method [11]

If the pulse of ultrasonic signal is transmitted via a sample along thickness (d) and reflected from the opposite wall, the echoes are produced. The echoes have a distance that is double the sample thickness d before it reaching

the transducer, the delay time (t) between two echoes is measured and consequently, the ultrasonic longitudinal velocity (V) can be determined through the following:

$$V = \frac{2d}{t} \quad \text{Eq. (2.14)}$$

where d is thickness of sample, t time of travelling ultrasonic wave [76].

2.10 Polymer Overview

Polymer materials can be defined as macro-molecules that are formed using multiple small components known as monomers. These monomers are joined together to form polymers. According to the morphology, polymers could be classified into amorphous or semi-crystalline polymers. An amorphous polymer has amorphous areas, wherein the molecules have a random organization, whereas the molecules are evenly packed in crystalline polymers. Since all crystalline polymers have amorphous areas to some extent, no polymers could be considered totally crystalline [87].

According to the random packing structures, amorphous polymers do not have sharp melting points, but rather a range of temperatures. They are regarded as glassy polymers when they exist in a glass state at room temperature and their glass transition temperature (T_g) is higher than the room temperature. As for rubbery and semi-crystalline polymers, T_g is lower than room temperature [87].

2.11 Polymers and Ultrasonic Waves

Ultrasonic surface wave testing is one of the most effective methods of detecting surface internal defects and evaluating through thickness stresses. Polymers are commonly adopted in the production of aerospace vehicles, automobiles and ships. They differ from metals in that they have lower stiffness and strength. They have a sensitive to defects and stress concentrations, and being rather weakly resistant to crack extensions [82]. This makes them

vulnerable to hazards resulting from both residual and working stresses. It is therefore important to ensure the proper evaluation of polymer work conditions and service life. The solution to these issues depends mainly on the non-destructive tests (NDT) of the component. The lack of efficient test methods leads to issues of wasted materials and hidden accidental dangers [82].

Polymers are sensitive to surface cracks and stresses, so the ultrasonic measurement of stress in polymers requires very great accuracy [7]. The linear acoustoelastic effect can be applied to assess the residual stresses quantitatively in polymeric products. In this case, the ambient temperature should be observed carefully throughout the measurements and correcting the temperature influences as the ambient temperature changes while testing [82, 7].

A polymer could be either amorphous or semi-crystalline. Amorphous areas in polymers are usually seen at low temperatures, at which the molecules vibrate slightly without significant movement. This is known as the glassy state, at which the polymer tends to be brittle, hard and rigid as glass. Heating this polymer enables its chains to wiggle around, making it soft and flexible like rubber, hence its name rubbery state [88].

The presence of double bands, aromatic groups, and/or larger side groups increased the melting point of the polymer, resulting from the limited flexibility of the polymer chain itself. On the other hand, the chain branches cause the melting point to reduce due to the defects that come along with branching [88]. Polymers are often described as a distinct type of modern materials. In spite of their light mass density, they have mechanical properties made them strong enough for a variety of applications in order to achieve suitable rigidity [89].

However, high Young's modulus is not the only necessary characteristic, polymeric materials should be ductile tolerating considerable bending. Ductile polymers involve different semi-crystalline polymers that have a lower (T_g), such as polyethylene (PE), polypropylene (PP), and amorphous glassy polymers

like polycarbonate (PC) and polyethylene terephthalate (PET). On the other hand, glassy polymers like polystyrene (PS) and poly methyl methacrylate (PMMA) with higher (T_g) seem to be rather brittle under ambient conditions [89].

2.12 Glass Transition Temperature of Polymers

Glass transition temperatures (T_g) can be defined as the point at which the glassy state transits into the rubbery state. It is a characteristic of the amorphous area in polymers, when crystalline areas are characterized by the melting point. Despite the fact that amorphous polymers have no melting point, all polymers have a glass transition temperature (T_g) [88]. This state is explained through Figure (2-34) where the relationship between specific volume and temperature due to cooling after melting is depicted, this relationship is including completely amorphous (A), semi-crystalline (B), and crystalline (C) polymers [90].

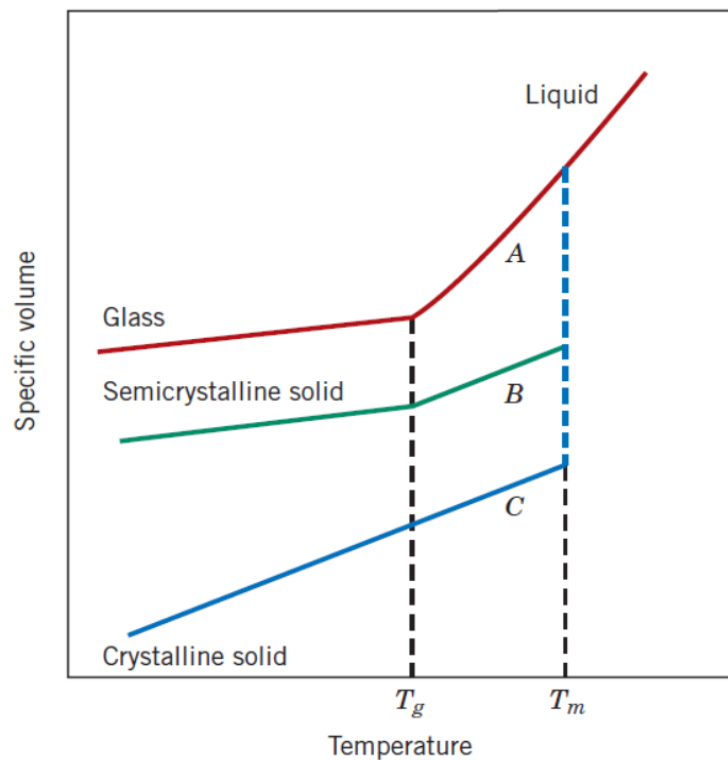


Figure (2-34): Relationship between specific volume and temperature [91]

The molecular chains of polymer in amorphous state are distributed randomly while the crystalline state in highly ordered chains are shown in Figure (2-35). In amorphous state of glassy polymers, the onset of molecular motion take place at the glass transition temperature (T_g), the melting temperature T_m of crystallites is greater than T_g . In a glassy state lower T_g , the low mobility of polymer chains causes stiffness and brittleness in material [92].

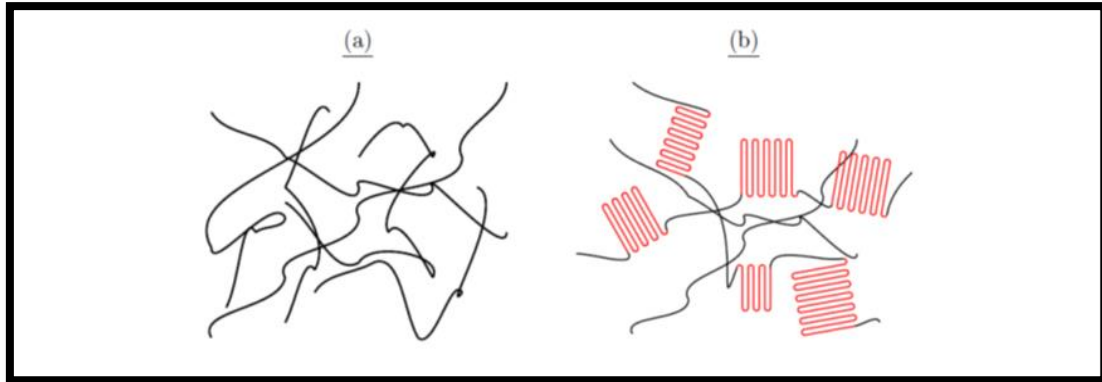


Figure (2-35): The molecular chains of (a) amorphous (b) crystalline polymer [92]

2.13 Glassy Polymers and Amorphous Structure

Glassy polymers are known for their amorphous non-crystalline structures whereby no regular pattern of atoms or molecules is found. Glassy polymers characterizes with high stiffness making them mechanically strong as hollow fiber membranes or porous flat films [90]. The molecular motion is increased with temperature and the physical properties of polymer altered due to undergoing a transition from a glassy state into a rubbery state till melting. Glassy polymers have favorable mechanical and manufacturing properties [92].

The glassy polymers are transformed into rubbery state according to raising of temperature above glass transition, addition of solvent(s) or other additives. The most common amorphous glassy polymers include polystyrene, polyvinyl acetate, polymethyl methacrylate, polysulfone, poly(ether sulfone), polyimide, and polycarbonate [93].

2.14 Applications of Glassy Polymers

The most important class of polymers is glassy polymers where there are various important applications of glassy polymers can be mentioned as following:

- 1- Aerospace composites, contact lens and automotive head/tail lights.
- 2- Thin films in solar cells, optical materials, fuel cells and lithography [94].
- 3- Systems of drug delivery [94].
- 4- Membranes for separating gasses in (gas, oil and petrochemical industries) [95].
- 5- Preservation of an inert atmosphere during transportation of flammable materials [95].
- 6- Electronic coating that requires adhesive strength, fracture toughness, wear resistance, tensile and compressive strength [95, 96].
- 7- Polymer matrix composites (PMCs) [95].
- 8- Corrosion prevention [96].
- 9- Substitute for glass in the electronics, automotive industry, machine guards and safety glass [88, 97].

2.15 Chemical Structure of Polystyrene (PS)

Polystyrene is one of the most broadly used thermoplastic glassy polymer, so it can be used as an important component in various fields ranging from domestic, industrial to automobiles, there is considerable improvement in physical properties of PS due to the combination with other materials [98]. Polystyrene is an atactic amorphous polymer, it is transparent with easy production, sustains thermal properties and have high mechanical strength, it is

brittle to some extent and mechanically stable, softens at 100°C, so it is suitable for sterilization [98].

Polystyrene is widely used for packing purposes. The general additives to PS are flame retardants, antioxidants and UV-stabilizers [98]. Polystyrene is an addition polymer, polymerized by a successive addition to the monomers of styrene. Most important addition polymers are polymerized using olefins and vinyl-based monomers [88, 97]. Polystyrene is aromatic polymer made from styrene monomer, it is one of the most widely used thermoplastics several billions kilograms per year, Figure (2-36) illustrates the chemical structure of PS [99].

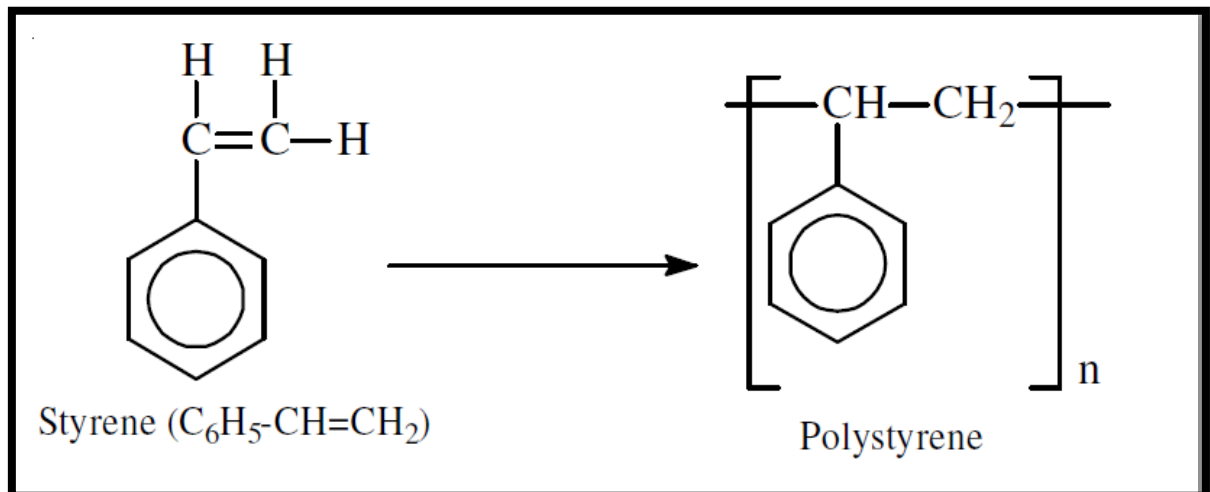
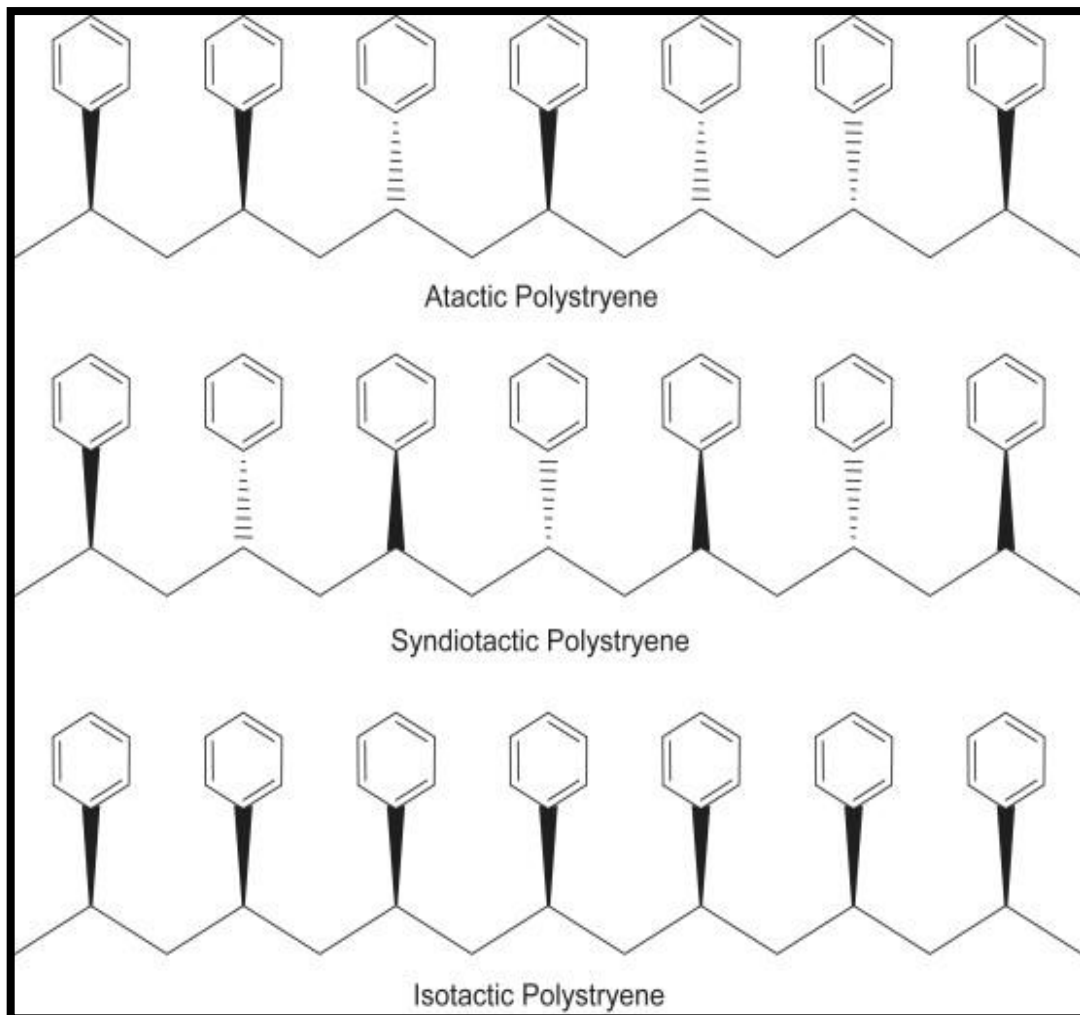
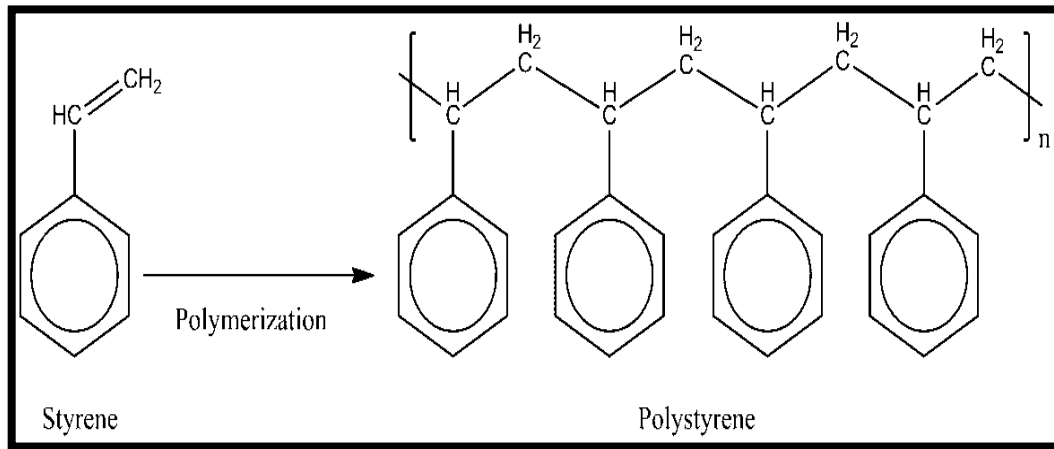


Figure (2-36): The chemical structure of PS [99]

There are three commercial produced grades of general purpose PS depending of the synthetic procedure: easy flow, medium flow and high heat flow. In injection molding, easy and medium flow PS are adopted whereas high heat flow is used in the applications of extrusion [100]. Polystyrene is also involved in polymer matrices when preparing polymer based nano-composites. The production of polystyrene involves the polymerization of styrene-monomer, as demonstrated in Figure (2-37a) [98].

Polystyrenes could be found in three different configurations, these configurations are atactic polystyrene, isotactic polystyrene and syndiotactic

polystyrene (SPS) as shown in Figure (2-37b), where the most commercially available polystyrene is atactic polystyrene [101].



**Figure (2-37):(a) The addition polymerization of PS from styrene- monomer [98]
(b)The various configurations of polystyrene [101]**

2.16 Properties of Polystyrene (PS)

Polystyrene is one of the most broadly used thermoplastic glassy polymer, so it can be used as an significant component in various fields ranging from domestic, industrial to automobiles, the physical properties of PS are significantly improved on combination with other materials, PS has some level of brittleness and mechanical stability [98]. Polystyrene is characterizes with fair density and dimensional stability, its processing methods are versatile, the specific grades of PS are possible on food contact, the density of PS is greater than polyethylene and polypropylene [98].

Polystyrene is amorphous without sharp melting point where the material softens over a wide temperature range. The glass transition temperature of PS is between (74 -105)°C, PS is hard and brittle below T_g, Polystyrene softens at relatively low temperatures and flows like a liquid at 100 °C or under stress, so it is easy to thermoform or extrude. There are sensitive properties to heat such as elongation at break and impact strength. PS is resistant to strong oxidizing acids, bases, alcohols, alkalis, vegetable oils, aliphatic amines, beverages, condiments, numerous foodstuffs, poly glycols and various pharmaceuticals, but PS is insoluble in aliphatic hydrocarbons.

The physical properties of PS are significantly improved on combination with other materials. Polystyrene is soluble in esters, aromatic and aliphatic hydrocarbons, aldehydes, aromatic amines, ethers, polyglycol ethers, ketones, chlorinated hydrocarbons insecticides, essential oils. Polystyrene has good resistance to hydrolysis. Polystyrenes displays good behavior under high-energy radiation, fire resistance is weak where PS burns easily and generates flames even after removing the source of ignition. PS is good insulator in a wet environment with high dielectric resistivity, fair rigidity with low loss factor [98].

2.17 Types of Polystyrene

A. General Purpose Polystyrene (GPPS)

GPPS is homopolymer and sometimes called crystal PS, General purpose PS is atactic and cannot crystallize, it is quite brittle material, its chemical resistance is poor, the barrier properties toward oxygen and water vapor are also poor, its impact resistance is weak, the scratch resistance is low, GPPS has low flexibility, it is used in high-performance and engineering products due to electrostatic build-up.

The GPPS is aromatic amorphous glassy polymer, it softens around 75 °C, its formation is easy, liquid at around 100 °C. GPPS has good luster, process ability, stiffness and hardness. Various grades of GPPS are designed for optical requests where the range of light transmission is (80% up to 98%) [102].

The mentioned disadvantages of polystyrene is overcome by adapting it into its copolymers and blends that represented one of the most versatile polymer materials [98]. The wide family of styrene polymers involved number of modified polystyrene variants as:-

A- High impact polystyrene (HIPS)

The development of high-impact polystyrene (HIPS) is carried out by rubber toughening of PS which expresses of improvement in impact resistance and barrier properties with reduction in transparency. The presence of rubber in HIPS is led to easy of thermoforming, good flexibility and low softening point [98].

B- Expanded PS (EPS)

EPS foam is produced in the form of large blocks, eco-friendly and cannot be recycled, it is found in various sizes, shapes and densities, effectively cost. The amount of consumed EPS is 15–30% of total consumed PS. Expanded

Polystyrene Aggregate Concrete (EPAC) is a lightweight eco-friendly material produced by replacing partially coarse aggregate with equal volume from chemically coated PS beads, it is used in both structural and non-structural applications according to its very attracting properties such as lightweight, thermal properties, capacity, durability, the feature of (EPAC) is expressed by Figure (2-38) [103, 104].

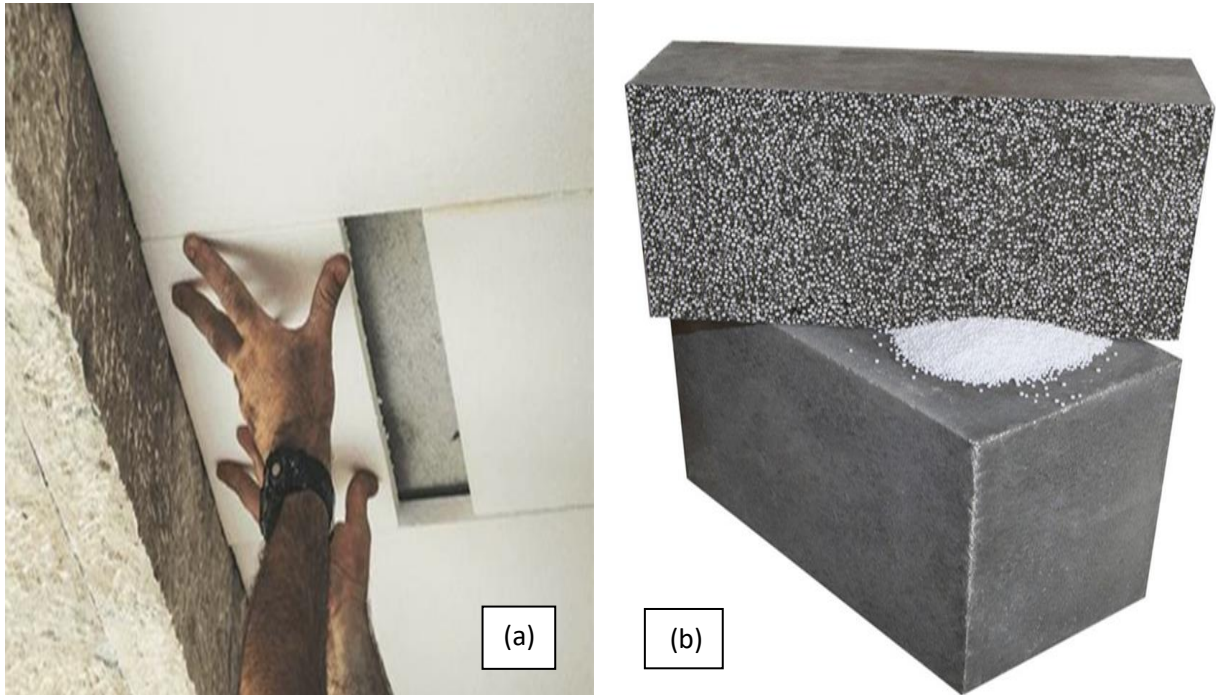


Figure (2-38): PS in building: (a) in construction (b) in concrete as aggregate [105]

C-Extruded polystyrene(XPS)

The trade name of extruded PS is Styrofoam, it consists of closed cell foam (cellular microstructure), it is usually used as an insulating material in heat-sensitive products, in packaging, cushioning agent, in art and craft field where it is easily cut into different shapes and sizes of excellent beauty for decorating [98]. Compound Styrofoam is introduced in the manufacturing of electronics as buttons of keyboards as shown in Figure (2-39) [106].

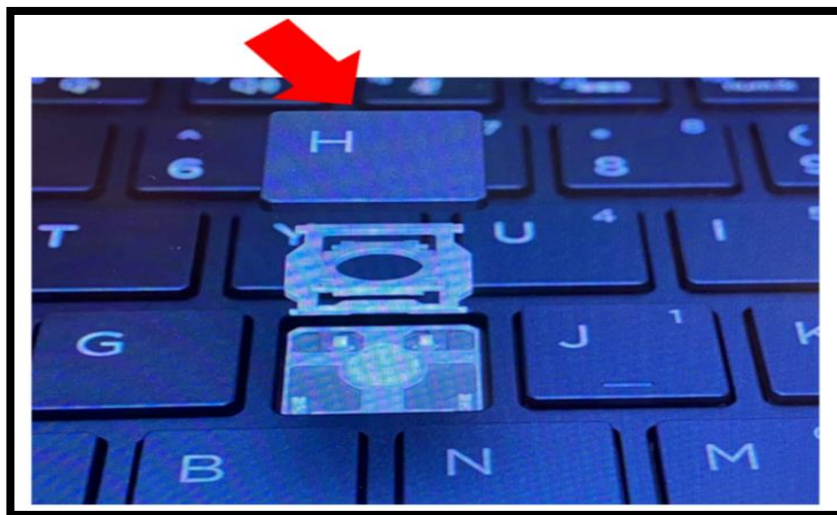


Figure (2-39):Compound Styrofoam into keyboard buttons

[106]

D-Branched PS

Branched polymers have some unique properties, such as lower solution and melt viscosities, increased solubility, and many more terminal groups. It is expected that these branched polymers will be used as polymer rheological modifiers [107].

E-Hydrogenated PS

Hydrogenated styrene–diene copolymers used as thickening (viscosity) additives to lubricating oils are considered. Specific features of the synthesis and hydrogenation of such copolymers are produced. The main requirements to thickening additives and the molecular structure–property relationships for the thickening power and viscosity index, mechanical stability, ability to disperse carbon black particles, heat resistance, and low-temperature properties are analyzed. The main producers of thickening additives based on hydrogenated styrene–diene copolymers are presented [108].

G-ABS and ASA copolymers

Acrylonitrile-butadiene-styrene (ABS) and acrylonitrile-styrene-acrylate (ASA) copolymers have outstanding scratch and chemical resistance as well as improvement in gas barrier properties [98].

H- Styrene - Acrylonitrile Copolymer (SAN)

The copolymers of styrene-acrylonitrile (SAN) are the most important products of PS. SAN and ABS is used in different fields as medicine, automotive, transportation, boats, appliance, recreational devices [98].

I- Syndiotactic Polystyrene (SPS)

Semi-crystalline syndiotactic PS is used through polymerization catalyst technology [98].

F- Copolymer (styrene - maleic anhydride)

The copolymerization of styrene and maleic anhydride improves thermal performance.

There are also other types of PS as: super PS (styrene-diphenylethylene copolymer), ethylene-styrene copolymers, oriented polystyrene sheet [98].

2.18 Applications of Polystyrene

Polystyrene is applied in construction and building (around 70%), packaging (around 25%) and other applications (around 5%) [109]. The description of PS applications in various fields are mentioned below.

a-Medical Field

PS and its products are more suitable for usage in not reusable medical applications as plates of tissue culture, conducting test trays, medical cups, tubes of test, kits for housing test through the biomedical research. PS is used in medical equipment due to its excellent clearness benefits for good visibility and

exceptional sterilization process for example diagnostic purposes and speculum [98]. One of medical applications is shown in Figure (2-40).



Figure (2-40):PS in medical devices

b-Construction Applications

PS is applied in the industries of construction and building for insulating boards, sliding, ceilings, walls, floors, sides, roofs due to its excellent capacity of insulation. PS is utilized in walls of sound proofing, units of bath and shower, fixtures of lighting and plumbing for buildings because of its good capability of processing and tremendous performance under all climatic conditions. PS also is used as architectural design models and replacement to corrugated cardboards [98]. PS is used as binding translucent materials between solar cells and Portland cement in the form of blocks and panels for exterior walls and partitions [110] as shown in Figure (2-41).



Figure (2-41): Use of PS in solar cells [110]

c-Automotive Industry

PS is used in automotive applications due to its characteristics: moisture free, inexpensive, thermally stable in a wider range of temperature, high mechanical strength with other elements, conductive in ionic form. The common industrial automobile products from PS are cores of bumper, void fillers, roof liners, head rests and head impact, knee supports, side protection from impact, seating of car, sun visors, liners of car air conditioning, liners of battery under bonnet, sound deadening under bonnet [98], there are exterior and interior automotive parts made from PS as shown in Figure (2-42).

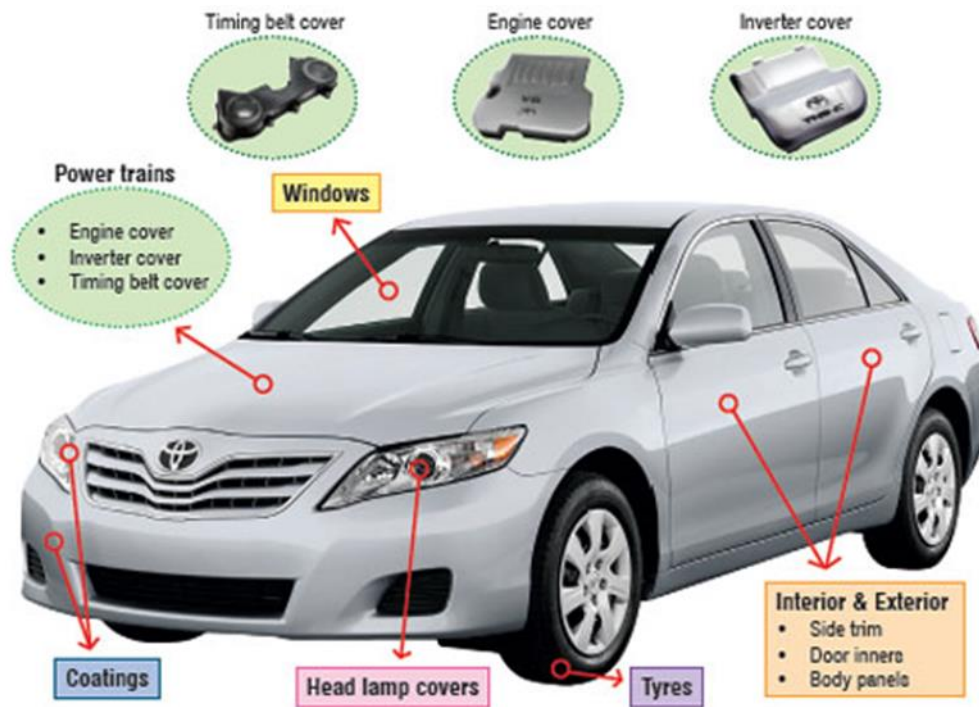


Figure (2-42): Parts of automotive that fabricated from PS [111]

d-Electronic Field

In electronic industry, PS is used in manufacturing computers with various types with respect to form, aesthetics, function, high performance, cost ratio and televisions. PS is used in consumer electronics for protecting CD and DVD, boxes of jewelers, cassette tape and many devices for information technology [98]. PS is used in the manufacturing of electronics as capacitors and can be shown through Figure (2-43).

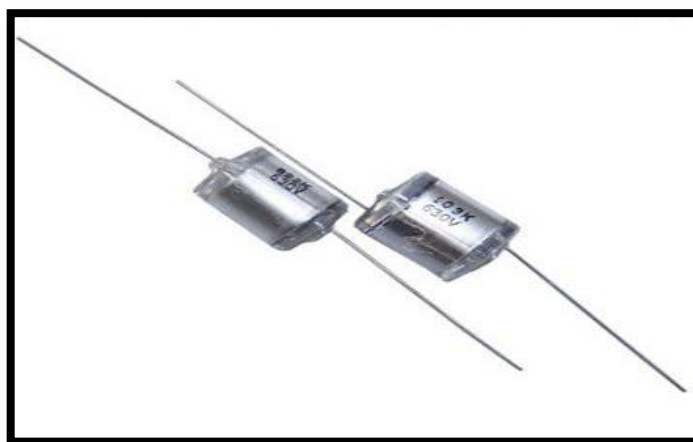


Figure (2.43): Capacitors made from Polystyrene

e-PS With Metals & Inorganic Compounds

PS is applied in removing of toxic metal ions from municipal, commercial and industrial effluents in order to protect our environment [99]. PS is included within different metallic and ionic membranes, it is mediated through inorganic composites as the synthesis of PS-supported ZrO₂ composites due to the easiness of production and inert behavior of PS for enhancing sorption of Pb(II) ions from water [112]. PS is applied in detecting of H₂O₂ because of its possibility for creating composite materials for electrodes [97].

f-Food Packaging

The exceptional insulator and protector material of food in the process of food packing is PS in order to prevent food meals from decomposition/spoiling like eggs, meat, fish, salads, dairy products and cold drink because PS is easy and cheap material for preserving food. PS has a great role in the industry of goods packaging, refrigeration and transportation, the materials of packaging are recyclable.

The transportation of shopper goods and health care products (pharmaceuticals, neutral cuticles) across the countries requires packing in boxes where PS is put as a supporting materials along boxes, it also offers insulation and protection from various exterior conditions like air, temperature, moisture in order to maintain the properties at all circumstances [99].

g-Household Appliances

There are various household appliances are made from PS as air conditioners, hot air and microwave ovens, refrigerators, blenders, vacuum cleaners with hand-held, disposable cutlery, equipment of garden, accessories of kitchen and bathroom, toys and other playing accessories, smoke detector housings [113, 114, 115].

2.19 Literature Review

2.19.1 Literature Review of Polystyrene

Rouabah F. et al.(2012) investigated the effect three thermal treatments on the thermal, mechanical, and thermo physical properties of polystyrene. First of them is the quenching from the melt state to different temperatures. Second is the quenching from $(T_g + 7)^\circ\text{C}$. The third is the annealing. The enhancement in the impact strength after a second quenching at 40°C . The enhancement in impact strength in expense the other properties as elastic modulus, density and hardness [4].

María Teresa, et al. (2014) analyzed the effect of molding temperature and cooling time on the residual stresses present in parts include two types of polystyrene. The part made in injection molding. Using the photoelasticity to determine the residual stresses. Concluding the photoelasticity technique can be applied in calculating residual stresses in injection molded crystal polystyrene parts [116].

2.19.2 Literature Review of Ultrasonic Test

Javadi, Yashar et al. (2012) presents a three dimensional thermo-mechanical analysis to evaluate welding residual stresses in dissimilar plate-plate butt weld joint geometry of AISI stainless steel 304 and Carbon Steel A106-B type. The materials tested are commonly used for pressure vessel applications. Four passes butt-weld joint geometry with 4mm root gap was used. Two calibration samples were extracted from A106-B and A240-TP304 base metal to determine acoustoelastic constants. The nominal frequency and diameter of the piezoelectric elements are 2 MHz and 24 mm, respectively. Two calibration samples were extracted from two base metals to determine acoustoelastic constants, then the results from ultrasonic stress measurements are carried out on both side of plates [77].

Raheem G. Kadhim (2014) searched the effect nanosilver particles on mechanical properties of polymer matrix containing polyvinyl alcohol and polyvinyl- pyrrolidone. The casting method used to prepare the samples (PVA-PVP-Ag). The percentage of nano silver in the range (0-16%). Using the ultrasonic method to determine the mechanical properties as absorption coefficient of ultrasonic wave, relaxation amplitude, bulk modulus and acoustic impedance. Increasing in density, relaxation amplitude, and absorption coefficient with increasing the amount of Ag [117].

Dawei Jia,et al. (2014) explored the effect of temperature and stress on the velocity of ultrasonic longitudinal waves in two amorphous polymers and two semi crystalline polymers. Calculating the acoustoelastic constants and temperature constant of polymers. The velocity alters linearly with stress and temperature, as well as there is an important effect of temperature as the acoustoelastic effect. It is necessary to ensure the ambient temperature in the test [7].

Xu, Chunguanget et al. (2015) carried out an experiment of residual stress testing of oil pipeline weld joint is carried out by using the ultrasonic detector. The material of pipeline is X70 steel and welding procedure is manual arc welding. The residual stresses are tested around straight weld joint in a section of pipeline. The test conditions are: frequency of transducers 5MHz, distance between transducers is 30mm, the material of the specimen is 6061 aluminium alloy and environment temperature is 23°C. In order to verify the accuracy of the test results, a hydrostatic test has been carried out, it is observed that the blasting area is consistent with the dangerous area evaluated by ultrasonic method [2].

Karrar Abd-Ali Obeid, et al. (2015) searched on blend of poly ethylene glycol and carboxy methyl cellulose PEG/CMC prepared by liquid mixing method. The mechanical properties was determined by ultrasonic

method. The adding of PEG on led to increasing density and the absorption of ultrasonic coefficient [118].

Hermawan Judawisastra, et al. (2019) determined the elastic modulus of three thermoplastic polymers and comparing with the elastic modulus from mechanical testing by using ultrasonic method-pulse echo. Determination the elastic modulus in pulse echo is more comfortable than transmission method. Polymethylmethacrylate (PMMA), low density poly ethylene (LDPE), and polyamide(nylon) were used. The outcomes of elastic modulus from pulse echo had a deep error in the range (98% -158%) particularly for the low density polymer and large ratio of viscous property to elastic property. The attenuation from ultrasonic method was operated by the viscoelastic properties and the elastic modulus from ultrasonic velocity reading was influenced by the density. The linear model for thermoplastic elastic modulus determination based on ultrasonic pulse echo testing has been improved and could decreased the error to 3.45% [119].

Sasmita et al (2019) calculated the elastic modulus of some polymers by using Ultrasonic method. Using five types of polymers were polyster, epoxy, polyamide 6, low density polyethelene and polymathyl methacrylate. There are a difference in value of elastic modulus especially for material of low density. Using lower probe frequency for testing enables easy alternating ultrasonic detection so it will allow the measurement of wave velocity [120].

Ye, Chong et al. (2019) used a laser/ electromagnetic acoustic transducer (EMAT) ultrasonic method where Q-Switched Nd:YAG laser is applied to generate a broadband ultrasonic wave with a reception bandwidth of (0.5MHz, 2.0MHz). An EMAT is attached to the welding plate in order to evaluate the surface/subsurface longitudinal residual stress distribution generated by gas metal arc welding (GMAW), the welding voltage was 25V and the welding speed was set as 0.375 in./s where the sample was joined by a

Miller Pulstar 450 GMAW machine. The velocity variation is experimentally measured due to the time of flight for travelling ultrasonic waves along a specific path parallel to the direction of the welding seam. The welding residual stress evaluation were carried out along each inspection row where 15 equally spaced points between 0 and 45mm away from the welding seam were chosen [83].

Yang, Shunmin et al. (2019) studied specimens of 304 stainless steel bars with dimensions of (390 mm x 60 mm x 6mm). To facilitate the experiments, the front surfaces were polished with a milling machine to a roughness (Ra) of 2.83 μm . The calibration sample is heat treated into 600 degrees Celsius and stayed 4 hours at that temperature, then followed by slow cooling in order to stress relief. Double receiving transducers are advantageous in that they eliminate environment effects (temperature and coupling conditions). Time-of-flight was measured using the zero crossing method between the two receiver echoes R1 and R2. The specimens were numbered from S1 to S10, with S1 being the reference specimen free of stresses. Samples S2 through S10 were tested for travel time by using the ultrasonic technique and each travel time was compared to the travel time of S1. for the 6 mm transducer. Test conditions are frequencies of transducers (5 , 2.5, 1) MHz, the distance between transmitting transducer and first receiving transducer is 37.6 mm, environment temperature 26 °C. The uncertain factors involved in measuring residual stress with LCR waves, such as the distance between the transmitter and receiver and the diameter and frequency of the transducer, have been investigated [121].

YANG, YANG (2020) measured the residual stresses for cylinder heads as cast engine components, six cylinder heads were manufactured from the same material composition. Four of them were kept for 5 hours after casting, and two of them had 10 hours, seven positions on each cylinder head were assigned as sample points for measurement due to high residual stresses and sharp residual stress gradients. The results are generated by averaging the speed

of waves within the covered region. Ultrasonic measurement were examined at several positions on cylinder heads. It comprises of 2MHz ultrasound ejector. Residual stresses at identical positions with 10-hour shakeout time are supposed to be smaller in magnitude than those with 5-hour shakeout time because longer shakeout time ensures gentle temperature reduction during cooling and results in less residual stresses. Longer shakeout time can lower the tensile stresses and develop more compressive stresses in the surface layer, and can also reduce the tensile strength slightly. the experiments are very scattered due to the complex geometry of the cylinder head [122].

Zhouyiao Zou (2020) used the ultrasonic longitudinal through transmission technique to determine the internal stresses in basin insulators inside gas-insulated metal-enclosed switchgear. An internal stress measurement system is advanced to discuss the relation between the uniaxial compressive internal stress and the velocity of ultrasonic wave. This research is provided the ultrasonic method is feasible in calculating the internal stress in epoxy composites [123].

Najm Sanaa S. (2021) calculated the physical properties of polymer solution of polyvinyl amid and poly ethylene glycol PVA/PEG by using ultrasonic method by dissolving various weight of powder PVA/PEG in water. Different concentrations of PEG in percentage (6%-14%)g/mol added to PVA. Increasing in acoustic impedance ,absorption coefficient and bulk modulus with increasing concentration of polymeric solution. The compressibility decreased with increasing the concentration [124].

Hwang, Young-In et al. (2021) used a probe consisting of one transmitter and two receivers was fabricated piezoelectric elements, the frequency and diameter of transducers were 2.25 MHz and is 0.75 inch respectively, the intervals between transducers were 29.3 mm. the dimensions of the welded plate were (270 * 40 * 6) mm. For the residual stress measurement

using the LCR wave, three rail samples were cut from different sites and used, the difference in residual stress distribution according to the characteristics of wheel-rail contact surface was analyzed from the obtained residual stress value. Received signals used for calculating travel times. it was verified how the difference in the arrival times of the LCR waves showed a trend as the tensile stresses increased. It was concluded that this non-destructive evaluation technique could be employed for accurate stress measurement of rails because differences in stress applied to the rail can be detected [125].

Zhi, Qimeng et al. used in this study A7N01P Al alloy plates with the dimension of (500×300×13) mm under aging condition (solution treated and naturally aged according to ISO 2107:2007) were used in this study. The welding joints were processed by the Metal Inert-Gas (MIG) technique and the welding direction was parallel to the rolling direction of the base metals. The welding wires of 1.6 mm diameter. In this work, the frequency of transducers was 4 MHz with the diameter of 6.8 mm. The distance between excitation and receiving transducer was 30 mm. The microstructure have significant effect on the acoustoelastic constant and consequently the acoustoelastic constant has significant effect on the measurements of residual stresses. The results indicated that the residual stresses obtained with correction are more accurate for structures design [126].

2.19.3 Literature Review of Optimization Method

M.F. Zamil, et al. (2019) used the modified bee colony algorithm to find the to discover the optimal operating situation for specific targeted production for polypropylene derivative .Working on *the ideal benchmark equations and complex case* of the polymerization of polypropylene in fluidized bed reactor. Algorithmic is placed by developing the examination knowledge of onlooker bee from meta-heuristic idea in search space. The optimization for the polypropylene reaction is implemented by the multi objective functions ABC

algorithm, and the objective functions are maximum production rate and melt flow index by monitoring operating temperature and pressure, superficial gas velocity, and concentration of feed propylene [127].

Xiaohui Guo (2022) predicted the natural aging life of 8016 ethylene propylene rubber carefully and fast. Depending on the time-temperature equivalent superposition precept, the artificial bee colony algorithm . This research inserted the digit the acceleration factor of the accelerated aging trial, and the computation of the acceleration agent was believed an optimization problem, which evaded the error superposition trouble caused by data fitting at each temperature. The final outcomes show that the artificial bee colony algorithm can fast and exactly identify the acceleration factor of the accelerated aging test [128].

Anton Chepurnenko (2022) studied the chance to use artificial neural networks to limit the rheological parameters of polymers from curves of stress relaxation. The feed forward back propagation neural network was chosen for this search. Neural networks were trained on theoretical stress relaxation curves structured . The value of the mean square error (MSE) was used as a criterion for the performance of the training. The structured model of the artificial neural network was examined on the experimental relaxation curves of recycled polyvinyl chloride. The type of the experimental curve approximation was quite good and was comparable with the standard methods for processing stress relaxation curves [129].

Chapter Three

Optimization and

Statistical Solutions

Chapter Three

Optimization and Statistical Solutions

3.1 Introduction

Back-propagation algorithm is one of the most widely used and popular techniques to optimize the feed forward neural network training. Nature inspired meta-heuristic algorithms also provide derivative-free solution to optimize complex problem. Artificial bee colony algorithm is a nature inspired meta-heuristic algorithm, mimicking the foraging or food source searching behavior of bees in a bee colony. Explaining steps of artificial bee colony ABC algorithm, feed forward neural network FFNA and hybrid of them will be discussed in this chapter.

3.2 The Optimization Method

The operation of calculating the best design or best representation is known as the optimization. This procedure can be applied in all fields of engineering, medicine, chemical and physical applications [130]. Any optimization problem can be solved depending on the type of problem by applying one of the following methods:

1.Traditional optimization methods: These can be helpful for dimensional problem with any number of dimension . Several methods are:(a) direct methods (b) Gradient methods (c) methods of linear programming (d) methods of interior point [131].

2.Progressive optimization techniques (meta-heuristic algorithms): large part of practical problems are complex, nonlinear , inconsistent and discontinuous. They have been used successfully in solving many real-world problems. The success of meta-heuristic algorithms has increased the interest in this field. Currently, there are more than 200 meta-heuristic algorithms. The equilibrium optimizer (EO), the marine predators algorithm (MPA), the slime mould

algorithm (SMA), the reptile search algorithm (RSA), the dandelion optimizer, the runge kutta optimizer (RUN), and weighted mean of vectors (INFO) are some of the current meta-heuristic algorithms recommended in these years. Artificial beecolony (ABC), cuckoo search (CS), particle swarm optimization (PSO), differential evolution algorithm (DE) and flower pollination algorithm (FPA) are some of the very popular meta-heuristic algorithms proposed in recent years [132].

3.3 Artificial Bee Colony Algorithm (ABC)

The artificial bee colony ABC turn out the most successful and powerful in resolving the problems that have more than action. The stochastic algorithm is depended on population that mimics the searching for food attitude of honey bee colonies to calculate the optimal parameter in the problem [133]. The social structure, quality of nectar and fertilization of crops are the few most important properties for making these species most famous. Due to various geographical locations and differences in weather pattern, the honey bees are found with different color, shape and nature, but irrespective of those differences there are some basic jobs that they perform on daily basis. The foraging or finding new food source and information sharing about new source are the most common jobs [134, 135].

Inside the algorithm three groups of bees. First of them is the working bees, second is the onlookers, third is the scouts. The algorithm consists of only one artificial bee used for each supply of food. The working bees (employed bees) go to their feed fountain and back to hive and dance in this region. The onlookers (unemployed bees) monitor the dances of working bees and select feed fountain according to the dances to take the best kind of feed [136].

The selection of the food source depends on many parameters. The food source is selected on the basis of the quality of nectar, distance of food source from the colony, quantity of nectar. The scout bee is one kind of unemployed bee which starts the searching of a food source without its knowledge.

Appearance of this kind of bee generally varies from 5-30% of the total population. The employed bees are the successful onlooker bee with the knowledge of food source [134].

The employed bees generally share the food source information with the other bee, and guide others about richness and the direction of food source. In reality the guidance of employed bees is reflected through their waggle dance in the specific dance area, and this dancing area is the main information sharing center for all employed honey bees. The onlookers bee is the most informative bee, as all the information about food source is available in dancing area [137].

On the basis of available information in the dancing area the onlookers bee selects the best one. Sharing information also depends on the quantity of food, and hence the recruitment of honey bee depends on the quantity and richness of food source. When nectar amount is decreased, the employed bee becomes an unemployed bee, and abandon the food source. The algorithmic process of artificial bee colony simulates the real life scenario of searching a food source, and maintain various types of bees involved in the searching and collecting the nectar [134].

The main steps of ABC algorithm are:

1. **First step** is started with the random leading bee, one of the leading bee is set up for fountaining feed and determining the concentration of food according to the objective functions, so the optimal location and the optimal fitness will be registered.

2. **Second step** is introduced each lead bee without prior planning to select a neighbor of leading bee and randomly choose one dimension, so the site is updated as in Eq. (3-1) [138]:

$$x_{ij} = x_j^{min} + rand(0,1)(x_j^{max} - x_j^{min}) \quad Eq. (3 - 1)$$

Where

$i=1,2,\dots,\dots,\dots,SN;$ $SN=$ Number of feed fountain

$j=1,2,\dots,\dots,\dots,D;$ $D=$ Number of optimization parameter

Every used bee is linked to only one of feed fountain, therefore; the number of feed fountain (in other words food sources) sites is equal to the numbers of used. While initialization is finished, employed bees generates a new solution based on ABC algorithm as in Figure (3-1).The used bee has produced changes to the feed fountain (solution) position in bee memory relying on information and detect the source of the neighbor's food and then assess its quality as in Eq.(3-2) [138]:

$$v_{ij} = x_{ij} + \phi_{i,j}(x_{ij} - x_{kj}) \quad \text{Eq. (3 - 2)}$$

Where $k \in [1,2,3, \dots, \dots, SN]$

According to without prior planning, the chosen index that has to be different from I and $\phi_{i,j}$ is a uniformly divided real random number in the range $[-1,1]$.

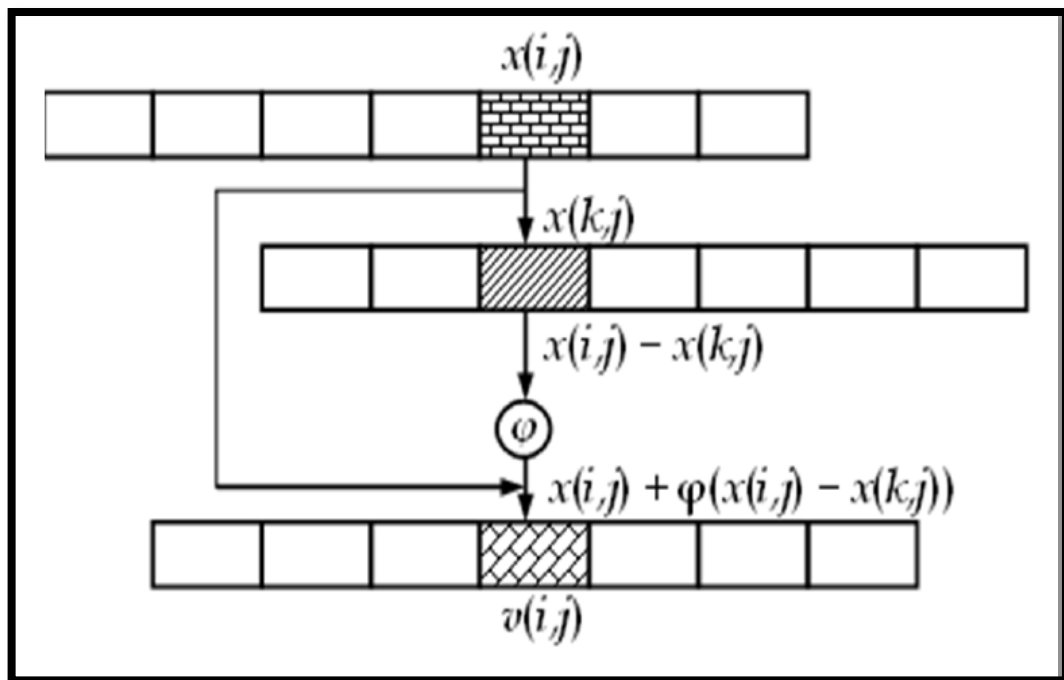


Figure (3-1): A simple position update scheme[139]

The fitness equation as following:

$$fit_i(x_i) = \begin{cases} \frac{1}{1+f(x_i)}, & f(x_i) \geq 0 \\ \frac{1}{1+f(x_i)}, & f(x_i) < 0 \end{cases} \quad \text{Eq.(3-3)}$$

where $f(x_i)$ refers to the value of the objective function for solving the trouble [128].

3-Third step all the used bees are terminated the fixative of their research, then they participated the datum with the number of nectar and their source situation where the onlooker bee in the hop region. There are several properties of bee fiction. An onlooker will estimate the datum of nectar taken from all the bees completed and choose the fountain of the food fountains with the prospect related with the magnitude of nectar [138].

This probabilistic chosen relays on the worth of fitness settlement in the population according to fitness as in Eq.(3-4) [128, 140]:

$$P_i = \frac{fit_i(x_i)}{\sum_{i=1}^{SN} fit_i(x_i)} \quad \text{Eq. (3 - 4)}$$

without prior planning real number within the range [0,1] is created for every fountain in the ABC algorithm.

4-Fourth step every follow bee would be advanced as a leading bee would choose in conformity with the roulette wheel design and the location would be updated agreement to Eq.(3-4). If the new position is preferable, the chosen bee would be updated in the present location, otherwise, the digit (best value) Base would plus 1. A leading bee can be chosen by many follow bees again and again, which denotes, that leading bee with larger fitness degree would be chosen with sizable probability.

5- Fifth step The position and focus of optimal feed fountains of this obstetrics would be registered .

6- Sixth step the leading bee with the extreme digit Base would be chosen, and the leading bee would be as a scout bee if the digit is larger than limits, so the

position, fitness and Bas would be initialized. The parameter Limit plays a function of reborn of lead bee with the long-term with no updating.

7- **Seventh step** if the generation digit is junior than the maximum digit, it should be go to the next generation at second step, otherwise, the results would output [140].

There is general flow chart concerning ABC is presented in Figure (3-2).

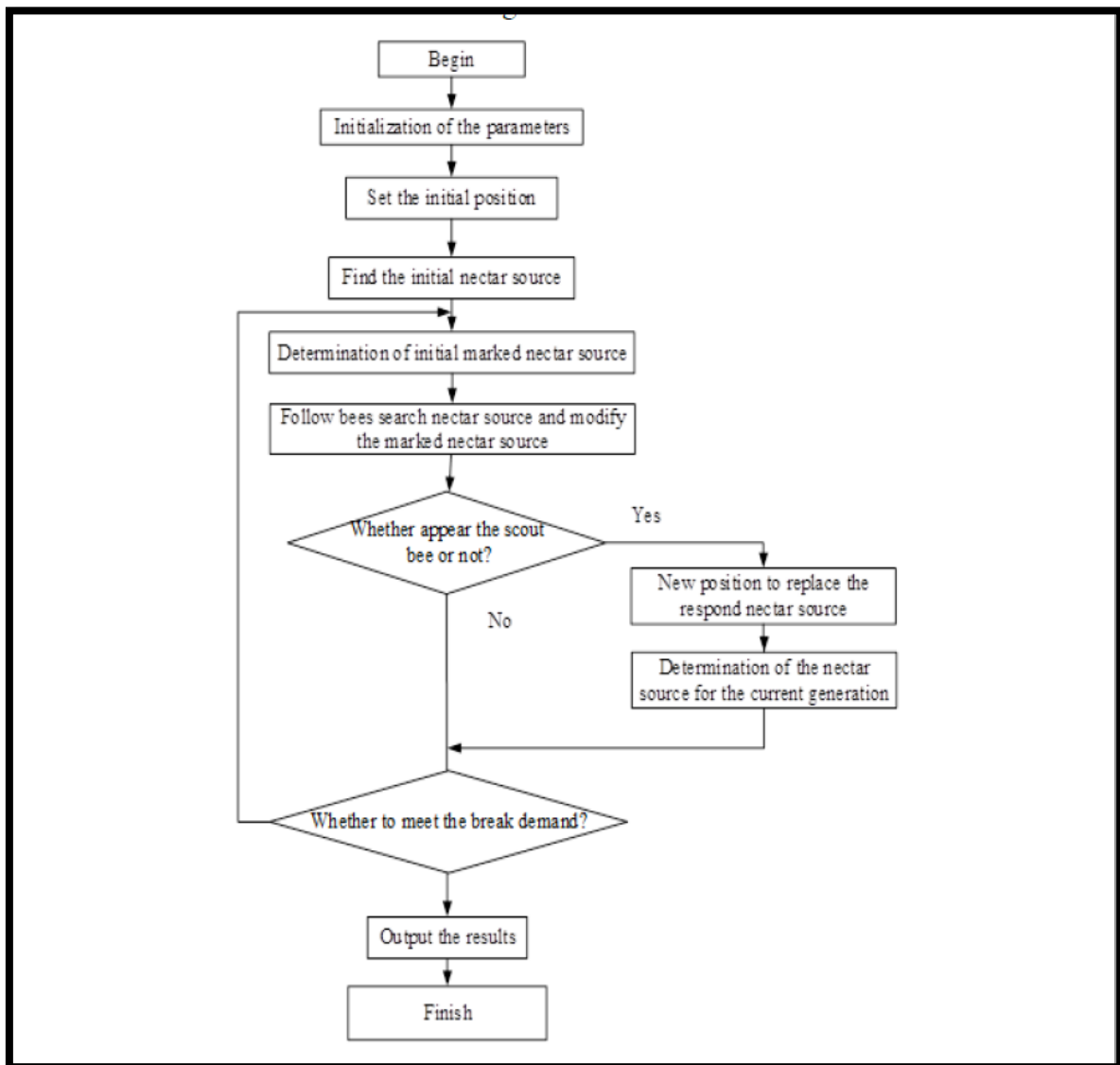


Figure (3-2): Flowchart of artificial bee colony ABC [140]

3.4 Artificial Neural Networks

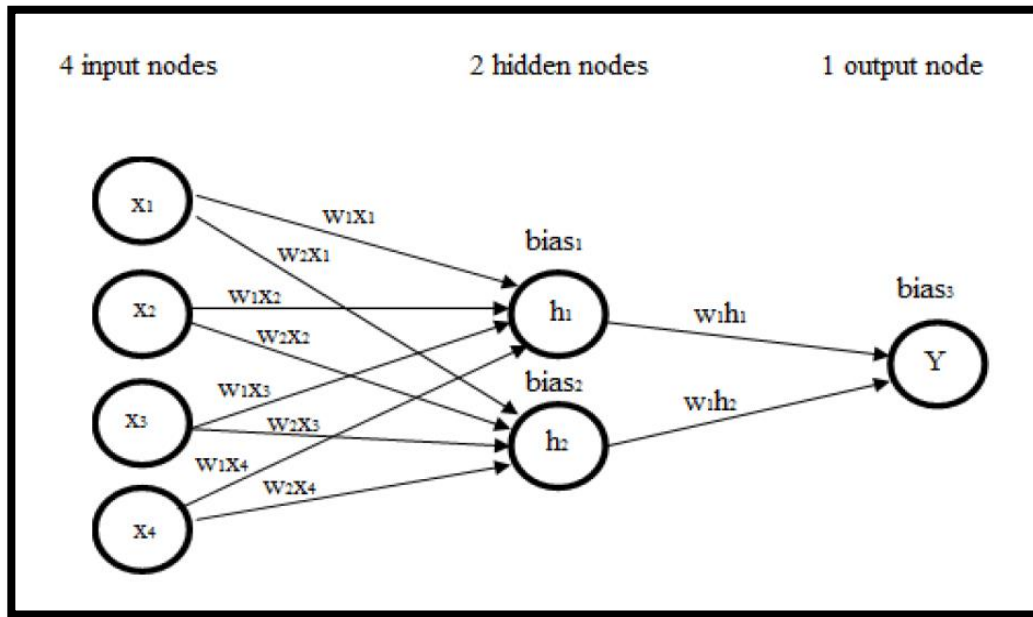
Artificial neural network ANN is one of the most important artificial intelligence techniques. It has been used to solve many real-world problems . Its

popularity is a result of its strong structure. Security, science, engineering, medical science, finance, education, energy, and manufacturing are some of the areas where ANN is used. One of the important capabilities of ANN is the learning feature. It can provide modeling of problems using existing data and can give information about data that it has never seen. The training process of ANN is very important. Successful modeling of a problem is directly related to the successful training process of ANN [135]

The artificial neural network is similar to the human brain installation. It composes of the input strata, pursued by hidden layer of neurons and the output strata. It stratifies in different area as: style rating/estimate, framework designing and symmetry, signal processing, image processing, monitoring systems and stock market predictions as well as some of the major areas of engineering and science. The reason is belonged to the numerous helpful sides of neural networks as their parallel structure, learning and adaptive capabilities, Very Large Scale Integrated (VLSI) implement ability and fault tolerance [141].

The ANN has simple units called neurons or nodes, each of which is interconnected with each other. These nodes are divided into three types: input, hidden and output nodes as in Figure (3-3). Input nodes represent the input data, hidden nodes are the main processing units that hold the calculation process, while the output nodes represent the ANN output results. However, the hidden nodes can be structured as a single or multiple layers of nodes that are connected to each other [142].

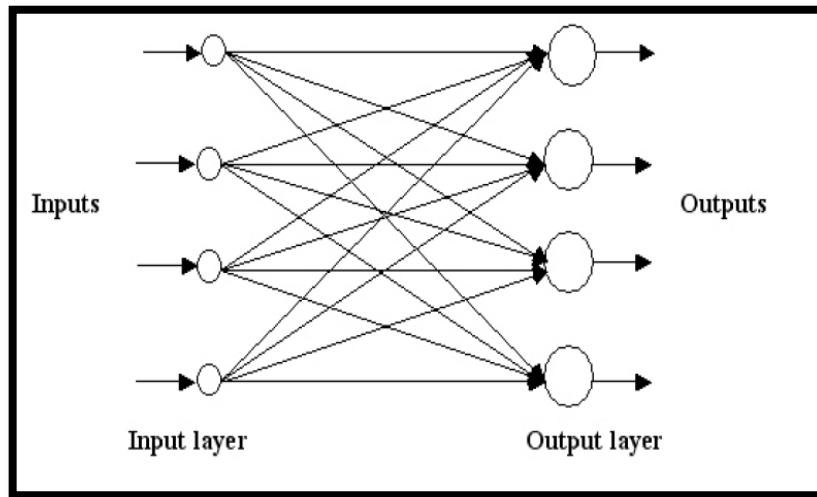
There are many types of the artificial neural network ANN such as feed forward (FF), Radial Basis Function (RBF), Recurrent Neural Network, Dynamic Neural Networks [158]. There are many types of the artificial neural network ANN such as feed forward (FF), Radial Basis Function (RBF), Recurrent Neural Network, Dynamic Neural Networks [143].



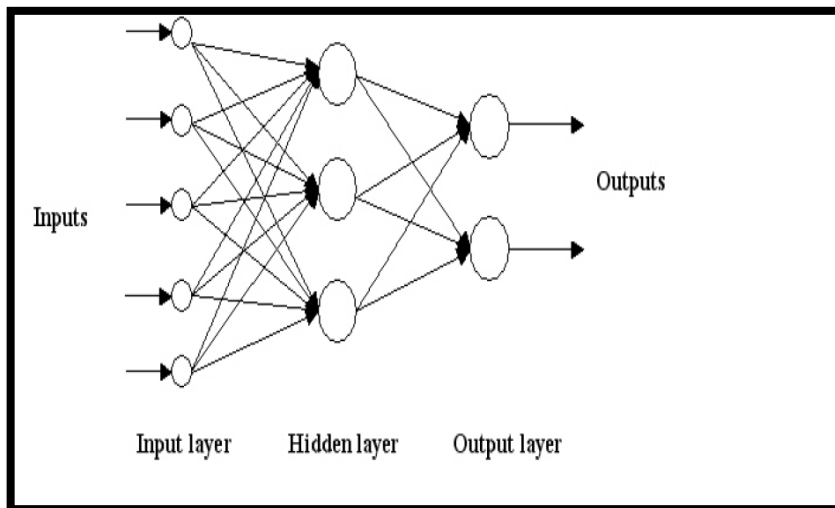
Figure(3-3): ANN basic unit [142]

The requisite building block of FF neural networks is a “*neuron*”. A neuron can be explained as a processing unit. Every neuron in a network picks weighted input through these synaptic links from the neurons that is linked to and produces an output by threading the weighted total of those input indicatives (either external inputs from the environment or the outputs of other neurons) through an activation function. If there is no feedback from the outputs of the neurons towards the inputs through the network, then the network is indicated to feed-forward neural network. Usually, neural networks are arranged in the shape of layers [144].

Feed-forward neural networks fall into two types relying on the digit of the layers, either one layer or multi-layer. Every neuron is consisted of an former weight and every neuron is linked to each other from one layer to the other. The feed forward network usually needs to be trained, as a human brain, with each training period the network gets more knowledge and precision since the weights are re-adjusting accordingly to the target [143]. The types of feed forward neural network input layer are expressed by Figure (3-4).



(a) single layer



(b) multi-layer

**Figure (3-4): Types of feed forward neural network
FFNN input layer [141]**

The training of the FFNN was depending on the back propagation function with trapezoidal function. Back-propagation multilayer feed-forward ANN is created by using the Neural Network Toolbox in Matlab [144]. The input values come in through the framework and determine the mean square error MSE. After that from the output the sensitivity is diffused back to the initial layer and the weight biases are updated. The output of the i th node of those hidden nodes can be described by Eq. (3-5) [142].

$$y_i = f_i \left(\sum_{j=1}^n w_{ij} x_j + \theta_i \right) \quad \text{Eq. (3 - 5)}$$

Where:

y_i : is the output of the hidden node i

X_j : is the j th input to the hidden node

w_{ij} is the connected weight between the hidden node and the input node x_j

θ_i is the threshold (bias) of that hidden node

f_i : is the hidden node transfer function

The number of neurons in the input and output layers of the ANN is identical to the number of input and output parameters, respectively. However, the number of neurons in the hidden layers of the neural network is calibrated during the training and validation process [144].

The training of the feed forward ANN is based on adjusting the corresponding weights and biases of the specified ANN structure in order to minimize the error rate between the target and the actual output of a supervised ANN. optimization search algorithms can be applied for ANN training, where the weights and biases of a fixed ANN structure can be fed into the algorithm as a vector of values representing the weights and biases of the corresponding nodes [142].

The training is the process of repeated applications of the back-propagation algorithm until the error becomes acceptable or some other criterion is achieved. Since the difference between the training data is larger, this will result in a larger ANN prediction error. Thus, it is necessary to normalize the experiment data before applying them to the network. Eq. (3-6) is The normalizing equation

$$x_k = \frac{x - x_{min}}{x_{max} - x_{min}} \quad Eq. (3 - 6)$$

where :

x is the real value of the variable before normalization

x_{min} and x_{max} are the minimum and maximum values of the variable x

The data for training and validation of ANN were obtained in MATLAB . The mean square error (MSE) of the network outputs and the target values are used as the network performance indicator. The equation of calculate MSE is a function to scale and reform the performance in neural network as shown [159].

$$MSE = \frac{1}{n} \sum_{k=1}^n (y_k - t_k)^2 \quad Eq. (3 - 7)$$

Where

n -total number of data patterns

y_k – the output produced from NN at point k

t_k – the target value at opoint k

It can be utilized with root mean square error (RMSE) to determine the real distance between the target and output due to Eq. (3-8) [143]:

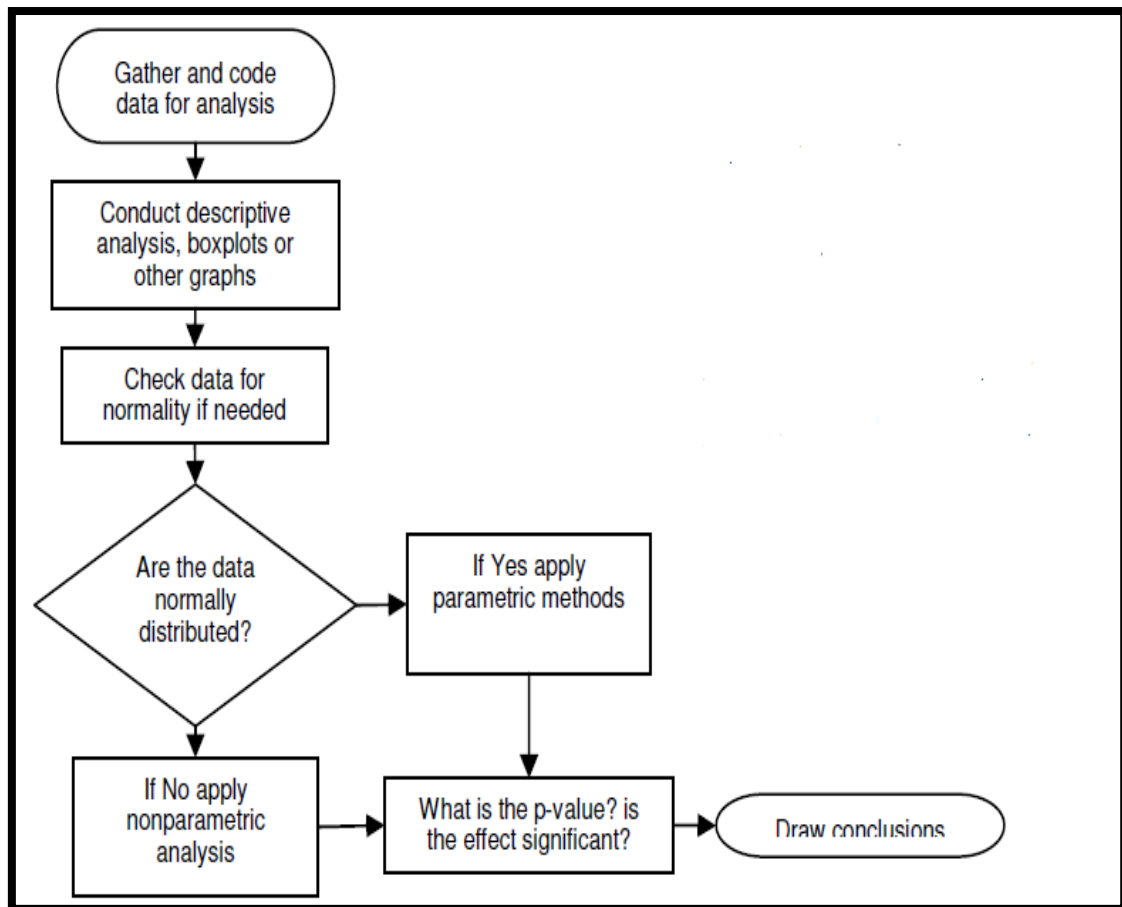
$$RMSE = \sqrt{\frac{1}{n} \sum_{k=1}^n (y_k - t_k)^2} \quad Eq.(3-8)$$

3.5 Statistical Software (SS)

The special computer programs that prepared for statistical information analysis are called statistical software (SS). It can be crossed as a graphical user interface or scripting. It is applied to resolve information emerging from a carefully orderly scientific operation of observation and experimentation, then

the analysis of data can make a result that can be explained to delivery scientific knowing. Sometimes data analysis can be applied to support research results in situations where integrity issues are suspected.[145, 146]

SPSS is popularly known as Statistical Package for the Social Sciences or Statistical Product and Service Solutions. SPSS is a widely used as statistical software for statistical analysis in social science and market analysis [146]. The main steps of SPSS flowchart are presented in Figure (3-5).



Figure(3-5): Flow chart of SPSS analyzing data of SPSS

Chapter Four

Experimental Part

Chapter Four

Experimental Part

4.1 Introduction

Large interest was introduced to determine the residual stresses in glassy polymers because of the technological importance of these materials. The detection of residual stresses was influenced on characteristics of molded polymers. This chapter will explained the stages of preparing PS specimens, the various instruments used to test them. The applying of non-destructive ultrasonic pulse-echo technique in order to evaluate through thickness residual stresses.

4.2 Properties of PS

PS granulates were supplied from Hebie Bona Import and Export Trade Co., Ltd-China. PS is colourless, odourless, tasteless and shiny. The basic properties of the used PS are listed in Table (4-1). The methodology of experimental work is shown in Figure (4-1).

Table (4-1) Basic Properties of PS

Property	Details
Average molecular weight (g/mol)	35000
Density (g/cm ³)	(0.96-1.052)
Transparency	88%-92%
Refractive index	1.59-1.6
Birefringence	Stress-optical effect
Heat distortion temperature	70°C-100°C
Melting temperature	150°C-180°C
Thermal decomposition	300°C

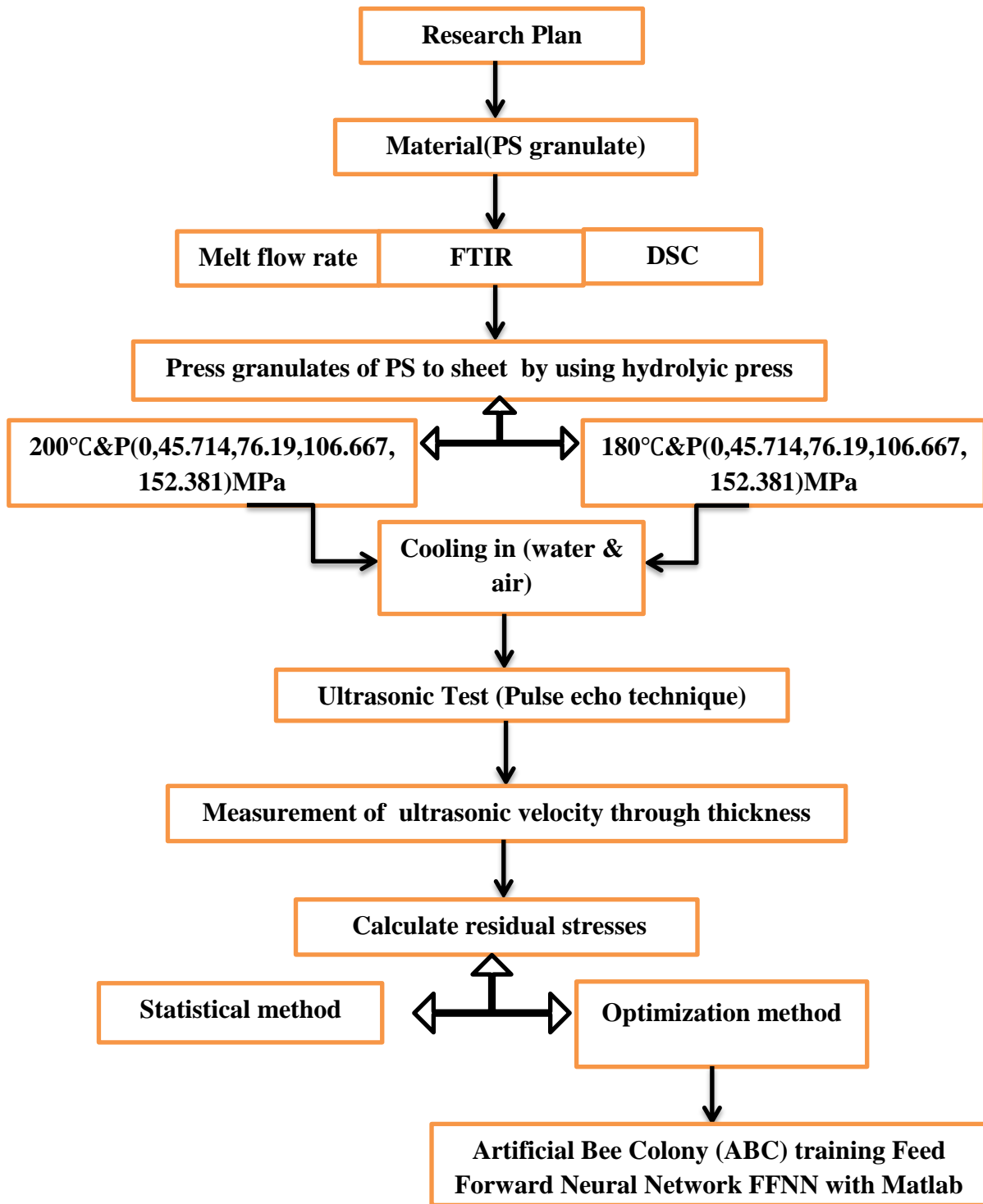


Figure (4-1): Research methodology

4.3 Preparation of Specimens

The specimens were prepared using pressed granulates of PS. The required amount of PS granulates was weighed and placed in the rectangular mold under hot press. The first step is placing PS granulates between two foils of aluminum inside metal mold in the form of rectangular plate with dimensions

of (150mm *70mm * 3mm) (length * width * thickness) as shown in Figure (4-2).

The used hydraulic press is found at laboratory of Material Engineering College/University of Babylon. The applied pressures from hydraulic press on the whole press area (40cm*40cm) were (3, 5, 7, 10)MPa. The actual applied pressures on rectangular metal mold were obtained by transforming the pressure of hydraulic press to the pressure applied on metal mold. The force is calculated from equation (4-1), then mold pressure is determined by using cross sectional area of specimen. This transformation is shown by table (4-2).

$$pressure = \frac{Force}{area\ of\ press} \quad Eq. (4 - 1)$$

Table 4-2 The transformation between pressures (MPa)

Hydraulic Pressures	Mold Pressures
0	0
3	45.741
5	76.19
7	106.667
10	152.381

There are several experiments for preparing PS specimens were carried out (approximately 65) experiments, many of these specimens were pressed during various time intervals and failed. According to these experiments, it could be reached that best times of stillness under the applied pressures by hydraulic press were (30, 20) minute at (180, 200)°C respectively.



(a)



(b)

Figure (4-2): (a) Hydraulic press (b) Metal mold

There are two manners used in preparing specimens:

1- Heating the press to 180°C, place PS granulates for 30 min in the mold at 180°C. Different pressures (0, 45.714, 76.19, 106.667, 152.381) MPa were applied for time (10) min. Five specimens were cooled in air and other five cooled in water. The temperature of air and water is (25)°C.

2- Heating the press to 200°C and place granulates for 20 min in the mold at 200°C. various pressure (0, 45.714, 76.19, 106.667, 152.381) MPa were

applied for time (10) min. Five specimens were cooled in air and other five cooled in water. There is additional two specimens for both annealing and tensile test, so the total number of effective specimens was (22).

The metal mold is very suitable for preparing PS specimens in order to obtain very smooth flat plates because:

- a- Ultrasonic technique is requires no surface polishing during preparation of specimen in order to maintain the original stress state and avoid causing damage to the material understudy.
- b- Ultrasonic technique is required avoiding surface roughness, imperfections (defects) and even small cavities that could possibly give inaccurate measurements.

The prepared specimen is shown in Figure (4-3) while the procedure of specimens preparation is shown in Figure (4- 4).



Figure (4-3): PS specimen (sheet)

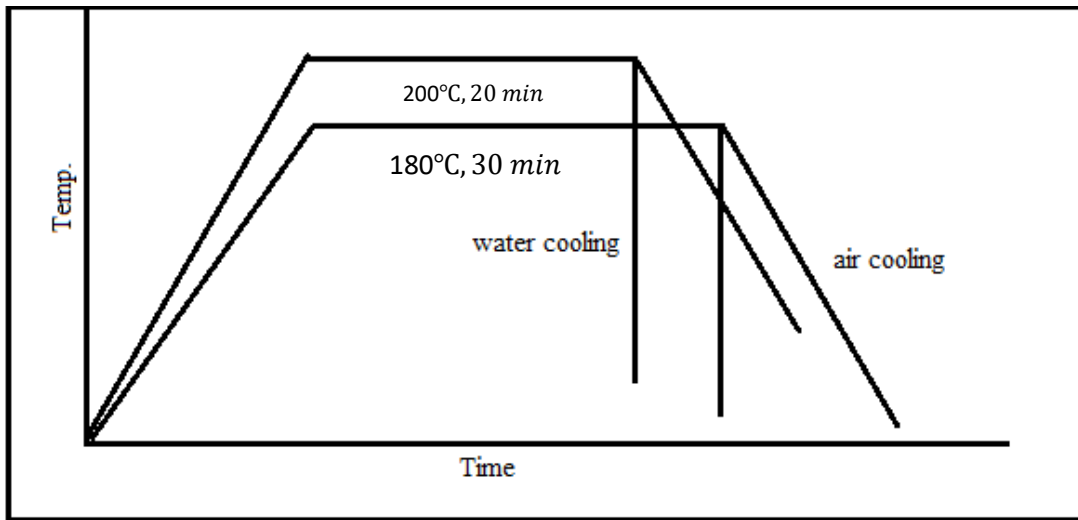


Figure (4-4): Procedure for preparing PS specimens

4.4 Annealing Treatment

The annealing treatment was carried out on PS specimen pressed under (76.19)MPa pressure at 180°C and cooled by air. The treatment was started by heating the oven temperature to 82°C for (1) hour in order to ensure the precise annealing treatment. The specimen was placed at 82°C for (12) hours in order to relax residual stresses and obtain stress free specimen [4] as shown in Figure (4-5). This specimen was adopted as reference specimen for evaluating through thickness residual stresses due to equation (2-13) which followed the principle of acoustoelasticity.

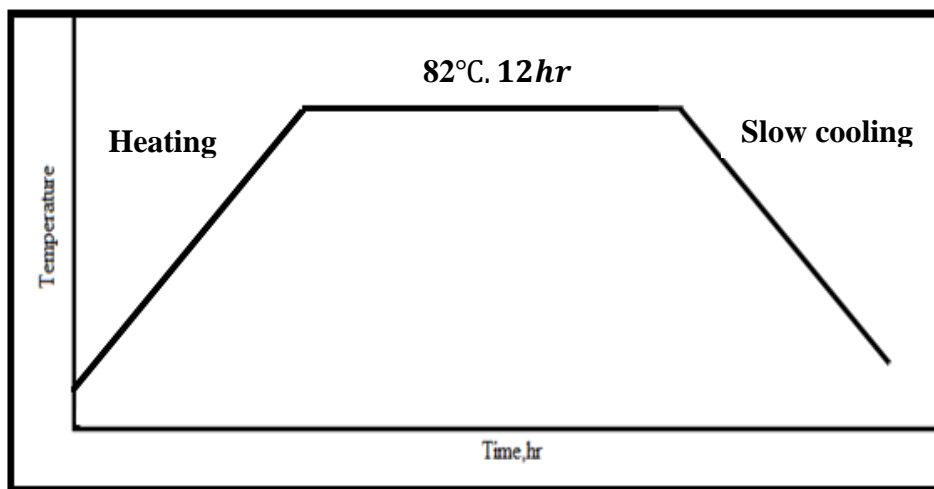


Figure (4-5): Annealing treatment of PS

4.5 Melt Flow Rate (MFR)

This instrument is used to study melt flow index. This test is a response to the needs of recycling facilities, which do not always need to know the technical parameters of the processed raw materials. MFI is often used to determine the polymer processing. For example, blow molding is more suitable than injection or rather pipe, film, or plates extrusion. MFR is compatible with standard ISO 1133 and ASTM D1238.

The melt flow rate testing instrument is SHI JIA ZHUANG ZHONG SHI TESTING MACHINE CO., LTD. It is found in the Engineering Materials College/University of Babylon. The measurement of melt flow index can be performed on (pellet, regrind, grind, powder, dry blend or cut pieces of the finished product (of 0.5cm size). The measurement is made under loading (0.325kg-21.6kg). MFI is often used to determine the polymer processing. Melt flow index MFI was calculated as average of (3) specimens. The applied weight is 0.063g, so MFI for PS is (3.72)g/10 min. at 180°C.

4.6 Differential Scanning Calorimeter

Thermal properties of materials were emphasized by differential scanning calorimeter (DSC) test. The hatch of DSC consists of two sample positions, one is employed as a sample and the other one as a reference where an inert material is used which does not have thermal transformations in the temperature scope under study. The differential scanning calorimeter is type TA-60 WS instrument (Shimadzu, Japan). It is available in laboratory of Materials Engineering College/University of Babylon.

Thermopile sensors were used to measure the variation in temperature between sample and reference and give the differential thermocouple voltage. The differential thermocouple voltage is transformed to energy per unit time by tool using the calibration constant. The heat flow rate versus temperature was obtainable for the sample and reference.

Glass transition temperature (T_g) is usually a range, over which the properties of an amorphous material change. Below T_g , materials exhibit a glassy, rigid structure; while above T_g , they are rubbery and flexible. Melting occurs over a temperature range in polymers due to the molecular weight distribution and range in crystal sizes as well as defects within the crystal. because amorphous materials can flow at higher temperatures but they do not melt.

4.7 Fourier Transform Infrared (FTIR)

In FTIR, Infrared radiation pass through the specimen. Some of the infrared radiation absorbed by the specimen and the other transmitted through it. The result of test refers to the molecular absorption and transmission creating molecular fingerprint of the specimen. Each molecular structure has single FTIR spectrum. FTIR device type IR Affinty-1(made in Japan) if found in Laboratory of Materials Engineering College/ University of Babylon. It is provided with a room temperature DTGS detector, mid-IR source. The wave length is (4000 to 400) cm^{-1} and a KBr beam splitter.

4.8 Density Test

Density test has been carried out for the verification of the material density by using high precision density tester type Densometer GP-120S with digital accuracy ($D = \pm 0.0001 \text{g/cm}^3$). The principle of Archimedes has been applied to measure the accurate balance using displacement method through the weight of samples. This device is found in Engineering Materials College /University of Babylon. The standard density of PS was $(1.05) \text{g/cm}^3$. According to air cooling from 180°C under (76.19MPa pressure), the specimen density was $(1.021) \text{g/cm}^3$. The cooling by water from the same temperature and pressure was produced increasing of density to 1.042g/cm^3 . There is no significant effect of applying pressure on density of specimens as compared with the standard density of PS.

4.9 Tensile Test

The dog bone tensile test specimen is cut according to ASTM D-638 type-V as shown in Figure (4-6). The load is increased continuously with deformation (stress with strain) until failure. The device of tensile test is Microcomputer Controlled Electronic Universal Testing Machine. It is found in Engineering Materials College / University of Babylon.

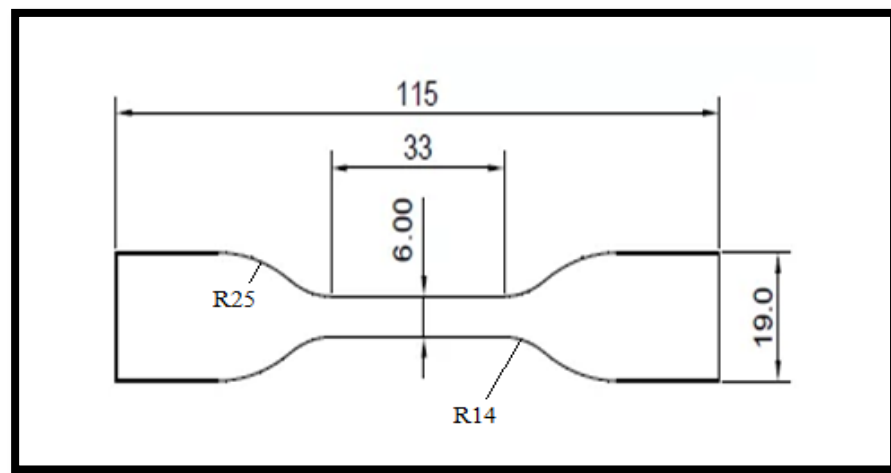


Figure (4-6):Tensile test specimen

4.10 Ultrasonic Pulse-Echo Test

The most popular non-destructive test is ultrasonic technique. It is capable to use within any field and gives fast scan for quality control test. The longitudinal ultrasonic waves were measured by using piezoelectric traducer which works as a transmitter and receiver in the same time. The acoustic couplant is a semi-liquid material. A couplant is placed between the specimen surface and transducer for enhancing the transmission of sound to the part in order to generate reliable inspection.

Pulse-echo test is easier to use as compared with transmission method and require only one side of the sample. In the state of pulse echo method, the emitter has employed to receive the ultrasonic signal. At an interface, the wave is reflected, then the signal go back to the transducer and revealed. The

ultrasonic wave then converted to an electrical signal by the same transducer and the electrical signal can be appeared on a screen.



Figure (4-7):The ultrasonic pulse echo device

The ultrasonic test is conducted with general purpose portable digital flow detector Siteman series Sonatest D-50 device with pulse-echo method to gain the longitudinal wave velocity of material as shown in Figure (4-7). The frequency and diameter of transducer are 2 MHz and 10 mm, the wave length is 0.0011m (11×10^5) nm. The device is made in United States of America.

The evaluation of through thickness residual stresses was carried out due to Equation (2-13) depending on the difference in ultrasonic longitudinal velocities between stressed specimens and stress free specimens. According to the principle of linear acoustoelasticity, the ultrasonic technique for stress measurement was depended on the linear relation between the propagation velocity of ultrasonic wave and mechanical stress of material. The measurement of residual stresses is based on the assumption of uniform acousto-elastic properties for tested material and a stable acousto-elastic constant (K). The

defects have negative effects on accuracy such as low homogeneity in materials texture, segregation in microstructure, cluster of inclusions.

According to the consideration of difference in morphology between batch to batch inside polymer components, through thickness residual stresses were determined twice in this work: first through thickness residual stresses in terms of K , second through thickness residual stresses are based on the acoustoelastic constant (K) for PS that determined experimentally from previous work. The acoustoelastic constant (K) of PS is $(-7.69 \times 10^{-4} \text{ MPa}^{-1})$ [7]. The two procedures in evaluating residual stresses were carried out at temperatures (180, 200)°C under various pressures (0, 45.714, 76.19, 106.667, 152.381)MPa. The ultrasonic velocity of reference (annealed) specimen (2260) m/s was approved in the evaluation of residual stresses.

Chapter Five
Results and Discussion

Chapter Five

Results and Discussion

5.1 Introduction:

The present material under study is (PS) that utilized as building material and fabricated as personal protective equipment. The quality of these products was affected by the distribution of residual stresses. This distribution was caused dimensionless changes, fractures and deformations. The residual stresses were made the manufactured parts unsuitable for use. The longitudinal ultrasonic velocity was measured for all specimens due to position under various applied pressure. Consequently residual stresses from pulse echo ultrasonic method were evaluated along specimen length and applied pressure.

5.2 Differential Scanning Calorimeter Test (DSC)

The differential scanning calorimeter (DSC) is obtained heat flow rate versus temperature and consequently the glass transition temperature (T_g). The average weight of specimen is $(8-10)\pm 5\text{mg}$ which placed into pans of aluminum. DSC test is carried out by heating the specimen from $(25-320)^\circ\text{C}$ with heating rate $10^\circ\text{C}/\text{min}$. The specimen is cooled down through the same rate into room temperature under an inert gas.

DSC curve of PS specimen is shown through Figure (5-1). The evaluated glass transition temperature of PS is $(93.52)^\circ\text{C}$ because of the presence of phenyl groups (benzene rings) into chemical structure that were responsible for high glass transition temperature [98]. The degradation of PS specimen is happened at $(320)^\circ\text{C}$. Melting in polymers occurs over a temperature range due to (molecular weight distribution, range in crystal sizes, defects within crystal). The melting range of PS is $(200-240)^\circ\text{C}$ because amorphous materials can flow at higher temperatures but they do not melt.

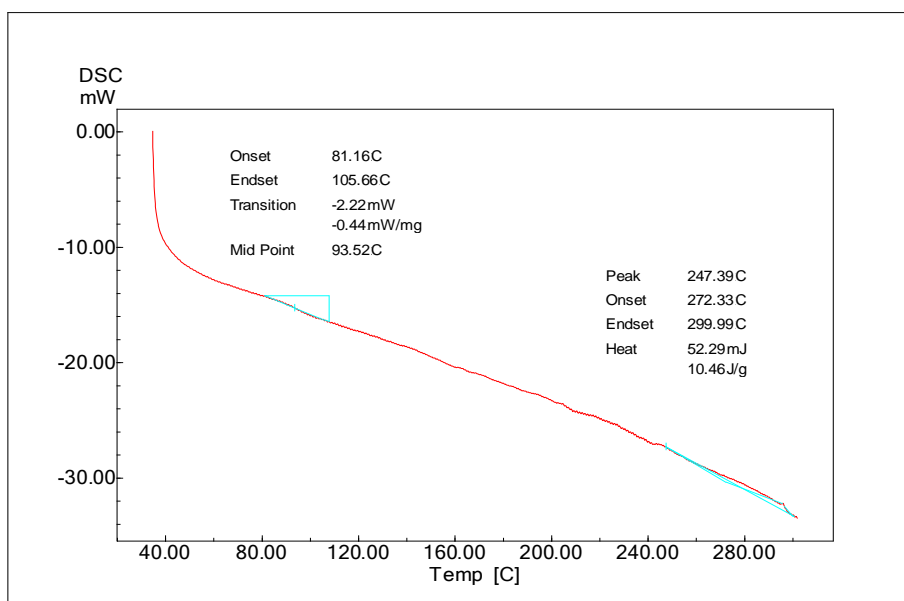


Figure (5-1):DSC curve of PS specimen

5.3 Fourier Transform Infrared Spectroscopy (FTIR)

One of the most famous tools is Fourier transform infrared (FTIR) spectroscopy. The role of FTIR role is identify and investigate the presence of different functional groups in polymers. Every molecule recognizes by the confirmed FTIR spectrum that refers to it. This tool is very important for materials analysis. Fourier transform infrared spectra technique was used for giving the fully characterization of prepared specimen from PS. FTIR is a relationship between percent of transmittance (T%) and wave number ($1/\text{cm}^{-1}$). Fourier transform infrared spectra of polystyrene in the range of wave number ($400\text{-}4000$) cm^{-1} is shown in Figure (5-2).

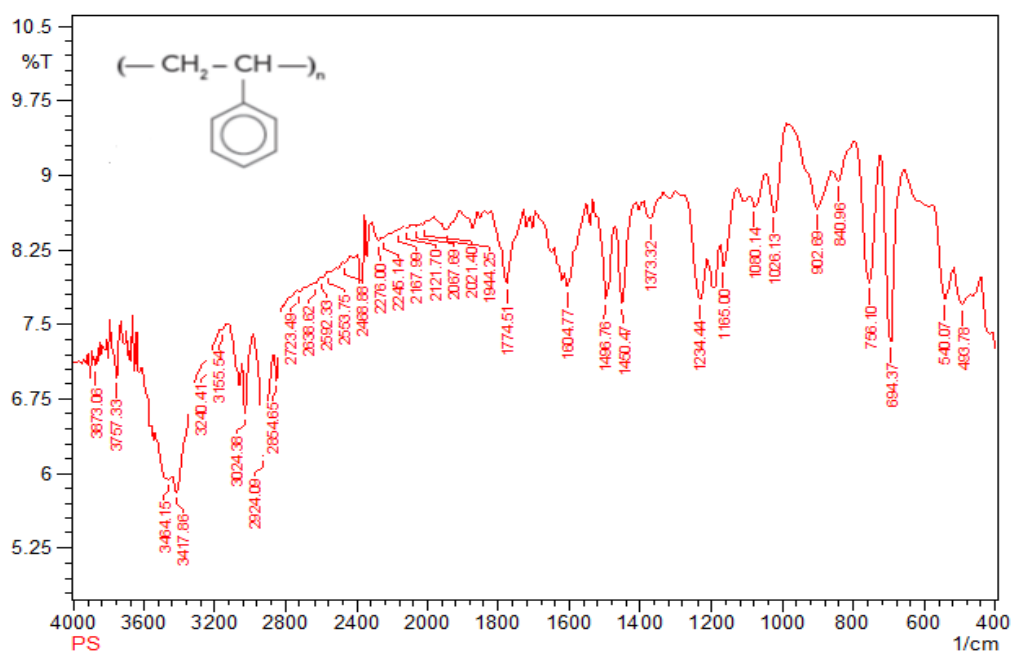


Figure (5-2): FTIR spectra of PS with standard and experimental bands

Table (5-1): Experimental and standard bands of PS

Type of band	Standard Polystyrene(cm^{-1})	Experimental Polystyrene(cm^{-1})
Aromatic C-H stretch	3025	3024
CH ₂ asymmetric and symmetric stretches	2923	2924.9
Aromatic ring stretch	1601	1604.77
Aromatic ring stretch	1492	1496.76
CH ₂ bond	1451	1450.47
Aromatic CH bond	1027	1025
Aromatic CH out of plane bend	753	756.1
Aromatic ring bend	694	694.37
Aromatic ring out of plane bend	537	540

5.4 Tensile Test

Tensile test is conducted to obtain the tensile strength and elastic modulus of PS specimen prepared with heating into 180°C, pressing under (5MPa). It was cooled rapidly by water and tested with strain rate (0.5mm/min). The stress-strain curve is shown at Figure (5-3). The tensile strength of PS specimen is (12)MPa, elastic modulus is (0.34)GPa. The standard tensile strength of PS is (16)MPa. The reduction in tensile strength produced from tensile test was belong to several sources:

- a-The presence of phenyl groups that is responsible for the resistance of polymer structure to rotation of chains that was lead to stiff and brittle polymer [98].
- b-The dependence of yield and post-yield stress on thermal history of polymer [147].
- c-The procedure of preparing PS specimen (application of pressure, water cooling) which was lead to generation of compressive residual stresses.



Figure (5-3) Stress-strain tensile curve of PS

It is important to characterize and monitor the elastic modulus of polymer in order to predict the lifetime of polymer component and prevent failure. The reduction in modulus of elasticity lead to structural failure [119]. The elastic modulus was obtained from tensile test is (0,34)MPa while the standard modulus is (1.5)GPa. The reason was belong to several reasons: the conditions of preparing specimen due to)temperature, pressure, cooling with water), branching, density and molecular weight (35000)g/mole as agreed with [119].

5.5 Ultrasonic Longitudinal Velocity

The distribution of ultrasonic longitudinal velocities that passed through air cooled and water cooled specimens from (180,200)°C under various pressures (0, 45.714, 76.19, 106.667, 152.381)MPa along the specimen length at the distances (25, 75, 125)mm on 150mm length were shown in Figures (5-4 to 5-7). The velocities of ultrasonic waves produced from pulse-echo test were varied in the range (2000-2500) m/s through Figures (5-4) and (5-5) due to air and water cooling from (180)°C. This range of velocity was consolidated with [7] except air cooled specimen under (152.381)MPa pressure where the longitudinal velocity was diminished approximately to (250m/s) at a distance of (25)mm along specimen length.

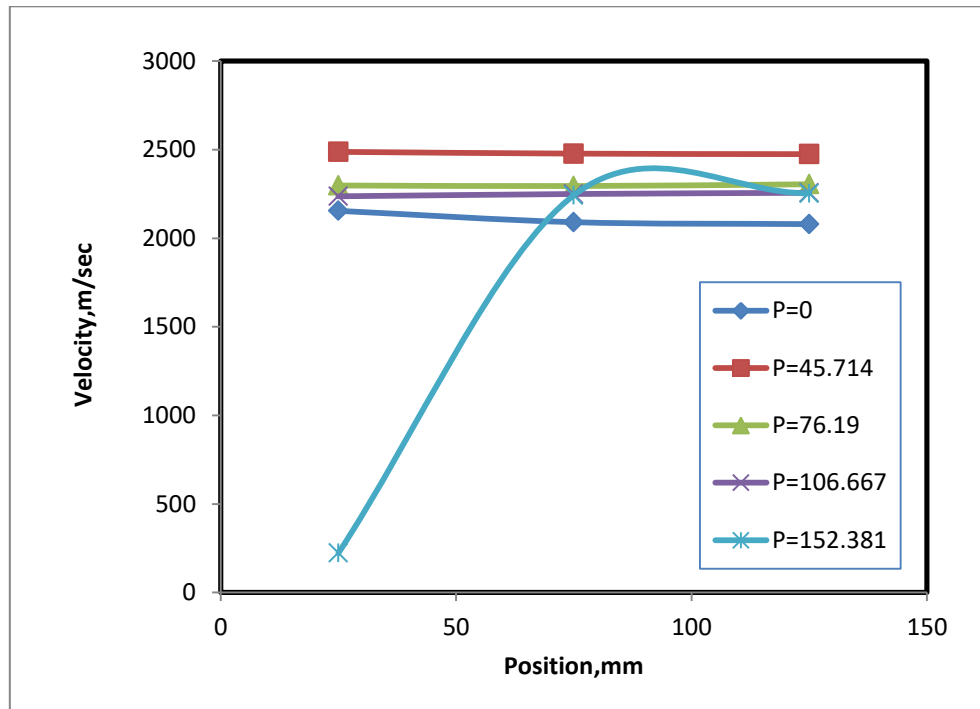


Figure (5-4): Longitudinal velocity along specimen length cooled by air from 180°C under various pressures

The applied pressure (45.714)MPa with air and water cooling was produced maximum velocity. Maximum pressures (106,667, 152,381)MPa were lead to maximum ultrasonic velocity as agreed with [119] where cooling by water was generated compressive residual stresses and the application of high applied pressures. These conditions were lead to increase in density and consequently ultrasonic velocity. The pulse-echo test of (2MHz) frequency is good for penetrating into thin and highly attenuated materials. Consequently, pulse-echo test gives more accurate ultrasonic velocities than transmission test as agreed with [119].

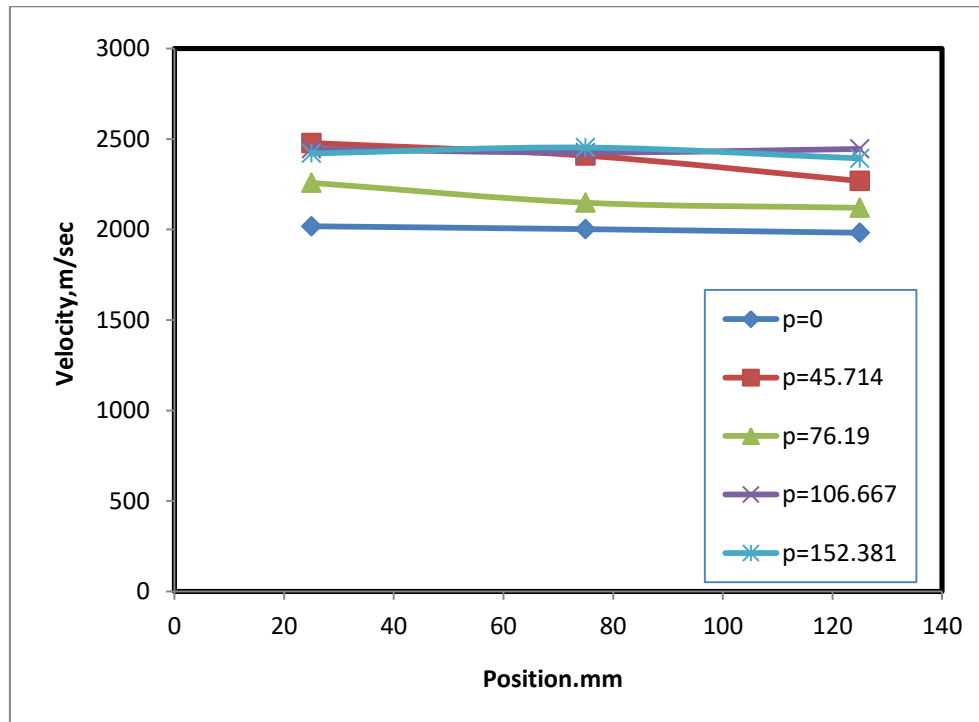


Figure (5-5): Longitudinal velocity along specimen length cooled by water from 180°C under various pressures

According to Figures (5-6, 5-7), the distribution of ultrasonic velocities was uniform and convergent in the range of (2000-2500) m/s due to air and water cooling that consistent with [148]. Maximum ultrasonic velocity greater than (2500)m/s was obtained at (152.381)MPa pressure due to slow and rapid cooling from 200°C, this behavior is agreed with [119] and suited to hypothetical behavior. This behavior was stated that increasing in applied pressure lead to increase in density and consequently ultrasonic velocity.

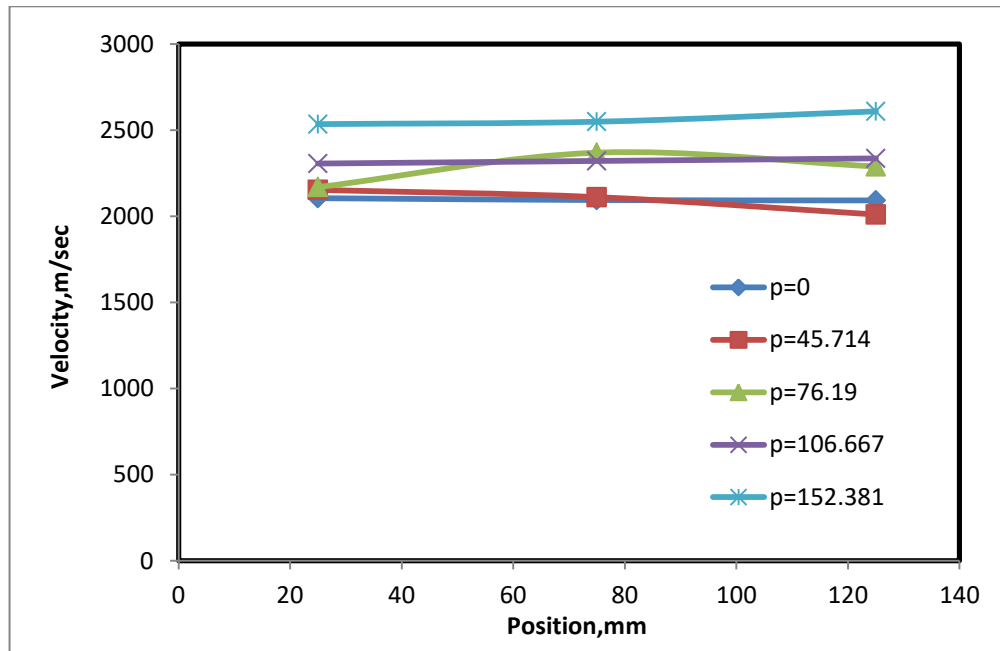


Figure (5-6): Longitudinal velocity along specimen length cooled from 200°C by air under various pressures

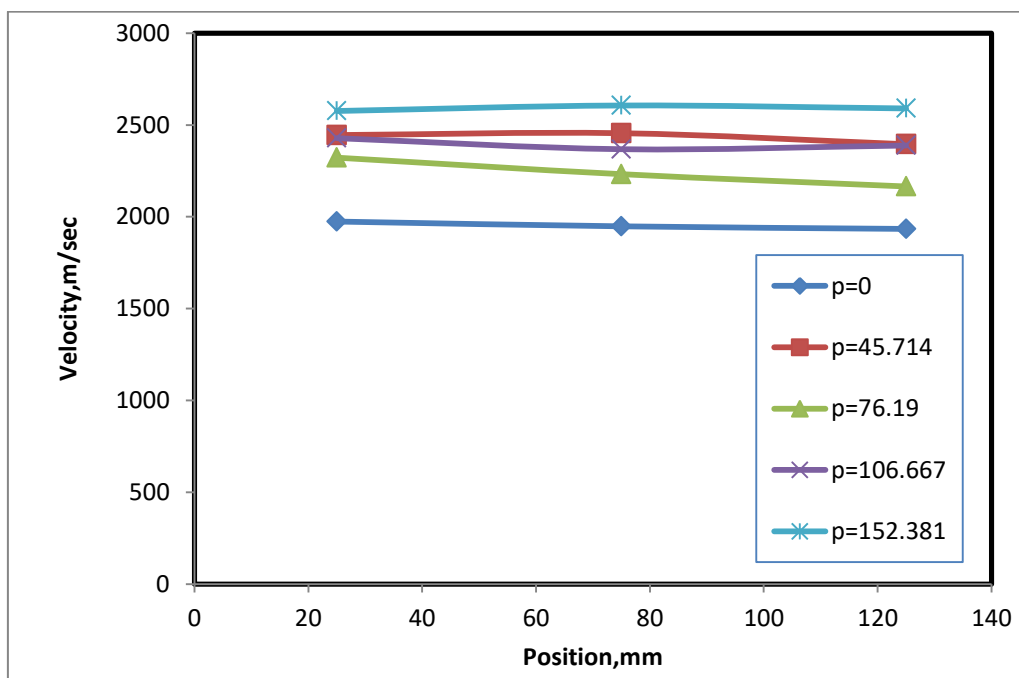


Figure (5-7): Longitudinal velocity along specimen length cooled from 200°C by water under various pressures

5.6 Residual Stresses in Terms of Acoustoelastic Constant

The evaluation of through thickness residual stresses was carried out due to Equation (2-11) depending on the difference in ultrasonic longitudinal velocities between stressed specimens and stress free specimens. According to the principle of linear acoustoelasticity, the ultrasonic technique for stress measurement was depended on the linear relation between the propagation velocity of ultrasonic wave and mechanical stress of material [81].

Through thickness residual stresses were determined and drawn twice: first through thickness residual stresses in terms of K , second through thickness residual stresses are based on the acoustoelastic constant (K) for PS that determined experimentally from reference [7]. The two procedures in evaluating residual stresses were carried out at temperatures (180, 200)°C under various pressures (0, 45.714, 76.19, 106.667, 152.381)MPa. The ultrasonic velocity of reference (annealed) specimen (2260) m/s was approved in the evaluation of residual stresses.

5.6.1 Residual stresses along specimens length

The residual stress distribution for PS specimens along their length under various pressures due to air and water cooling from 180°C were sketched in terms of acoustoelastic constant (K) because of the unfeasibility of determining it over this thesis work. According to figure (5-8), maximum tensile and compressive residual stresses due to uniform air cooling were obtained under (zero, 45.714)MPa respectively. On the other hand, minimum residual stresses (approximately zero) were happened under high applied pressures (106.667, 152.381) MPa.

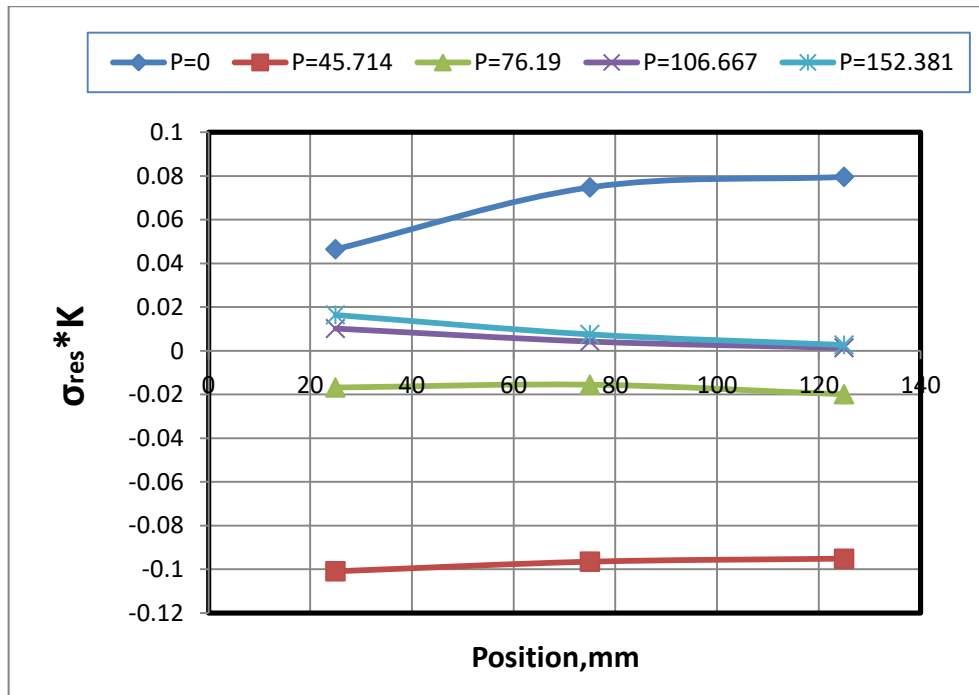


Figure (5-8): Residual stresses in terms of K along air cooled specimen from 180°C under various pressures

Figure (5-9) was represented the generation of tensile residual stresses without applied pressure and under (76.19)MPa pressure due to water cooling. The corresponding compressive residual stresses were occurred under (45.714, 152.381)MPa pressures. According to pressure (106.667)MPa, there was increasing to maximum compressive residual stress (-0.8/K)MPa at 25mm from one limb of specimen.

Figure (5-10) was shown for PS specimens cooled from 200°C with uniform temperature distribution by air cooling. The increasing in applied pressure lead to transform the residual stresses from tensile to compressive under (76.19)MPa. It could be observed that maximum applied pressure (152.381)MPa was produced maximum compressive residual stresses. The pressure (0,45.714)MPa was induced maximum tensile residual stresses.

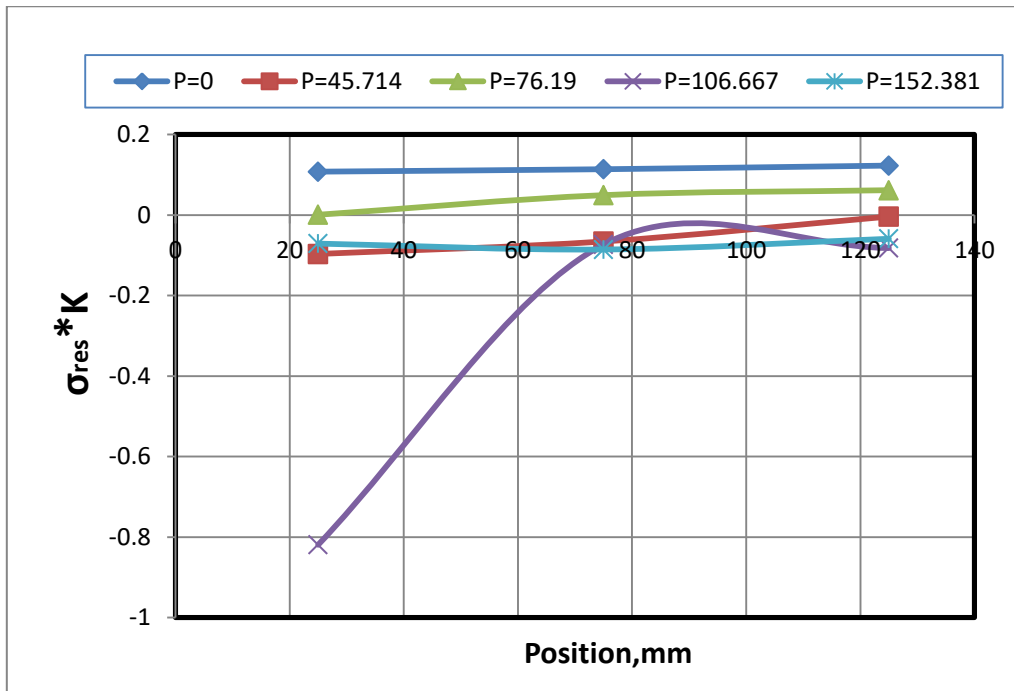


Figure (5-9):Residual stresses in terms of K along water cooled specimen from 180°C under various pressures

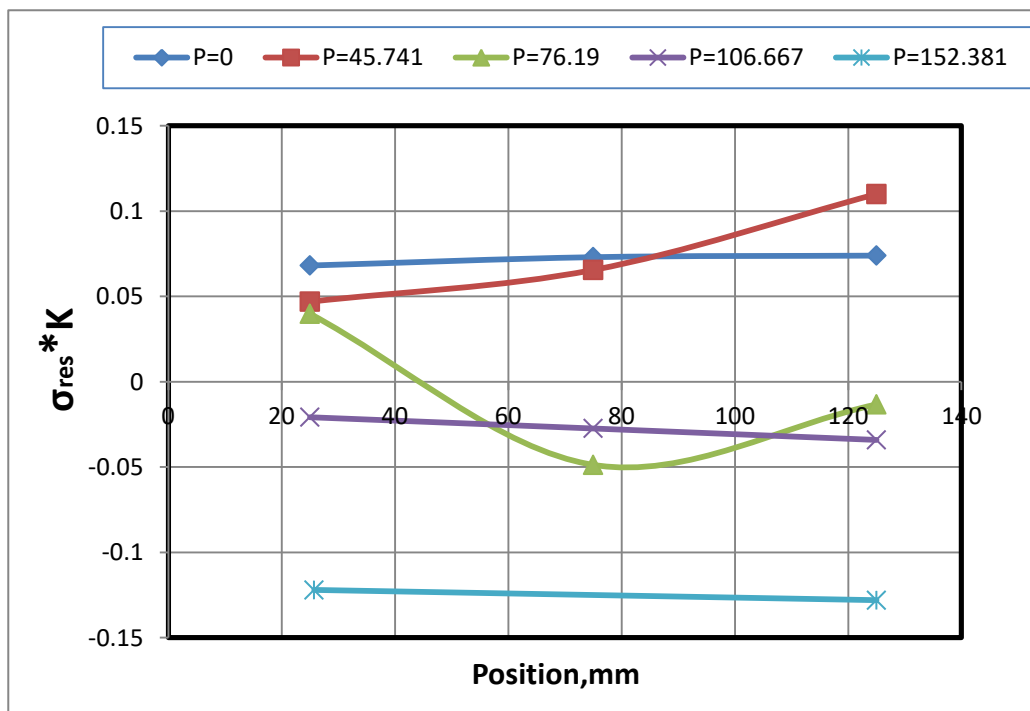


Figure (5-10):Residual stresses in terms of K along air cooled specimen from 200°C under various pressures

According to Figure (5-11), maximum tensile and compressive residual stresses were obtained without applying pressure and under (152.381)MPa

respectively. The pressure (76.19)MPa was caused transition in residual stresses from compressive to tensile along the specimen length.

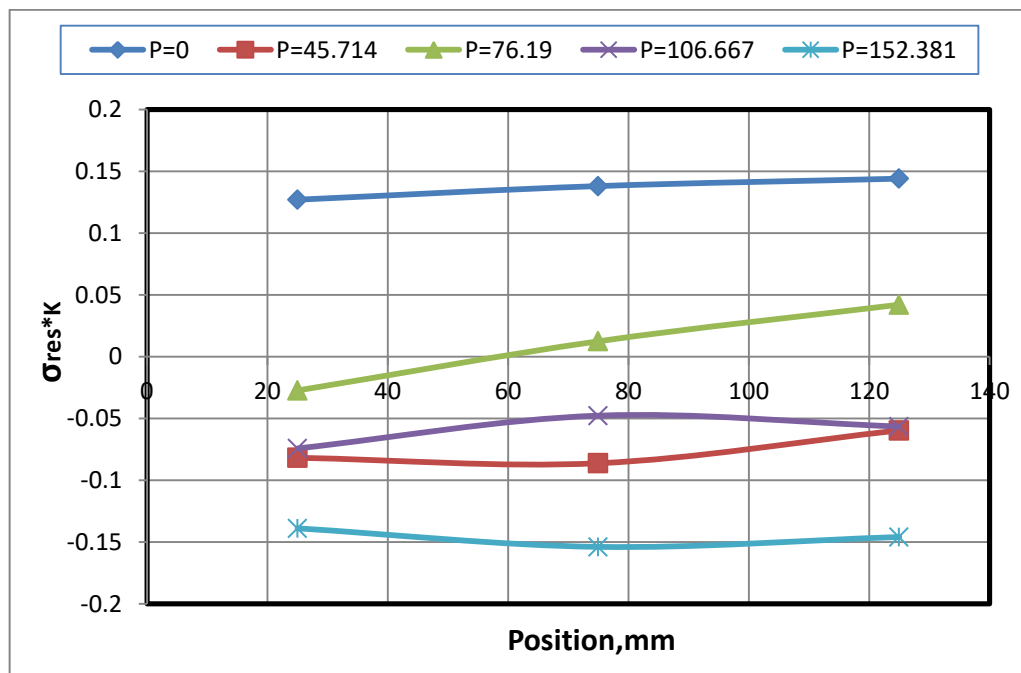


Figure (5-11): Residual stresses in terms of K along water cooled specimen from 200°C under various pressures

The discussed results through Figures (5-4 to 5-11) for both air and water cooling from (180, 200)°C were verified the approval with theoretical rule. This rule is referred to that compressive residual stresses were corresponded with increasing the ultrasonic velocity. On the other hand, tensile residual stresses were related with decreasing in ultrasonic velocity that guaranteed with [19].

5.6.2 Residual stresses due to various applied pressures

The residual stresses in terms of K for PS specimens cooled by air and water from 180C under various pressures at the three distances (25, 75, 125)mm along the specimen length were described in Figures (5-12, 5-13, 5-14). For (25)mm distance under air cooling through Figure (5-12), the behavior of residual stress is transformed from tensile at zero pressure to compressive at (45.714, 76.19)MPa, then transforms to tensile at higher pressures (106.667,152.381)MPa. The same behavior was shown at the distances (75,

125)mm from Figures (5-13, 5-14) respectively. The uniform cooling system in air was essential to reduce the risk of environmental stress cracking in moldings [37]. On the other hand, the behavior under slow cooling was conformed with [16] where the compressive residual stresses were converted into tensile residual stresses by applying external pressure.

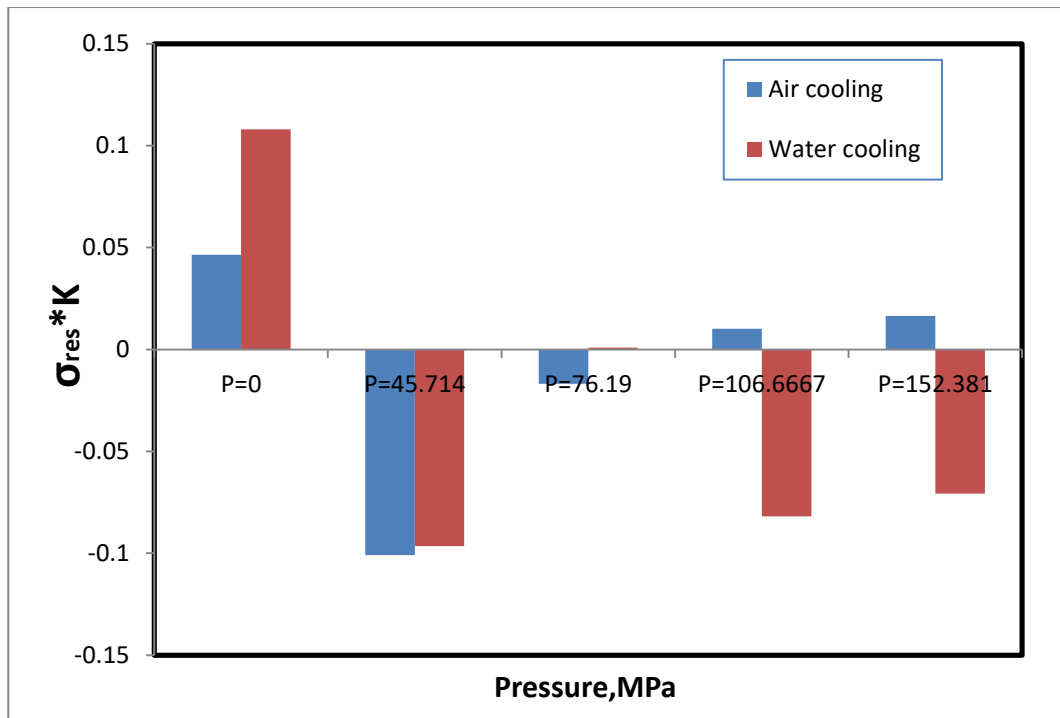


Figure (5-12): Residual stresses in terms of K at 25mm for all specimens cooled from 180°C

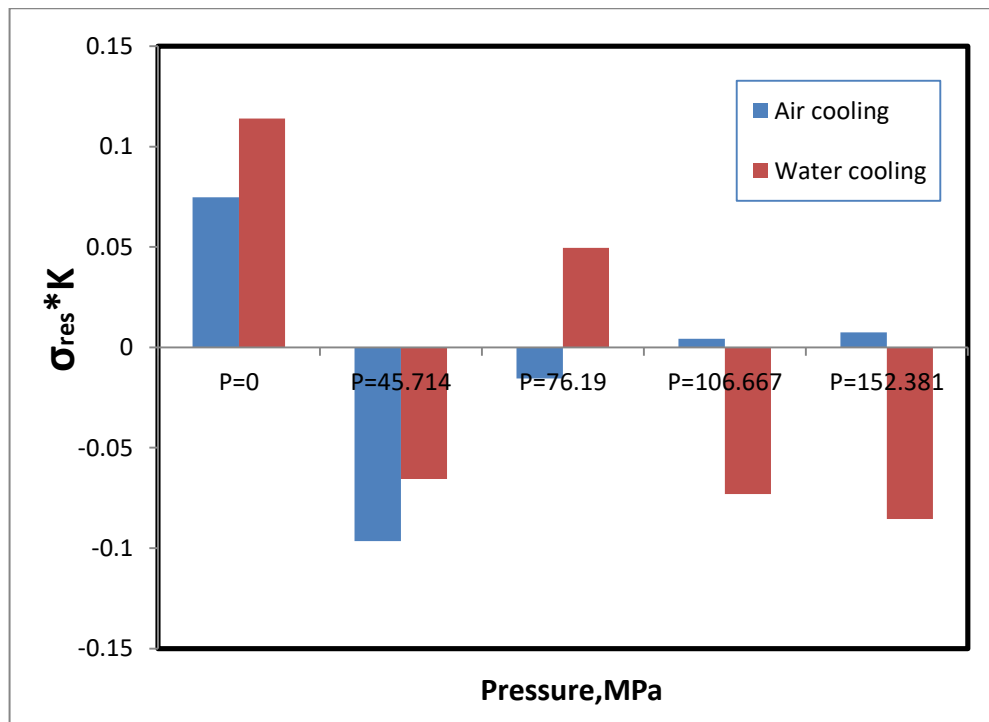


Figure (5-13): Residual stresses in terms of K at 75mm for all specimens cooled from 180°C

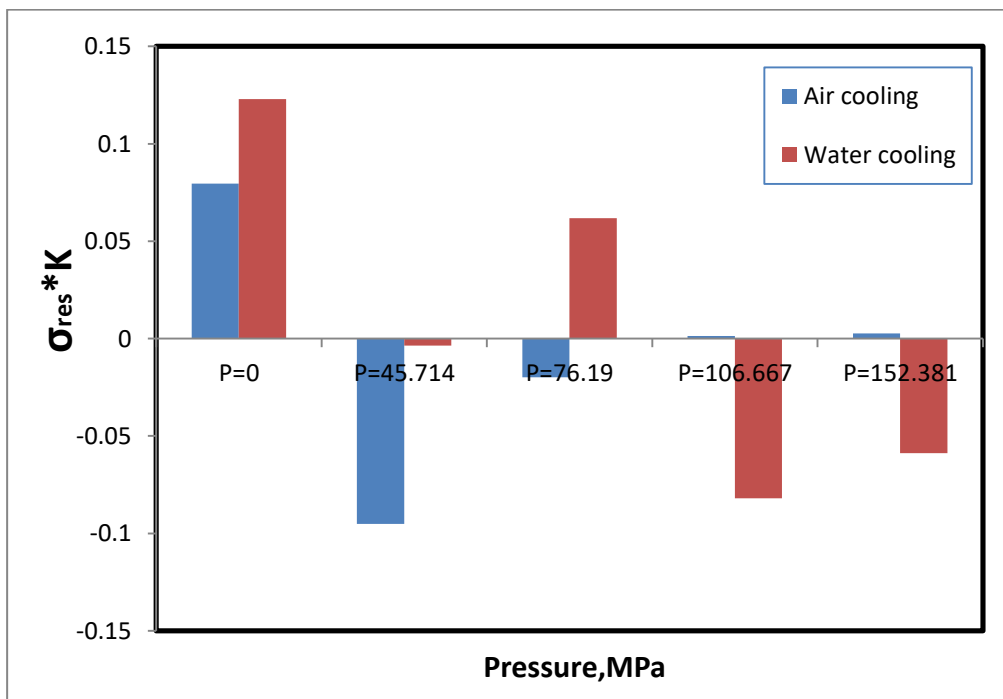


Figure (5-14): Residual stresses in terms of K at 125mm for all specimens cooled from 180°C

For (25)mm under water cooling, the behavior of residual stresses from Figure (5-12) was transformed from tension under zero pressure to compression under (45.714)MPa. There are two other transformations one to tension under (76.19)MPa and another to compression under higher pressures (106.667, 152.381)MPa. The same pattern of behavior was represented at distances (75, 125)mm through Figures (5-13, 5-14) respectively. The generation of compressive stresses under (45.714)MPa was a natural result to the rapid quenching. The tensile stresses under (76.19)MPa were produced because the compressive residual stresses were converted into tensile residual stresses by applying external pressure as stated in [16].

Finally, the origin of generation compressive residual stresses under (106.667, 152.381)MPa was belong to high pressures of pressing and fast cooling with water. This behavior was guaranteed with [119] where the rapid cooling in water with high applied pressures were increased material density and consequently ultrasonic velocity. Consequently increase in velocity was indicated the presence of compressive residual stresses [77].

The residual stresses in terms of K for PS specimens cooled by air and water from 200°C under various pressures were described over Figures (5-15, 5-16, 5-17) at three distances (25, 75, 125)mm along the specimen length. According to air cooling, the behavior of residual stress was transformed from tensile at (0, 45.714, 76.19)MPa pressure to compressive at higher pressures (106.667,152.381)MPa.

The behavior at the distances (75, 125)mm through Figures (5-16, 5-17) was transformed from tension under (0, 45.714)MPa to compression under (76.19, 106.667,152.381)respectively. Generally, the lower pressures was formed tensile residual stresses while higher pressures formed compressive residual stresses. The generation of tensile residual stresses were particularly dangerous as they were directly exposed to chemical contamination and

therefore significantly increase the risk of environmental stress cracking in components made from PS [37].

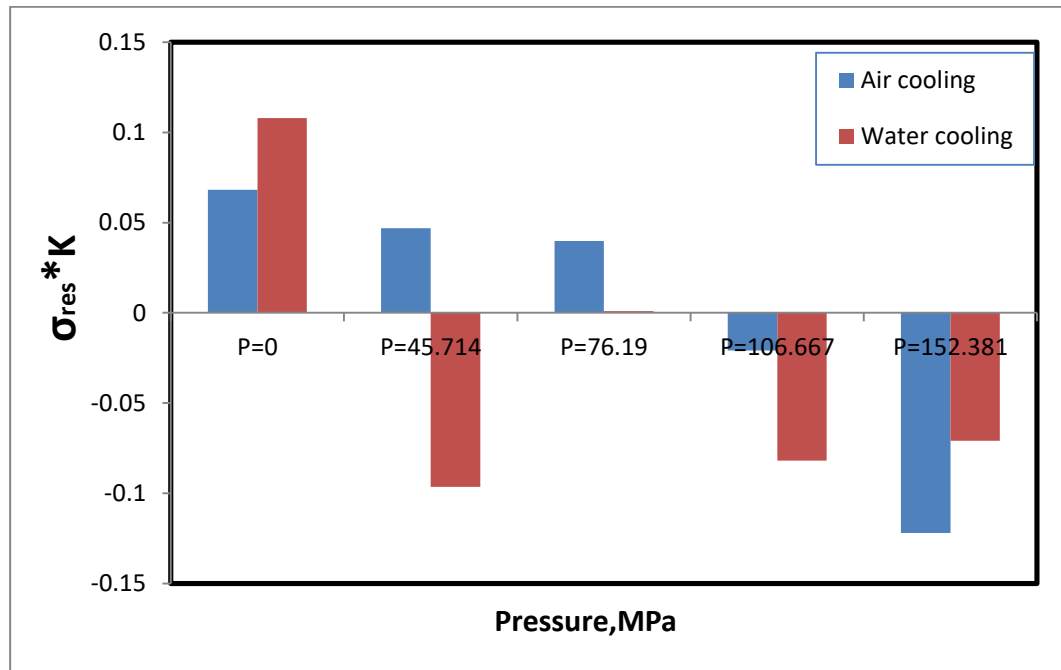


Figure (5-15): Residual stresses in terms of K at 25mm for all specimens cooled from 200°C

For (25)mm under water cooling, the behavior of residual stresses from Figure (5-15) was transformed from tensile under zero pressure to compression under (45.714, 76.19, 106.667, 152.381)MPa. The behavior at distances (75, 125)mm in Figures (5-16, 5-17) respectively was transformed from tensile under zero pressure to compressive under (45.714)MPa.

There was another transformation to tensile at (76.19)MPa and consequently to compressive due to higher pressures (106.667, 152.381)MPa. The reason was that water quenching lead to formation of compressive residual stresses. The range of residual stresses was between (-0.15 to 0.15) for PS specimens.

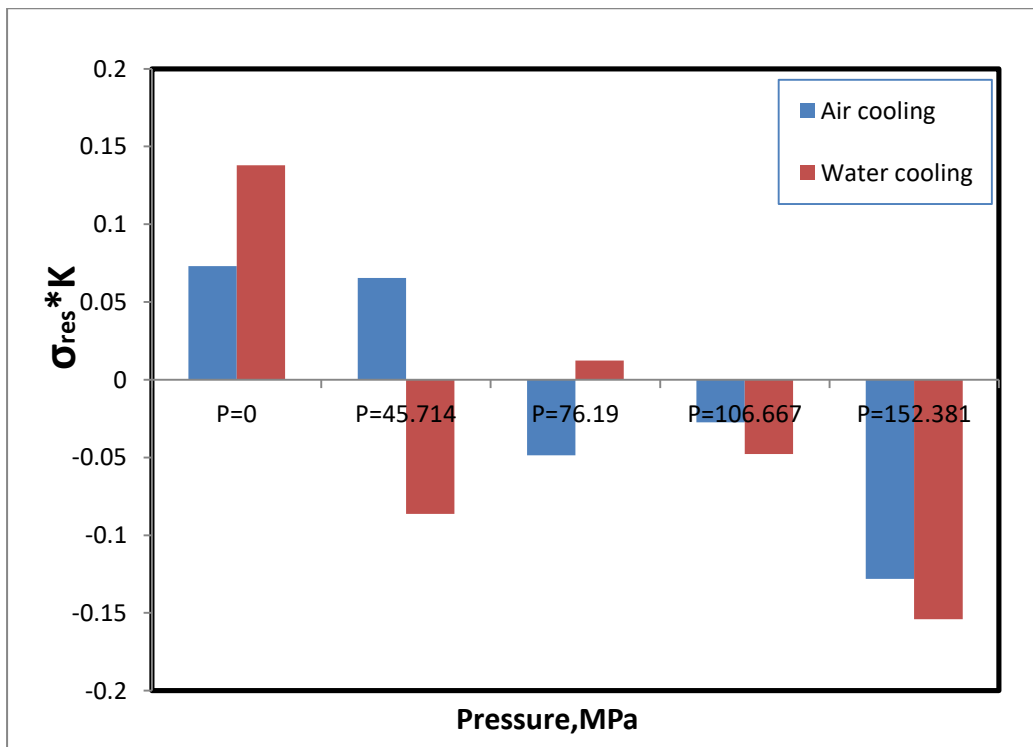


Figure (5-16): Residual stresses in terms of K at 75mm for all specimens cooled from 200°C

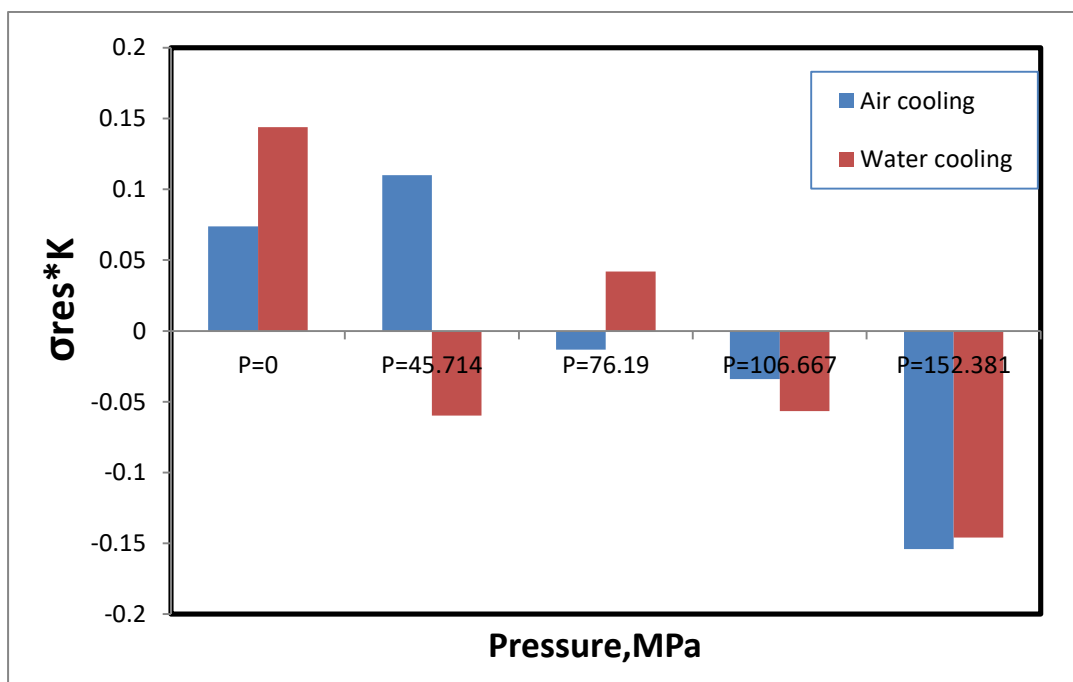


Figure (5-17): Residual stresses in terms of K at 125mm for all specimens cooled from 200°C

5.7 Evaluated Residual Stresses

5.7.1 Residual stresses along specimen length

The evaluated residual stresses for PS specimens cooled from (180, 200)°C by air and water were expressed under various pressures along the length of specimens through Figures (5-18 to 5-27). From Figure (5-18), it can be observed that maximum tensile and compressive residual stresses were obtained under (0, 45.714)MPa due to air cooling. According to water cooling from Figure (5-19), maximum tensile and compressive residual stresses were obtained under (0, 45.714, 106.667, 152.381)MPa pressures respectively. On the other hand, the higher pressures (106.667, 152.381) due to slow cooling were diminished residual stresses into approximately zero.

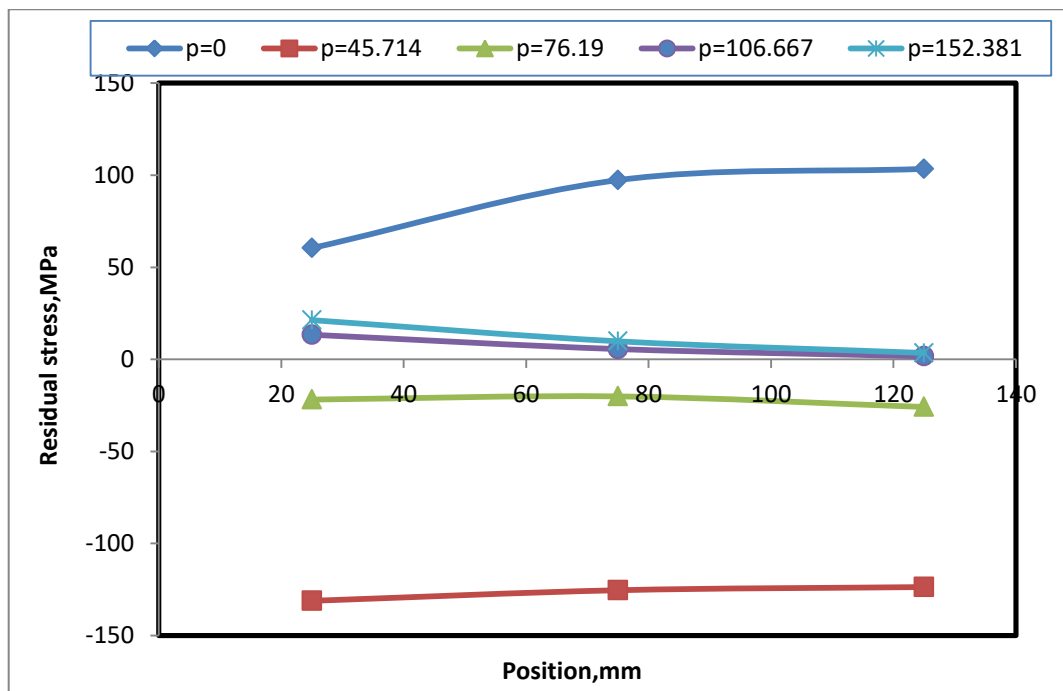


Figure (5-18): Evaluated residual stresses along air cooled specimens from 180°C under various pressures

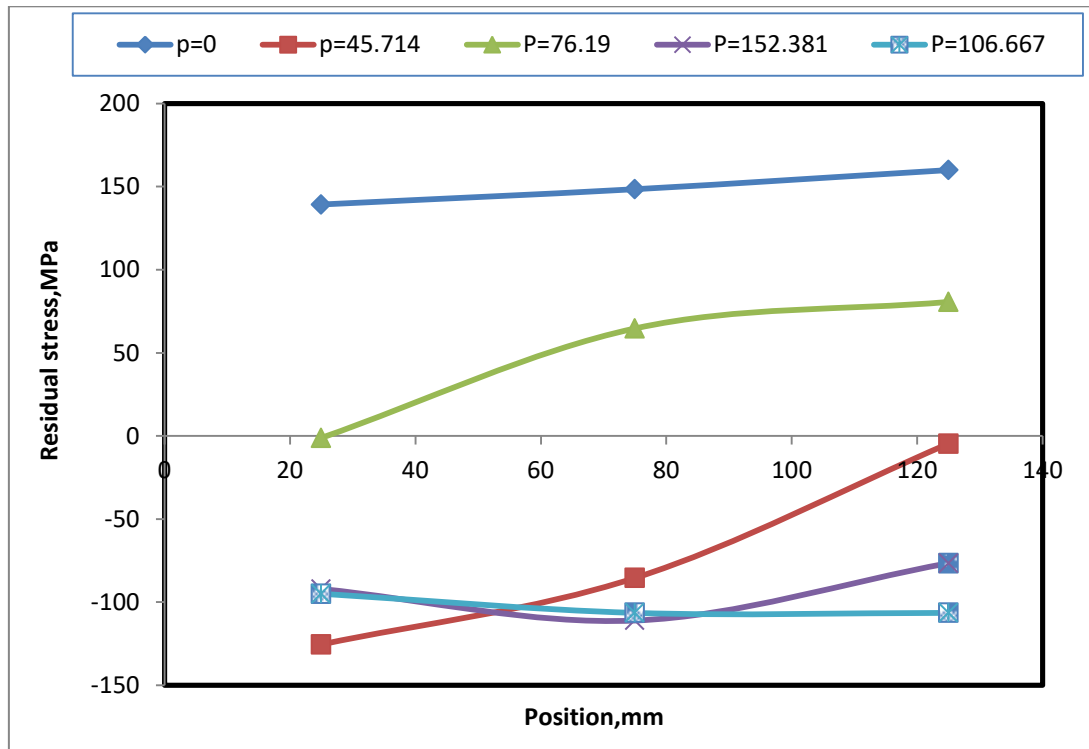


Figure (5-19): Evaluated residual stresses along water cooled specimens from 180°C under various pressures

In Figure (5-20), The distribution of air cooled residual stresses along specimens length under various pressures was shown tensile residual stresses under pressures (0, 45.714)MPa. The prepared specimens under (76.19, 106.667, 152.381)MPa pressures were undergone compressive residual stresses. Maximum compressive stress was obtained at pressure (152.381)MPa in the range of residual stresses between (-200 to 150)MPa.

The distribution of residual stresses versus position for water cooled specimens was varied. The variation was from tensile under zero pressure to compressive under (45.714, 106.667, 152.381)MPa. The range of residual stresses (-200 to 200)MPa as shown in Figure (5-21). The residual stress under (76.19)MPa was at equilibrium between compressive and tensile through the specimen thickness.

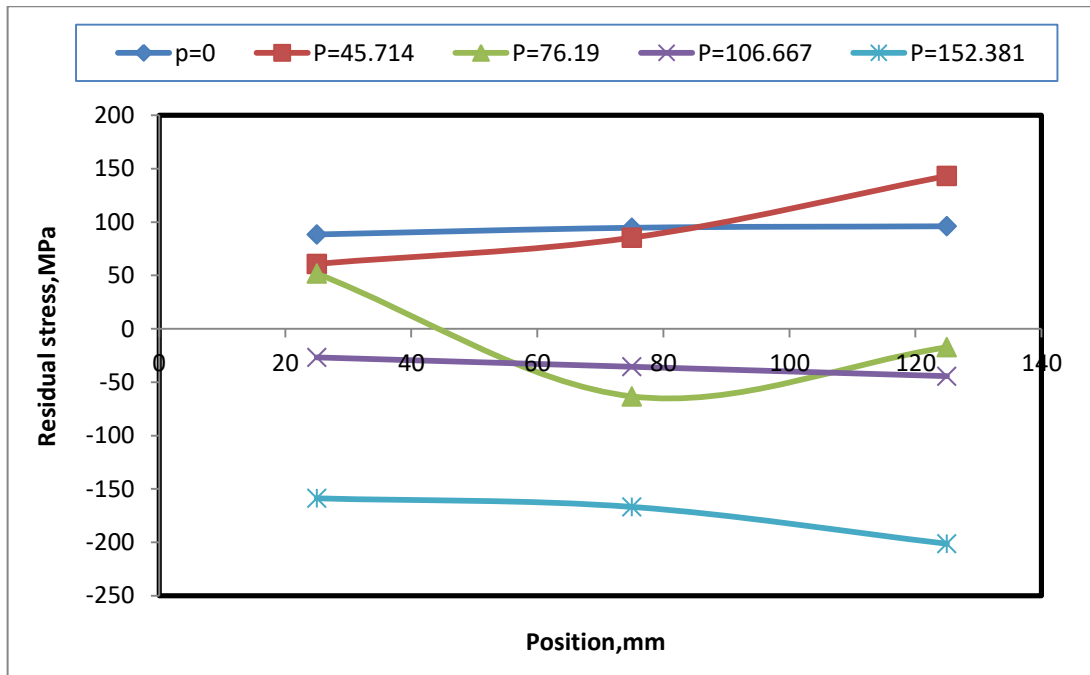


Figure (5-20):Evaluated residual stresses along air cooled specimen from 200°C under various pressures

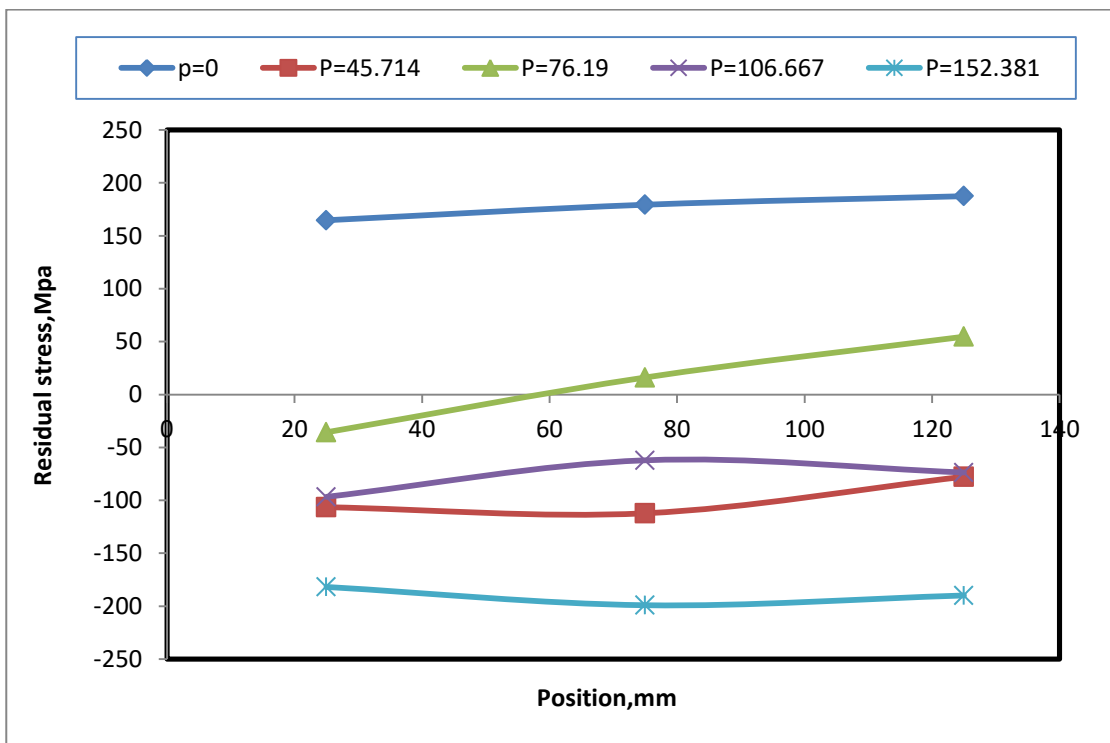


Figure (5-21):Evaluated residual stresses along water cooled specimen from 200°C under various pressures

The comparison between distribution of residual stresses and ultrasonic velocities through Figures (5-18, 5-19, 5-20, 5-21 and 5-4, 5-5). The results

were approved with theoretical rule. This rule was stated that compressive residual stresses were corresponding to increment in velocity. On the other hand, tensile residual stresses were related with velocity decrement [77, 19]

5.7.2 Residual Stresses According to Various Applied Pressures

The evaluated residual stresses along specimens length cooled from 180°C with air and water under various applied pressures were described through Figures (5-22, 5-23, 5-24). For (25)mm distance under air cooling through Figure (5-22), the behavior of residual stress was transformed from tensile under zero pressure to compressive at (45.714, 76.19)MPa. There was other transformation to tensile under higher pressures (106.667,152.381)MPa.

The same pattern of behavior was appeared at the distances (75, 125)mm from Figures (5-23, 5-24) due to air cooling. The air cooling was essential to reduce the risk of environmental stress cracking in moldings [37].

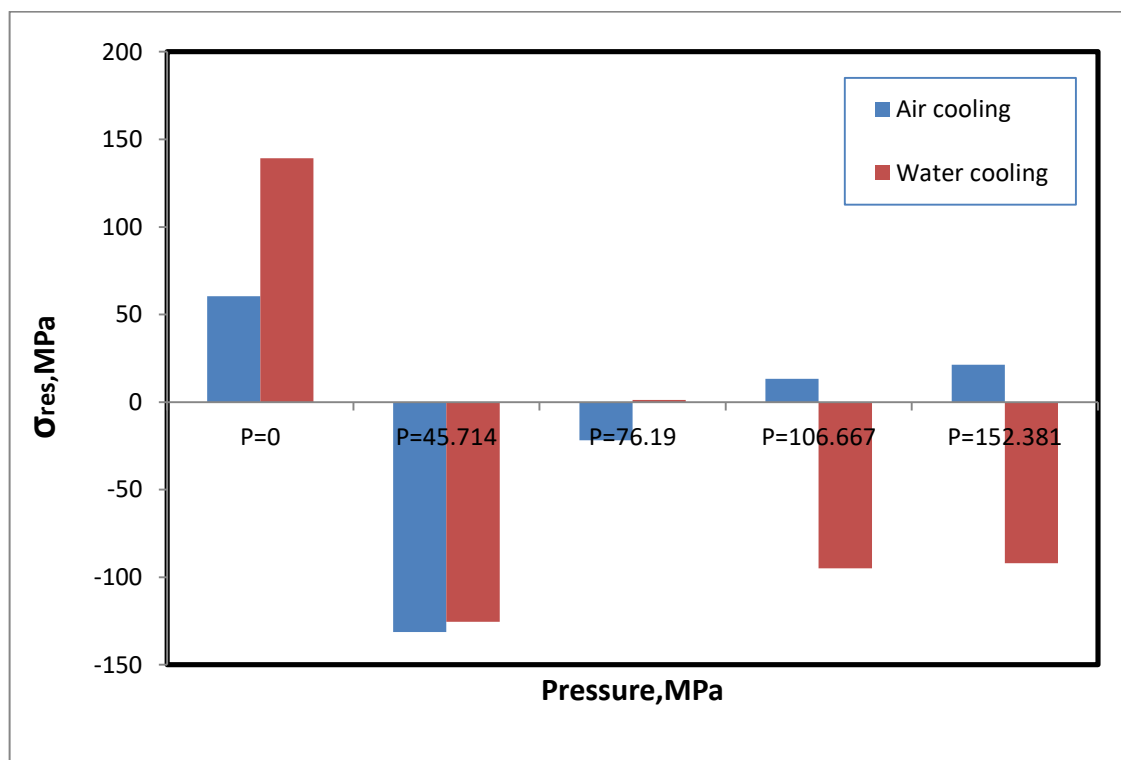


Figure (5-22): Evaluated Residual stresses at 25mm for all specimens cooled from 180°C

For (25)mm under water cooling, the behavior of residual stresses from Figure (5-22) was transformed from tensile under zero pressure to compressive under (45.714)MPa. There is another transformation into tensile under pressure of (76.19)MPa. Finally the behavior was become compressive under (106.667, 152.381)MPa. The same pattern of behavior was observed through Figures (5-23, 5-24) due to the distances (75, 125)mm.

According to the distance (75)mm, the sequence of through thickness residual stresses was as follows: (97.342, -125.436, -20.139, 5.569, 9.782)MPa with respect to air cooling and the same sequence of applied pressures. It was noted that the tensile stresses under higher pressures were less than tensile strength of PS (12)MPa. For water cooling, the residual stresses were (148.452, -85.432, 64.666, -106.448, -111.051)MPa. The evaluated residual stresses were guaranteed with [86, 76, 25] and similar to the corresponding behavior from water cooling from 180°C without introduction of (K) through Figures ((5-12), (5-13), (5-14)).

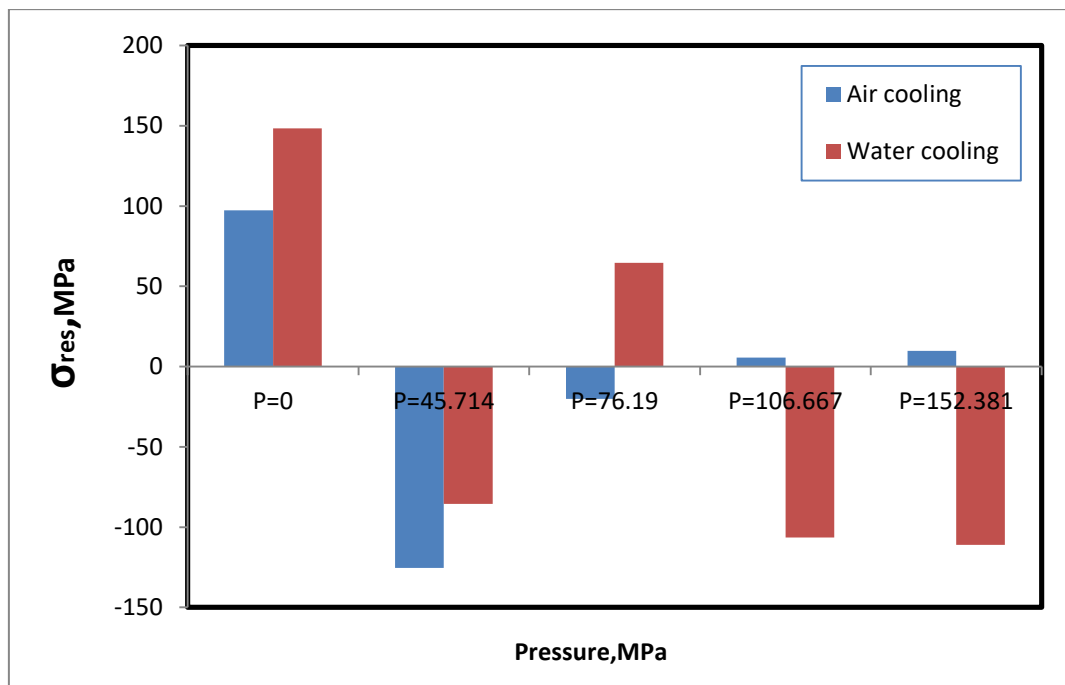


Figure (5-23): Evaluated Residual stresses at 75mm for all specimens cooled from 180°C

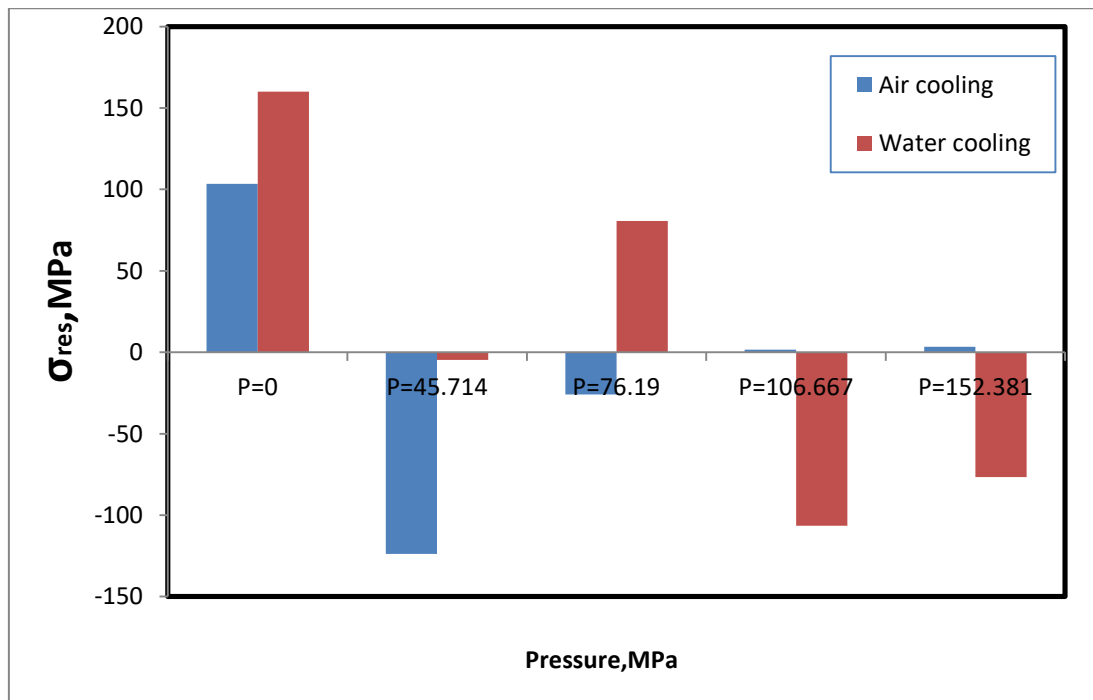


Figure (5-24): Evaluated Residual stresses at 125 mm for all specimens cooled from 180°C

The evaluated residual stresses at three distances (25, 75, 125)mm with air and water cooling from 200°C under various applied pressures were expressed through Figures (5-25, 5-26, 5-27). According to air cooling, Figure (5-25) was described the residual stresses at (25)mm where the behavior was transformed from tension under pressures of (0, 45.714, 76.19)MPa to compression under (106.667, 152.381)MPa.

The same previous pattern of behavior was observed in Figures (5-26, 5-27) due to the distances (75, 125)mm except residual stress under (76.19)MPa was compressive instead of tensile. The uniform slow cooling is essential to reduce the risk of environmental stress cracking in moldings [37].

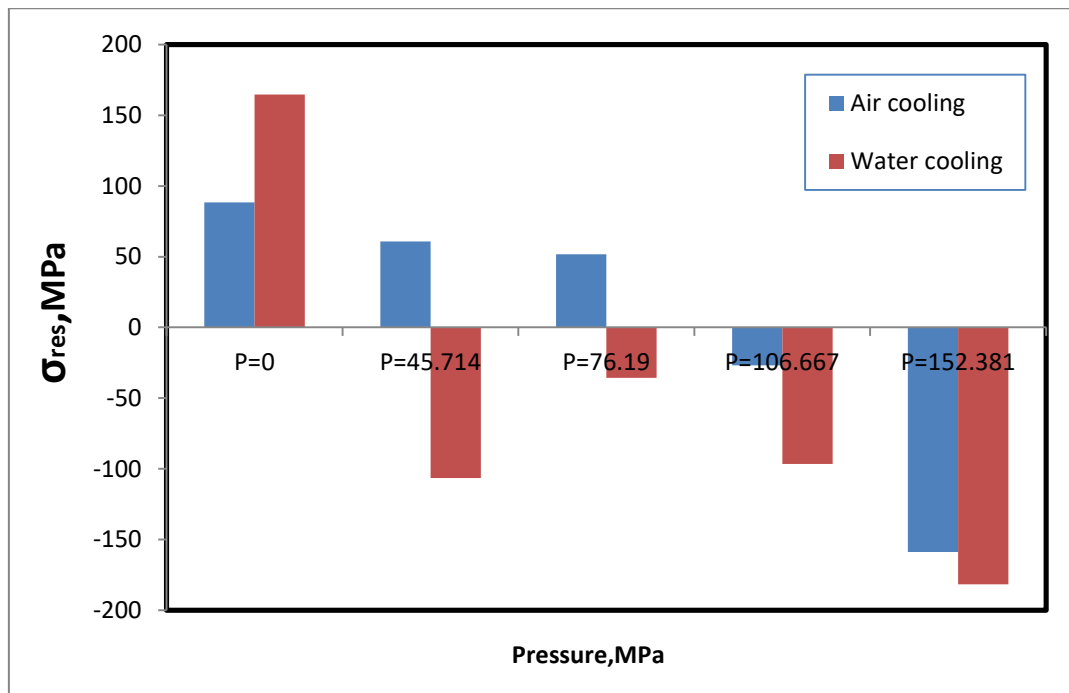


Figure (5-25): Evaluated Residual stresses at 25 mm for all specimens cooled from 200°C

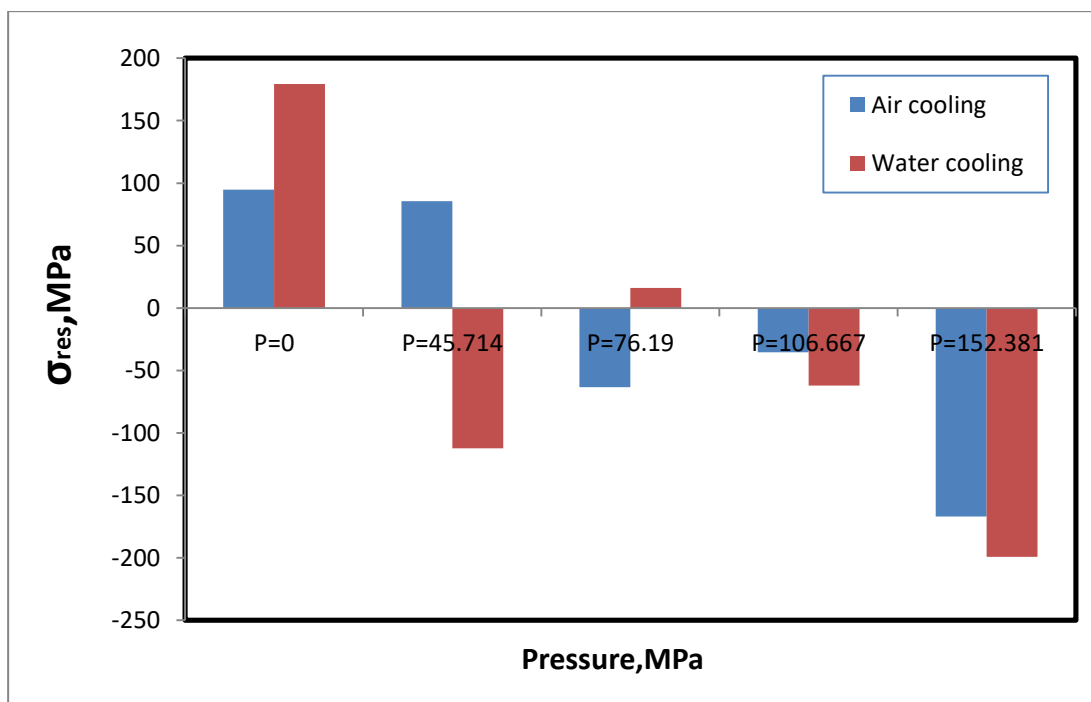


Figure (5-26): Evaluated Residual stresses at 75 mm for all specimens cooled from 200°C

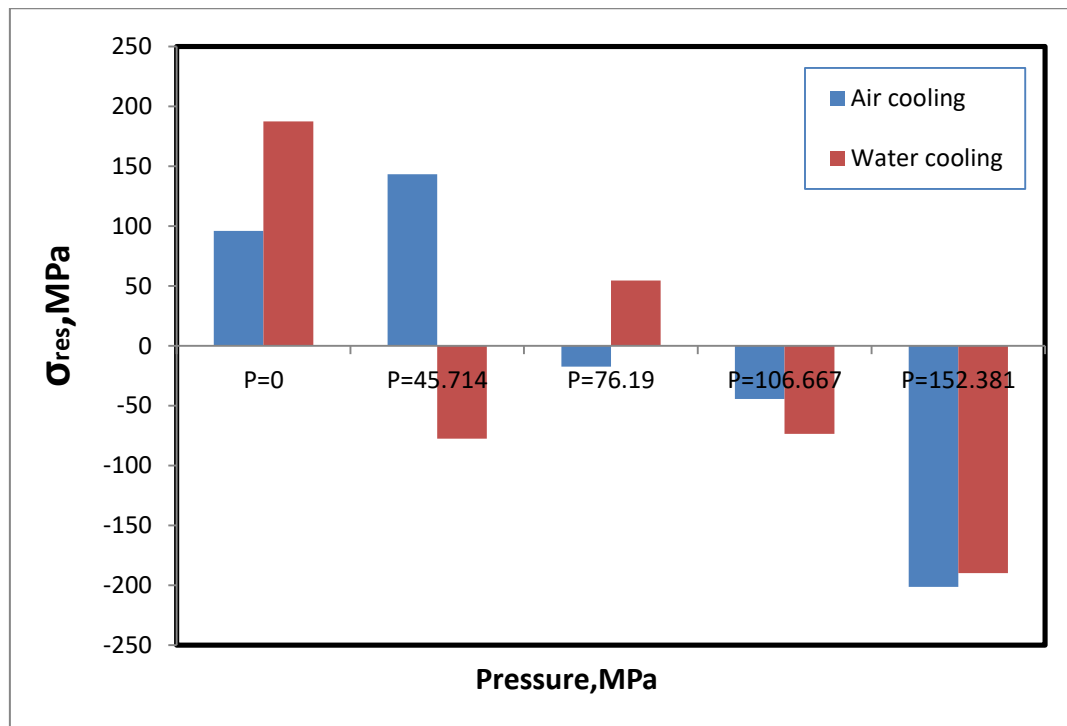


Figure (5-27): Evaluated Residual stresses at 125 mm for all specimens cooled from 200°C

According to water cooling, Figure (5-25) was described the residual stresses at (25)mm. The behavior was transformed from tension under zero pressure to compression under other pressures. The expressed behavior through Figures (5-26, 5-27) at the distances (75, 125)mm was altered from tensile under zero pressure to compressive due to (45.714)MPa.

The residual stresses were converted to tensile at (76.19)MPa. Finally, the residual stresses were compressive due to (106.667, 152.381)MPa. In the middle of specimen at (75)mm, the residual stresses due to air cooling were: (94.678, 85.436, -63.293, -35.553, -166.864)MPa. According to water cooling, the stresses (75) mm were: (179.352, -112.202, 16.11, -62.143, -199.086)MPa.

The compressive residual stresses were belong to the addition of compressive stresses from two sources: fast water cooling and high applied pressure. The water cooling was introduced thermal residual stresses at yield which caused material distortion or cracking. The high residual stresses have belonged to the great heat fluxes with high gradients in temperature near

material surface and between intermediate layers [149]. Generally, the range of residual stress was between (-200 to 200)MPa.

5.8 Statistical Package For Social Science (SPSS)

This software program is used by researchers in various types of quantitative data analysis. The behavior of mean velocity are represented opposite relationship with the mean stress according to the calculations of statistical analysis SPSS software, This behavior is guaranteed with [7, 82] where maximum residual stresses corresponding to the minimum ultrasonic velocities and vice versa.

According to SPSS, all tests of significance were given (p-value). The statistical power of the test is p-value. The widely used critical value for p is (0.05). The hypothesis is null and rejected for $p \leq 0.05$. In most tests, this p-value ($p \leq 0.05$) means that general findings were considered as general population. Generally, , the sample is externally valid and can be generalized onto the population.

Figure (5-28) represents the assessment of mean ultrasound velocity for the reference specimen with all other specimens. In SPSS, the number of the reference (annealed) specimen is (100). There are many differences between the reference specimen and others The behavior of interchanging altitude and declining of residual stresses for various specimens that inspected by ultrasonic test is agreed with [74, 82], Figure (5-29) represents the mean stress for all specimens with respect to the reference specimen.

All the specimens can be changed to the following numbers in order to determine (p-value) in SPSS. Comparing. Table (5-2) is represented (p-values) where (p-value) is effective ($p \leq 0.05$) depending on circumstances of specimens. For specimens (1, 2, 3, 4 , 8, 10) that cooled from 180°C depending on reference specimen, (p-value) is effective ($p \leq 0.05$). On the other hand, for

specimens produced by cooling from 200°C which represented with (11, 12, 13,14,18,19, 20), (p-value) is effective ($p \leq 0.05$).

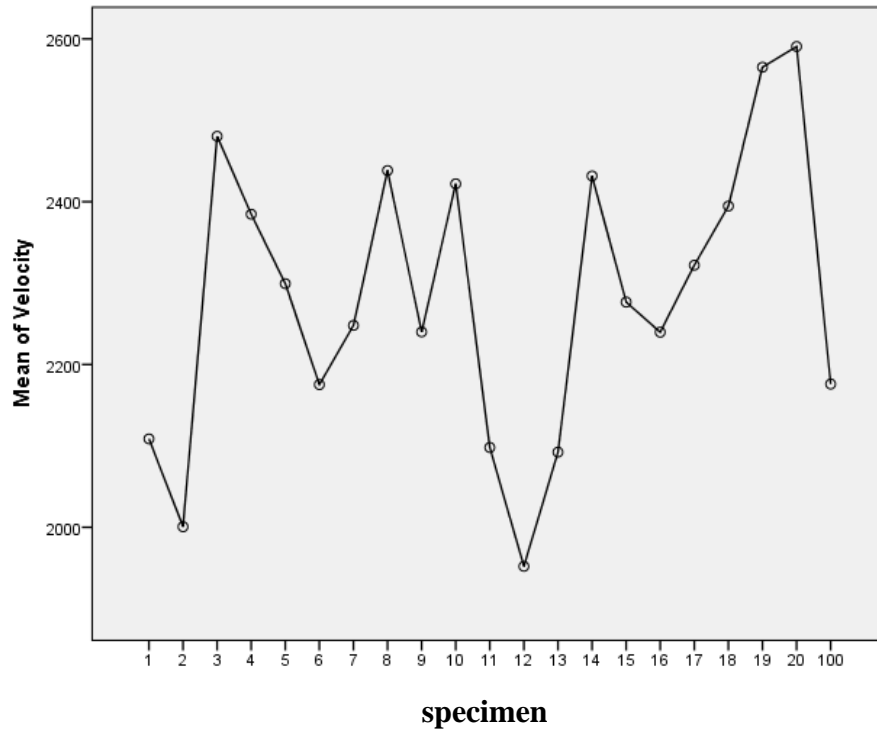


Figure (5-28): Mean velocity for all specimens due to SPSS

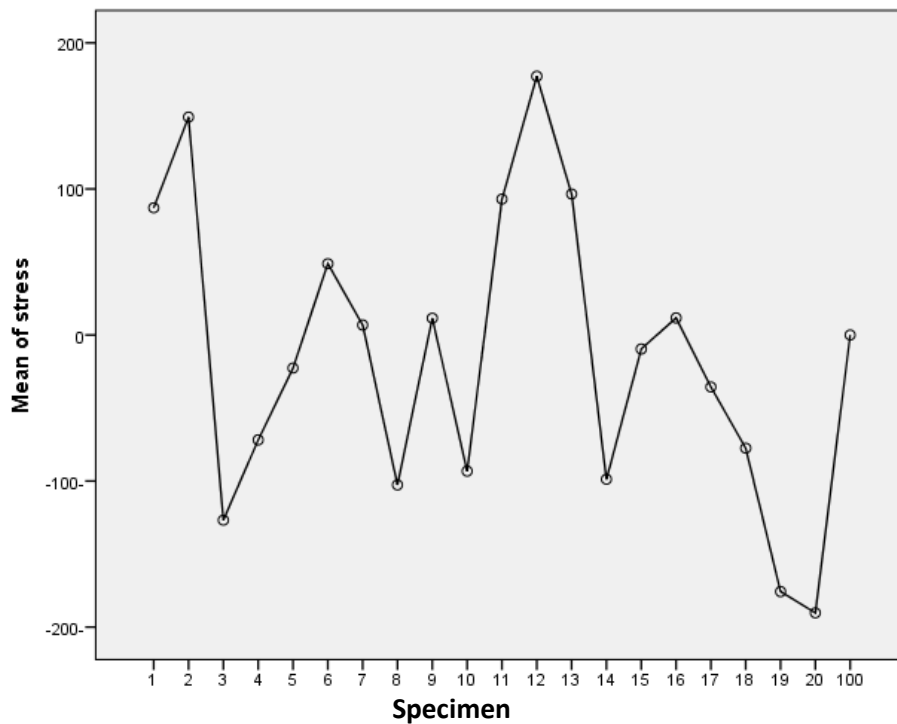


Figure (5-29): Mean stress for all specimens due to SPSS

Table 5-2:SPSS, p-value of ultrasonic velocities and residual stresses

Temperature	Medium of cooling	Pressure	Symbol	p- value of velocity	p-value of stress
180°C	air	0	1	.124	.000
	water	0	2	.000	.000
	air	45.714	3	.000	.000
	water	45.714	4	.000	.002
	air	76.19	5	.006	.311
	water	76.19	6	.988	.033
	air	106.667	7	.100	.758
	water	106.667	8	.000	.000
	air	152.381	9	.143	.605
	water	152.381	10	.000	.000
200°C	air	0	11	.076	.000
	water	0	12	.000	.000
	air	45.714	13	.058	.000
	water	45.714	14	.000	.000
	air	76.19	15	.024	.666
	water	76.19	16	.145	.599
	air	106.667	17	.001	.115
	water	106.667	18	.000	.001
	air	152.381	19	.000	.000
	water	152.381	20	.000	.000

5.9 Hybrid ABC and FFNN Flowchart

Artificial neural networks have large possibility in resolving the issues of polymers characteristics. In this work, hybrid artificial bee colony with feed forward neural network (HABCFNN) algorithm is built by the language of technical Computing MATLAB R2010a in order to obtain the optimized manufacturing conditions with appreciable values of residual stresses.

The procedure is started after evaluating the residual stresses for all specimens and entering these magnitudes in algorithm to find the optimum conditions for preparing PS specimens with respect to applied pressures and residual stresses. MATLAB is a systematic program which control the

functions of a computer's hardware to give the incorporated numeric estimation and graphic imagining in elevated scale programming language.

The evaluated through thickness residual stresses are produced under various pressures and two manner of cooling (air, water) are entered in Matlab program. The flowchart of through thickness residual stresses program is shown in Figure (5.30). The optimal results of HABCFFNN algorithm are expressed through table (5-3) as well as the parameters of HABCFFNN are displayed.

Table (5-3) The parameters of (HABCFFNN)

Max. No. of Iterations	1000
Colony Size (No. of Onlooker Bees)	100
Regression	1
Training function	Levenberg Marquardt
Training ratio	70/100
Validation ratio	15/100
Test ratio	15/100
No. of Decision Variables	5
Lower Bound of Decision Variables	100
Upper Bound of Decision Variables	100
Data Division	Random
No. of Hidden Neurons (hidden layers)	20
<i>Optimum Values</i>	
Residual stress (180) °C and water cooling P=(106.667)MPa , σ_{res} = (-70.003)MPa	
Residual stress (200)°C and water cooling P=(76.19)MPa , σ_{res} = (10. 579) MPa	

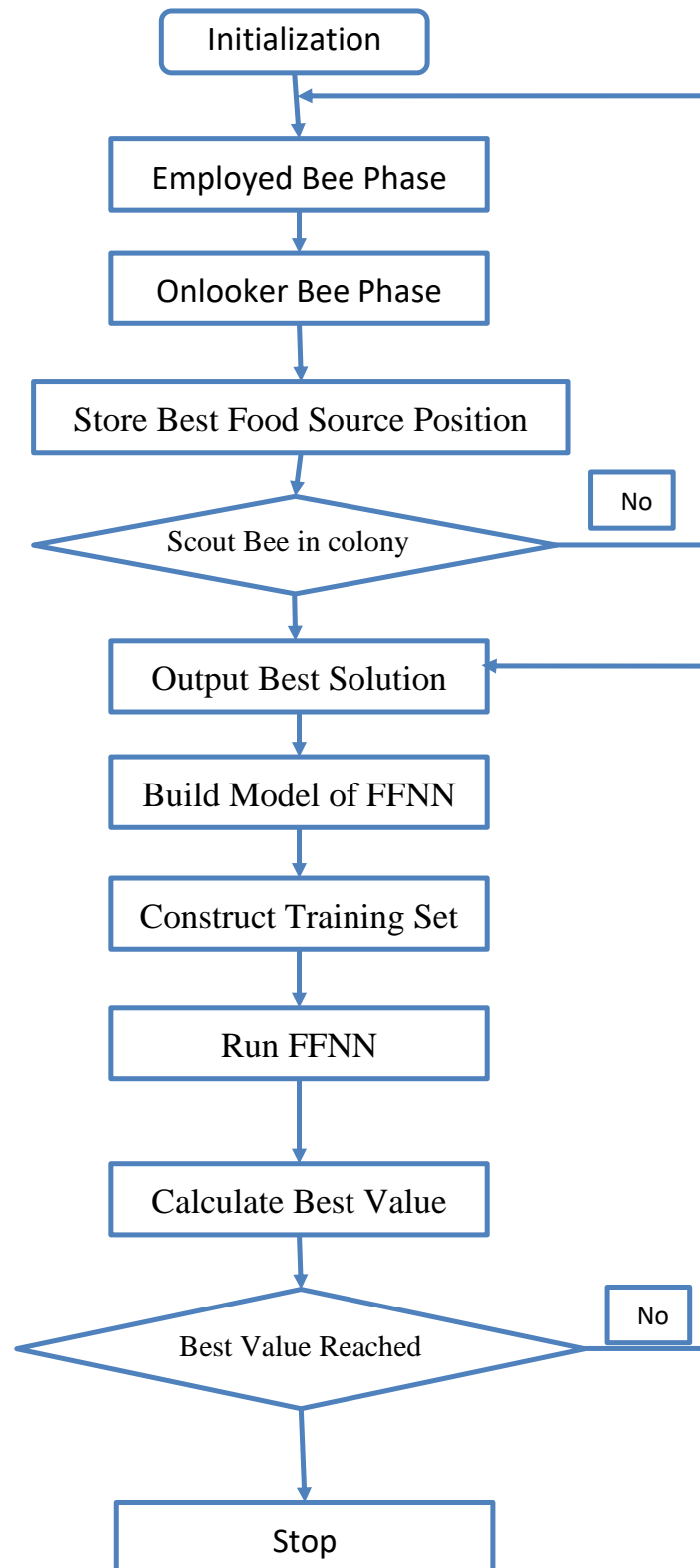


Figure (5-30): Flowchart of HABCFNN

The types of neural network functions are shown in Figure (5-31). The relationship between ABC and FFNN is represented in Figure (5-32). The Input included layers of feed forward neural network FFNN are shown in Figure (5-33), while Figure (5-34) is represented the hidden layers of FFNN.

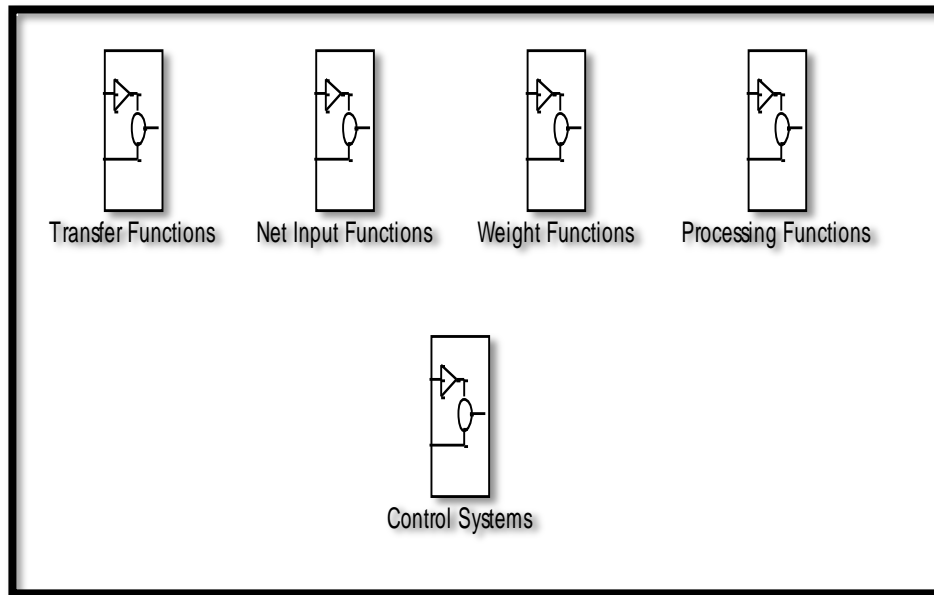
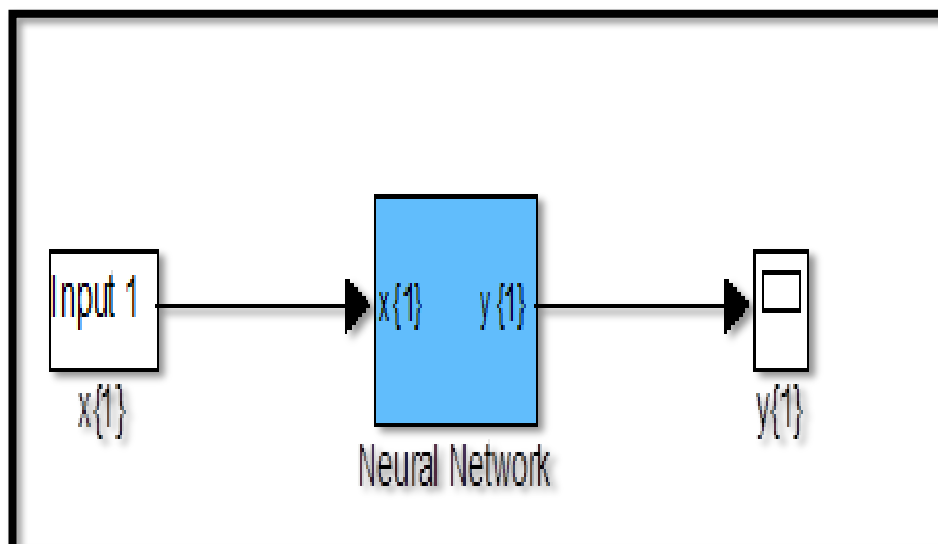


Figure (5-31):Types of functions in neural network



Figure(5-32): The related block between ABC-FFNN

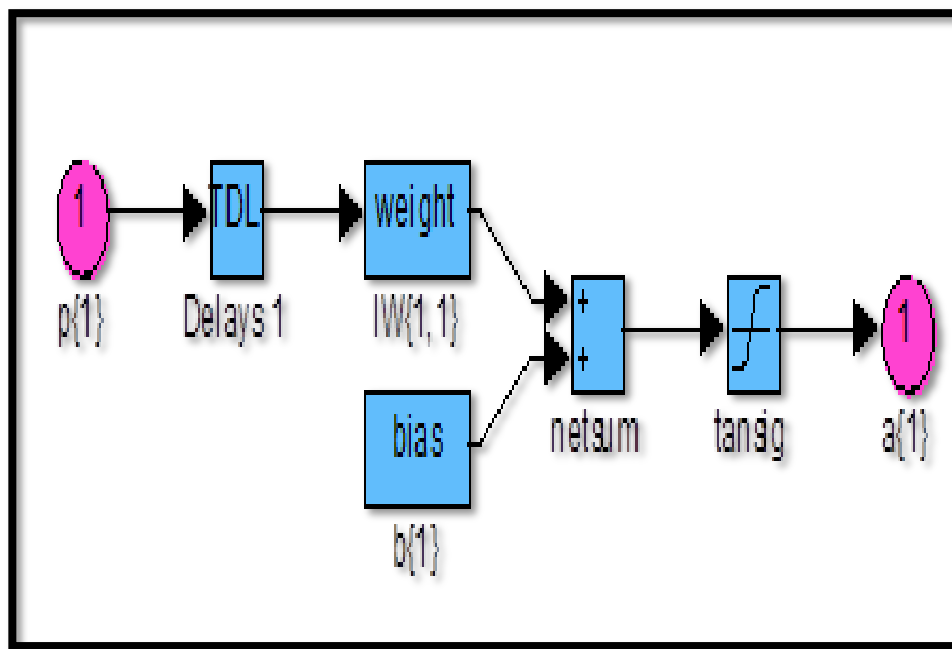


Figure (5-33): Input included layers of FFNN

5.10 Results of (HABCFNN) Algorithm

According to HABCFNN algorithm, artificial bee colony was training the neural network. The training process is carried out for (70) times at two temperatures under various pressures and types of cooling. Figures (5-35), (5-36) are referred to one training process at (180, 200)°C respectively.

The performances of residual stresses for PS specimens that pressed under pressures (45.714, 76,19, 106.667, 152.381) MPa and cooled from (180, 200)°C are shown in Figures (5-37, 5-38) respectively. It can be shown that (training, validation, test) are identical. The regression curve is characterized in Figure (5-39) (R=1) which refers to the accurate solution of optimization.

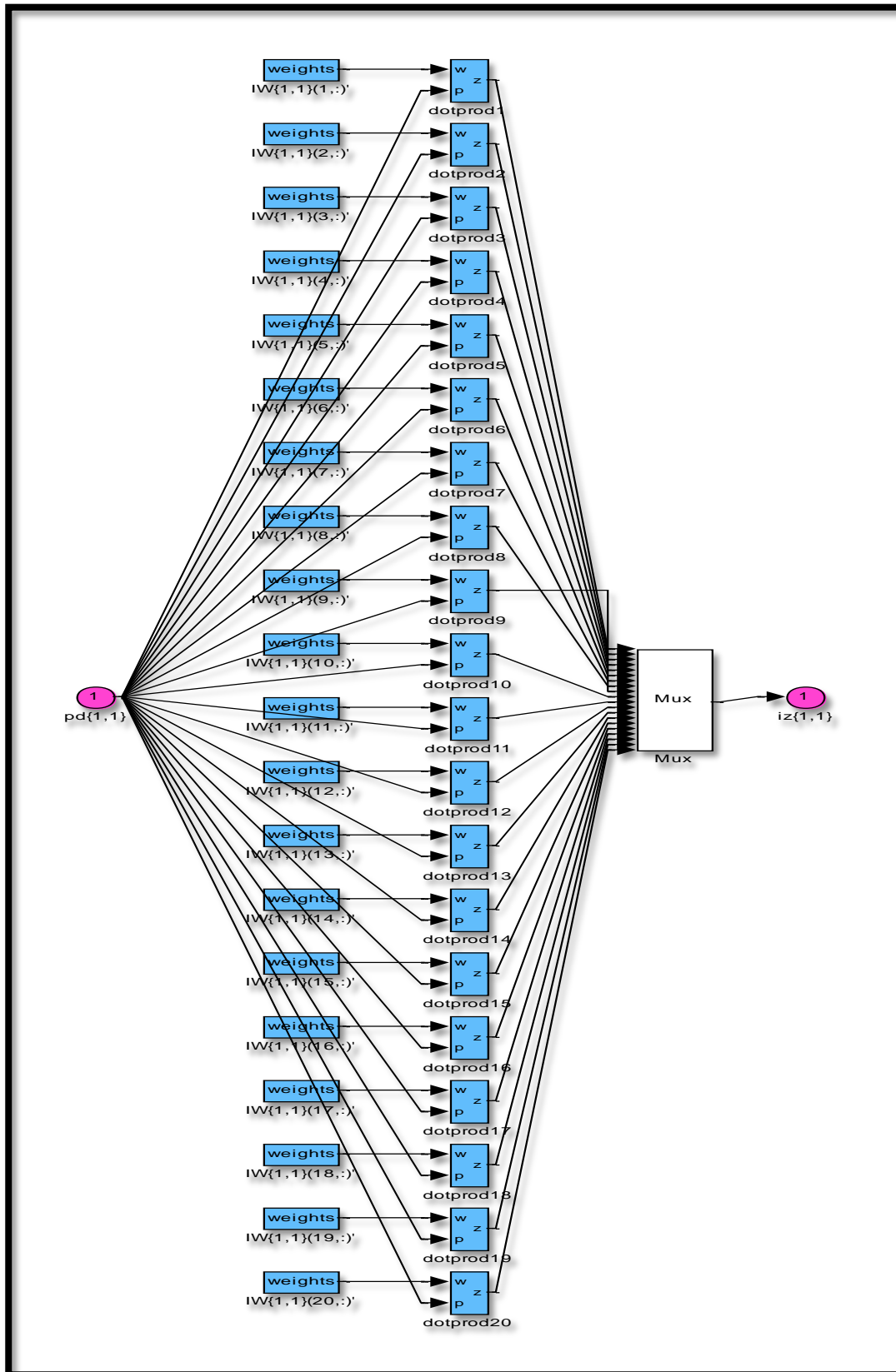
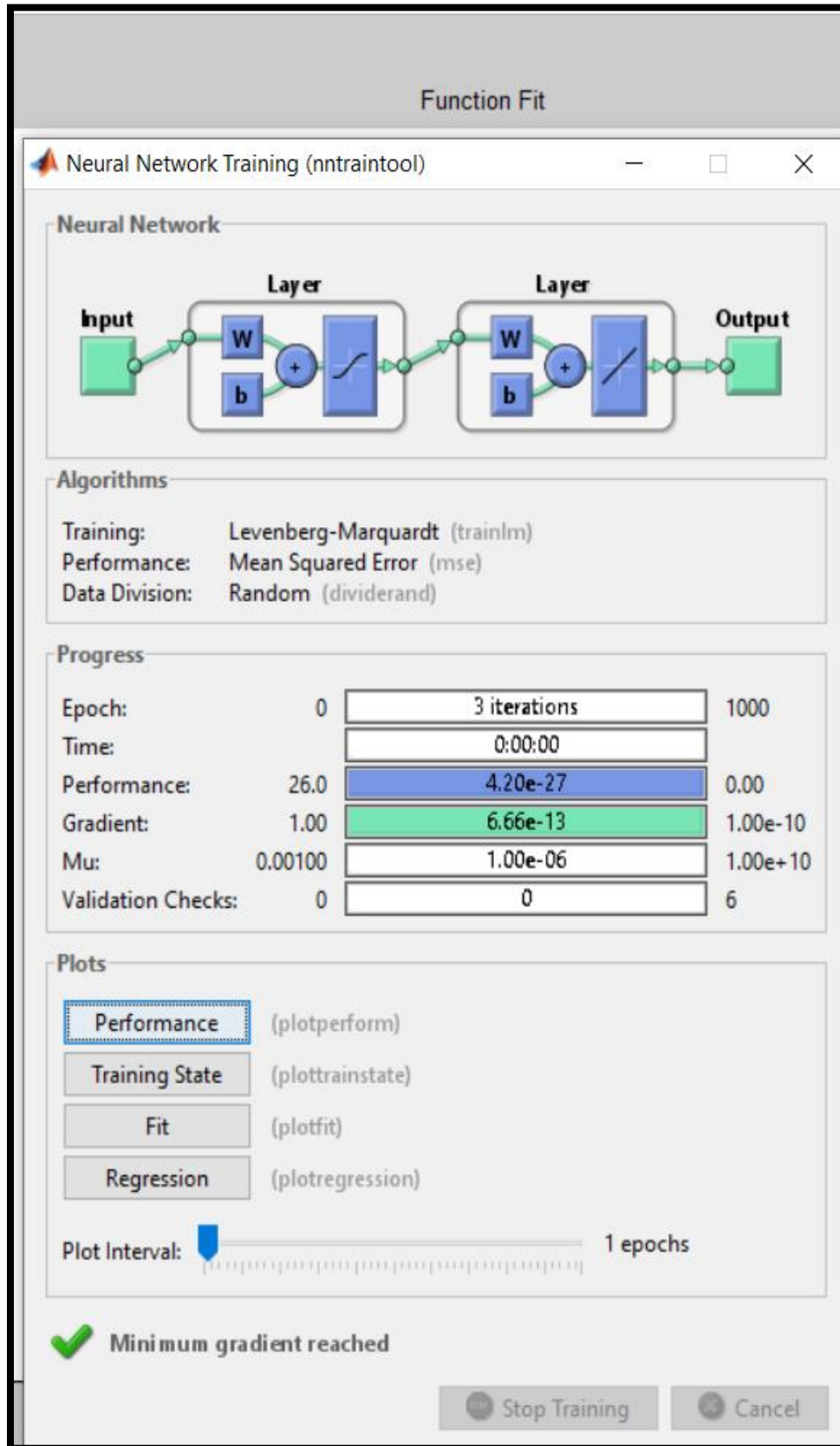


Figure (5-34): Hidden layers of FFNN



Figure(5-35): Representation of one training process (180)°C

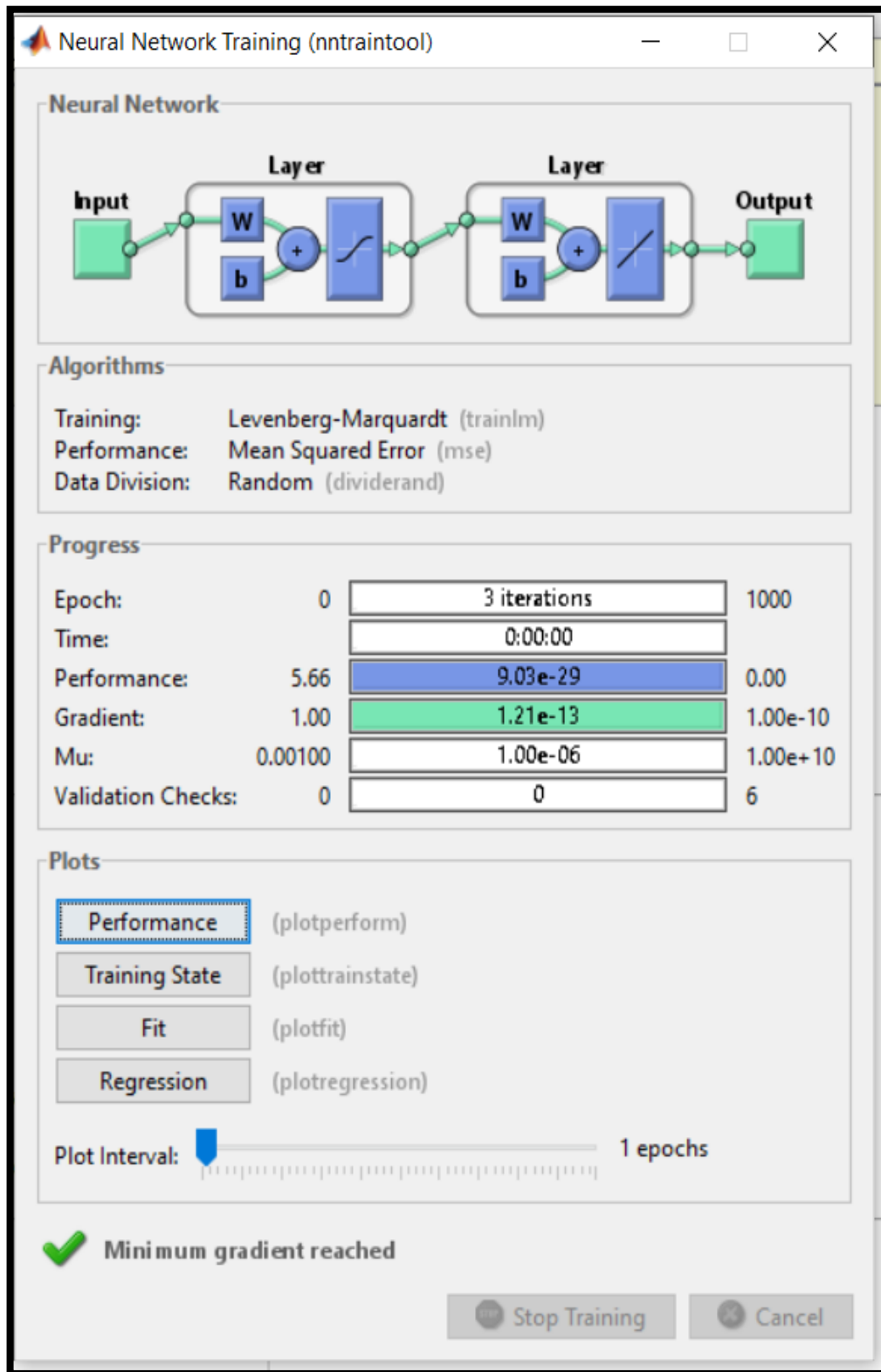


Figure (5-36): Representation of one training process (200)°C

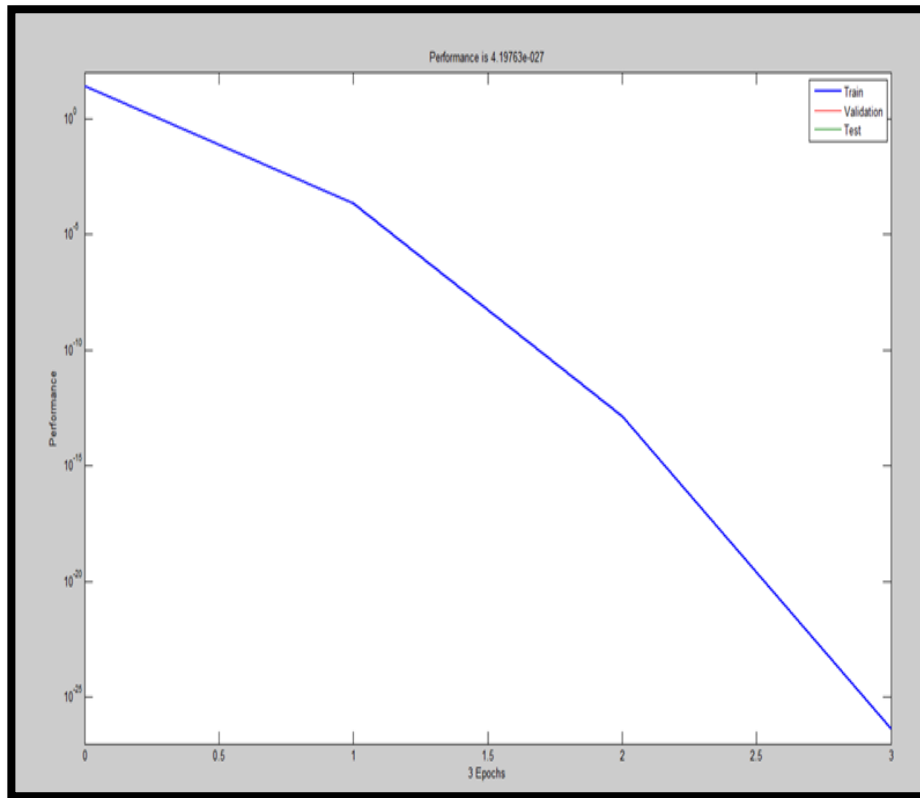


Figure (5-37): Performance of residual stresses for PS specimens (180)°C

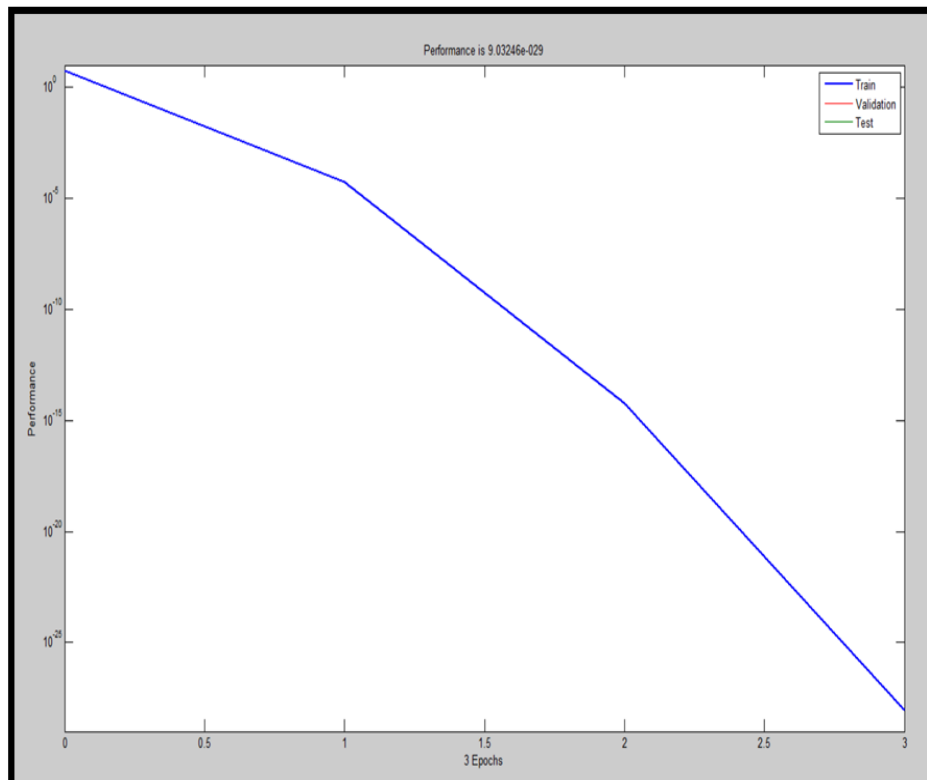


Figure (5-38): Performance of residual stresses for PS specimens (200)°C

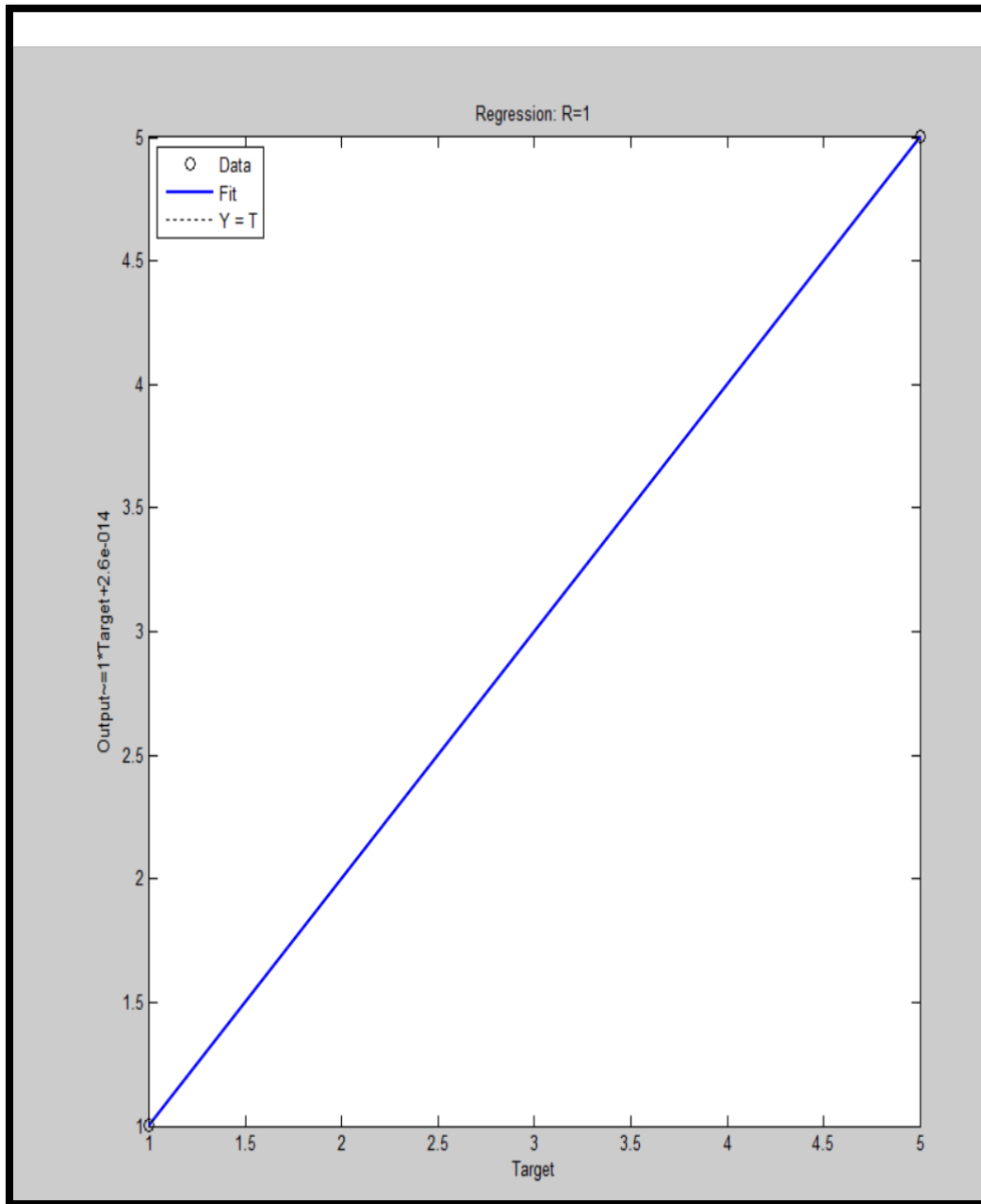


Figure (5-39):Regression plot of HABC-FFNN

Chapter Six
Conclusions &
Recommendations

Chapter Six

Conclusions and Recommendations

6.1 Conclusions

There are numerous conclusions could be deduced from this dissertation work:

1- Maximum ultrasonic velocity approximately (2500)m/s is obtained at (152.381)MPa pressure due to slow and rapid cooling from 200°C as well as from from rapid cooling at 180°C.

2-The compressive residual stresses in terms of K for PS specimens cooled from (180, 200)°C by air and water were corresponded with increasing in ultrasonic velocity while tensile residual stresses are related with decreasing in ultrasonic velocity.

3-The optimal pressures from (HABCFNN) were obtained under (106.667, 76.19)MPa while the optimal through thickness residual stresses due to water cooling from (180, 200)°C were (-70.003, 10.579)MPa.

4- The air cooled PS specimens from 200°C have maximum ultrasonic velocity against maximum applied pressure.

5- There is different behavior was obtained at a distance of (25)mm for water cooled state from 200°C where through thickness residual stresses behaved as tensile under zero pressure and compressive under all applied pressures.

6-The determined through thickness residual stresses were an addition of (thermal stresses due to cooling type, over load pressures of pressing, restraining of polymeric sheets inside metal molds).

7-At the middle of PS specimen (75)mm cooled by air from 180°C, the higher pressures (106.667, 152.381)MPa are given tensile stresses (5.569, 9.782)MPa less than tensile strength of PS MPa.

8-According to (p-value) from SPSS software, in two temperatures (180, 200)°C the more significant residual stresses are (tensile without pressure) for air and water cooling.

9- In SPSS, the significant pressure on residual stresses due to water cooling from (200)°C was 152.714.

10-The range of ultrasonic velocity produced from pulse-echo test were (2000-2500) m/s due to air and water cooling from (180, 200).

6.2 Recommendations

1- Detected the presence of residual stresses from tensile test.

2-Manufacture of polystyrene by another manufacturing process such as injection molding and compression molding, then measure residual stresses.

3-Use another non-destructive methods in measuring residual stresses such as Neutron diffraction and X-ray diffraction.

4-Studying the influence of residual stresses on cyclic loading.

5-Examination the relationship between creep strength and manufacturing stresses.

References

References

- 1- Rossini, N. S., M. Dassisti, K. Y. Benyounisb, Abdul-Ghani Olabi. 2012."Methods of Measuring Residual Stresses in Components." *Journal of Materials & Design*, Elsevier, Vol.35, pp. 572-588, ISSN 0261-3069.
doi.org/10.1016/j.matdes.2011.08.022
- 2- Chunguang, Xu, Wentao Song, Qinxue Pan, et al. 2015. "Nondestructive Testing Residual Stress Using Ultrasonic Critical Refracted Longitudinal Wave." *Physics Procedia* , Elsevier, Vol.70, pp.594 – 598.
- 3- Alberto, Cazzato .2016. "Residual Stress Evaluation in Innovative Manufacturing Techniques: FSW and FDM." PhD Diss. Politecnio Di Bari University.
- 4- Rouabah, F., a D. Dadache, and N. Haddaoui.2012." Thermophysical and Mechanical Properties of Polystyrene: Influence of Free Quenching." *International Scholarly Research Network ISRN Polymer Science*, Vol. 2012.
- 5- Kenney Timothy .2017." Polycarbonate Residual Stress." ASTM D4093,info@nhml.com.
- 6- Raghuwanshi, R. K. and V. K. Verma.2014."Mechanical and Thermal Characterization of AeroGrade Polymethyl Metha Acrylate Polymer used in Aircraft Canopy." *International Journal of Engineering and Advanced Technology (IJEAT)*, Vol. 3, No.5.
- 7- Dawei Jia, G. Bourse, S. Chaki, M. F. Lacrampe, C. Robin, and H. Demouveau .2014. "Investigation of Stress and Temperature Effect on the Longitudinal Ultrasonic Waves in Polymers.", American Society for Nondestructive Testing, Tylor & Francis Group, France, Vol. 25, pp 20–29,doi: 10.1080/09349847.2013.820371.

8- "Residual Stress in Plastics Part," Korea Engineering Plastic Co., Ltd. (KEP), 2017. www.kepital.com

9- Ho Sung Kim, Chae Hwan Kim, Hwajin Oh, et al.2007. "Residual Stresses and Viscoelastic Deformation of an Injection Molded Automotive Part." *Korea-Australia Rheology Journal* ,Vol. 19, No. 4, pp. 183-190.

10- Kandil, F. A., J. D. Lord, A. T. Fry, P. V. Grant. 2001."A Review of Residual Stress Measurement Methods a Guide to Technique Selection." National Physical Laboratory Materials Center (NPL), UK.

11- Rosato, D.V. 1995. *Injection Molding Handbook*. Chapman and Hall, NY, pp. 1011.

12- Dreier Steven, and Berend Denkena. 2014"Determination of Residual Stresses in Plate Material by Layer Removal with Machine-integrated Measurement." *Procedia CIRP*, Vol. 24 , pp.103 – 107.

13- Maxwell A.S., and A. Turnbull. 2000."Measurement of Residual Stress in Polymeric Materials." *Proceedings of Sixth International Conference on Residual Stress*, Institute of Materials, Oxford.

14- Turnbull A., A. S. Maxwell, and S. Pillal.1999." Residual Stress in Polymers—Evaluation of Measurement Techniques", NPL, *Journal of Materials Science*, Vol.34, pp. 451– 459, UK.

doi:10.1023/A:1004574024319.

15- Gabriela dos Santos Kotila .2018. "Photoelastic Stress Analysis of Polyethylene Terephthalate", MSc. Thesis, *Arcada University*.

16- Maxwell A.S. .2005. "Measurement of Residual Stress in Plastics", *National Physical Laboratory (NPL)*, permission of the controller of HMSO, DEPC (MN) 027, ISSN 1744-3911, UK.

- 17- Paul Nicolas Henry. 2015." Measurements and Modelling of Residual Stresses during Quenching of Thick Heat Treatable Aluminium Components in Relation to their Precipitation State." PhD Diss. University of Ottawa.
- 18- Zhang Jingyu. 2005. "Experimental Study of Stress Cracking in High Density Polyethylene Pipes." PhD Diss. Drexel University.
- 19- Omar ,Suliman Zaroog , Chong Yap Wee Ken, and Abreeza Noorlina Abd. Manap. 2014."Current and Challenge of Residual Stress Measurement Techniques." International Journal of Science and Research (IJSR), Vol. 3, No. 9. www.ijsr.net Paper ID: 02015924.
- 20- Yang Shunmin, Mingquan Wang, and Lu Yang. 2019. "Investigation of Uncertain Factors on Measuring Residual Stress with Critically Refracted Longitudinal Waves." *Applied Science*, Vol.9, No.485.
- 21- Prime B. Michael, Mark A. Newborn, and John A. Balog. 2003. "Quenching and Cold- Work Residual Stresses in Aluminum Hand Forgings : Contour Method Measurement and FEM Prediction." *Materials Science Forum*, Vols. 426-432, pp. 435-440.
- 22- Octavio Cesar .2015. "Relaxation of Residual Stresses in Plastic Cover Lenses with Applications in the Injection Molding Process", PhD Diss. University Autonoma De San Luis Potosi.
- 23- Maxwell A. S., and A. Turnbull. 2003. " Measurement of Residual Stress in Engineering Plastics using the Hole-drilling.", *Polymer Testing* ,Vol.22, pp.231-233.
- 24- Nuutinen, Minna . 2019. "Development of Annealing Process for Injection Molded PPSU Fittings to Reduce Residual Stresses". MSc Diss. LUT School of Energy System, LUT Mechanical Engineering, Lahdessa.

25- Hearn, E. J.1997. "Mechanics of Materials 2", The mechanics of Elastic and Plastic Deformations of Solids and Structural Materials, The Third Edition, Elsevier Science & Technology, Oxford.

26- Hughes D.J., E.L. Heeley, and C. Curfs. 2010. " Residual Stress in HDPE Pipeline Using Synchrotron XRD: a New Tool for in Polymer Engineering." *Materials Letters*.

27- Shukla, A. 2006. "Dynamic Fracture Mechanics", World Scientific Publishing Co Pte Ltd, Singapore.

28- Hibbeler, R.C. 2014. "Mechanics of Materials", Pearson Prentice Hall, The Ninth Edition, New Jersey.

29- Sciammarella, A.C. and M.A. Sciammarella .2012. "Experimental Mechanics of Solids", John Wiley & Sons, First Edition, Chischester.

30- Foltz, Erik .2018. "Accounting for Residual Stress in Injection Molded Parts", The Madison Group, Madison, WI53711, USA. www.madisongroup.com/.

www.eiseverywhere.com/ehome/315321&t.

31-Song, Young Joo .1996. "Residual stress analysis of sputtered Tantalum Silicide thin film", MSc Thesis, New Jersey Institute of Technology.

digitalcommons.njit.edu/theses.

32- Feingold, Joel M .2019."Stress Diagnose it Before it Ruins Your Parts-Plastic Technology", Gardner Business Media, Inc. www.ptonline.com.

33- Maxwell, A.S. & A. Turnbull .2003. "Chemical Probe Technique for Assessing the Susceptibility of Polymeric Moldings to Environment Stress Cracking", *Polymer Testing*, Vol. 22, pp.259-265.

34- Solvay Specialty Polymers .2014. [web document]. Available: www.solvay.com/en/product/radel-r-5100#product-documents

- 35- Guevara-Morales, A., & Figueroa-López, U. 2014. "Residual Stresses in Injection Molded Products.", *Journal of Materials Science*, Springer, Vol.49, No.13, pp. 4399-4415.
- 36- ASTM D7474-17. 2017. Standard Practice for Determining Residual Stresses in Extruded or Molded Sulfone Plastic (SP) Parts by Immersion in Various Chemical Reagents. United States: ASTM International.
- 37- Maxwell, A. S. &Turnbull, A. 2000. "Characterization of Environment Stress Cracking Susceptibility of Weld line Defects by The Chemical Probe Technique", Chemical probe report v6.doc, NPL Report CMMT (A) 269, permission of the controller of HMSO, NPL, UK.
- 38-Solvay Specialty Polymers .2015. [web document]. Available: www.solvay.com/en/product/radel-r-5100#product-documents
- 39- Shah, Vishu .1998. "Hand Book of Plastics Testing Technology", second edition, John Willy & Sons.
- 40- Allen. W.S & Baker, P.N. .2004. *Hand Book of Plastics Technology*, Vol.2, CBS Publishers, New Delhi.
- 41- O. Bílek , I. Lukovics , D. Sámek, and J. Knedlová, "An Approach for Residual Stress Determination by Mechanical Indentation Technique," *Journal of Scientific Proceedings*, Bratislava, vol. 20, Issue 1, pp.1-6, December 2012.
- doi:10.2478/v10228-012-0001-z
- 42- B. X. Xu, B. Zhao, and Z. F. Yue, "Investigation of residual stress by the indentation method with the flat cylindrical indenter," *Journal of Materials Engineering and Performance*, vol.15, pp. 299–305. June 2006.
- 43- S.- J. Wu, P.- C. Chin, and H. Liu, "Measurement of Elastic Properties of Brittle Materials by Ultrasonic and Indentation Methods," *MDPI, Journal of Applied Science*, vol. 9, no. 2067, May 2019.

doi:10.3390/app9102067

www.mdpi.com/journal/applsci

44- P.-L. Larsson and P. Blanchard, " On the invariance of hardness at sharp indentation of materials with general biaxial residual stress fields," *Journal of Materials and Design*, Sweden, vol. 52, pp.602–608, 2013.

45- Olivera. E. Kesler, " Residual Stresses and Properties of Layered and Graded Coatings," PhD Dissert., Department of Materials Science and Engineering, Massachusetts Institute of Technology, September 1999.

46- P.- L. Larsson, "Principal Stress Ratio Effect at Residual Stress Determination Utilizing the Variation of Indentation Hardness," MDPI, *Journal of Lubricants*, Department of Solid Mechanics, Royal Institute of Technology, Stockholm, Sweden, vol.7, no.50, June 2019.

doi:10.3390/lubricants7060050

47- Z. Yao, "Development of an indentation method for material surface mechanical properties measurement," PhD. Dissert., College of Engineering and Mineral Resources, West Virginia University, Morgantown, West Virginia , 2005.

48- S. Carlsson and P. - L. Larsson, "On the Determination of Residual Stress and Strain Fields by Sharp Indentation Testing: Part I. Theoretical and Numerical Analysis," *Journal of Acta Materialia*, vol. 49, pp. 2179–2191.2001.

49- A. Rydin and P.- L. Larsson, "On the Correlation Between Residual Stresses and Global Indentation Quantities: Equi-Biaxial Stress Field," *Journal of Tribology Lett.* vol. 47, pp. 31–42, 2012.

50- Q. Wang , K. Ozaki , H. Ishikawa, S. Nakano, and H. Ogiso, "Indentation Method to Measure the Residual Stress Induced by Ion Implantation," Elsevier, *Journal of Nuclear Instruments and Methods in Physics Research*, Japan, section B, no. 242 , pp.88-92. January 2006.

doi:10.1016/j.nimb.2005.08.008

51- P. - L. Larsson, "On the Influence of Elastic Deformation for Residual Stress Determination by Sharp Indentation Testing," *Journal of Materials Engineering and Performance*, Sweden, vol.26, no.8, pp. 3854–3860, August 2017.

doi: 10.1007/s11665-017-2816-2

52- T. Y. Tsui, W. C. Oliver, and G. M. Pharr, "Influences of stress on the measurement of mechanical properties using nanoindentation: Part I, Experimental studies in an aluminum alloy," *Springer, Journal of Materials Research*, vol.11, pp.752–759 1996.

53- J. - I. Jang, "Estimation of residual stress by instrumented indentation: A review," *Journal of Ceramic Processing Research*, Korea, vol.10, no. 3, pp.391-400, 2009.

54- M. T. Attaf, "Connection between the loading curve models in elastoplastic indentation," *Elsevier, Journal of Materials Letters*, Canada, vol.58, no. (27-28), pp.3491–3498, August 2004.

55- P. - L. Larsson, " On the Variation of Hardness Due to Uniaxial and Equi-Biaxial Residual Surface Stresses at Elastic–Plastic Indentation," *Journal of Materials Engineering and Performance (JMEPEG)*, Sweden, vol.27, pp.3168–3173, May 2018.

doi.org/10.1007/s11665-018-3393-8.

56- M. Jamal, "Characterization & Evaluation of Thermally Treated Recycled Glass For Mass Finishing & Super finishing Processes," PhD. Dissert, Liverpool John Moores University, August 2015.

doi.org/10.24377/LJMU.t.00004580

57- M. R. VanLandingham, " Review of Instrumented Indentation," Journal of Research of the National Institute of Standards and Technology, Gaithersburg, vol. 108, no. 4, pp. 249-265, 2003.

58- F. Ali safaei and C.- S. Han, "Indentation Depth Dependent Mechanical Behavior in Polymers, Review Article," Hindawi, Journal of Advances in Condensed Matter Physics, USA, July 2015.

doi.org/10.1155/2015/391579

59- L. Zhu, B. Xu, H. Wang, and C. Wang, "Measurement of residual stresses using nanoindentation method," Journal of Solid State and Materials Sciences, vol.40, no.2, pp.77-89, 2015.

[doi:10.1080/10408436.2014.940442](https://doi.org/10.1080/10408436.2014.940442)

60- J. HP, Y. WY, and Y. L., "Development of an Improved Energy Based Method for Residual Stress Assessment," Philosophy Magazine , vol.92, no.4, pp.480–499, 2012.

doi.org/10.1080/14786435.2011.61.16867

61- J. HP, Y. WY, and Y. L., " Determination of Residual Stresses and Material Properties by an Energy-Based Method Using Artificial Neural Networks," Journal of Academic Science, vol.61, no.4, pp.296–305, 2012. doi: 10.3176/proc.2012.4.04

62- C. M. Lepienski et al., " Factors limiting the measurement of residual stresses in thin films by nanoindentation," Elsevier, Journal of Thin Solid Films, vol. 447, pp.251-257, 2004.

63- X. Zh and L. Xd, "Estimation of Residual Stresses from Elastic Recovery of Nanoindentation ," Philosophy Magazine, vol.86, no.19, pp. 2835–2846, 2006.

doi.org/10.1080/14786430600627277

64- J. Dean, G. Aldrich-Smith , and T.W. Clyne, "Use of Nanoindentation to Measure Residual Stresses in Surface Layer," Elsevier, Journal of Acta Materialia, UK, vol.59, no. 7, pp.2749-2761, January 2011.

doi:10.1016/j.actamat.2011.01.014

65- J. G. Swadener, B. Taljat, and G. M. Pharr, " Measurement of Residual Stress by Load and Depth sensing Indentation with Spherical Indenters," Journal of Materials Research, vol.16, no. 7, pp.2091–2102, 2001

doi.org/10.1557/JMR.2001.0286

66- Kudryavtsev ,Yuriy, Jacob Kleiman.2016."Ultrasonic Measurement of Residual Stresses in Welded Elements and Structures." 19th World Conference on Non-Destructive Testing.

67- Sadeghi, S., M. A. Najafabadi, Y. Javadi, M. Mohammadisefat.2013. "Using Ultrasonic Waves and Finite Element Method to Evaluate through Thickness Residual Stresses Distribution in the Friction Stir Welding of Aluminum Plates." Journal of Materials and Design, Vol.52, pp.870-880,doi.org/10.1016/j.matdes.2013.06.032 .

68- Gokhale,Shailesh.2007."Determination of Applied Stresses in Rails Using the Acoustoelastic Effect of Ultrasonic Waves." MSc Diss., Civil Engineering, Texas A&M University.

69- Mao, Hanling, Yuhua Zhang, Hanying Mao, Xinxin Li, and Zhenfeng Huang. 2018."Stress Evaluation of Metallic Material under Steady State Based on Nonlinear Critically Refracted Longitudinal Wave", Journal of Results in Physics , Elsevier, Vol.9,pp.665–672.

doi.org/10.1016/j.rinp.2018.03.029

70- Castellano, Anna, Aginaldo Fraddosio, Salvatore Marzano, Mario Daniele Piccioni. 2017. " Some Advancements in the Ultrasonic Evaluation of Initial Stress

States by the Analysis of the Acoustoelastic Effect", *Procedia Engineering*, Vol.199, pp.1519–1526.

71- Zhu, Q., C. Burtin, and C. Binetruy.2014." Acoustoelastic Effect in Polyamide 6: Linear and Nonlinear Behavior." Elsevier, *Journal of Polymer Testing*, Vol.40, pp.178-186.

doi.org/10.1016/j.polymertesting.2014.09.007 0142-9418

72- Ramasamy, R., Z Ibrahim, and H K Chai.2017." Numerical Investigations of Internal Stresses on Carbon Steel Based on Ultrasonic LCR Waves." IOP Conference Series: Journal of Physics: Conf. Series 908 – 012044.

doi :10.1088/1742-6596/908/1/012044

73- Zuohua, Li, Jingbo He, Jun Teng, and Ying Wang. 2016."Internal Stress Monitoring of in-Service Structural Steel Members with Ultrasonic Method." *Journal of Materials*, Vol.9, No. 223.

doi:10.3390/ma9040223

74- In Hwang, Young, Geonwoo Kim, Yong-II Kim, Jeong-Hak Park, Man Yong Choi, and Ki-Bok Kim.2021." Experimental Measurement of Residual Stress Distribution in Rail Specimens Using Ultrasonic LCR Waves." *Journal of Applied Science*, MDPI, Vol.11.

doi.org/10.3390/app11199306

75- Manchem, Lakshmi Divya, Malur N. Srinivasan, and Jiang Zhou.2015. "Analytical Modeling of Residual Stress in Railroad Rails Using Critically Refracted Longitudinal Ultrasonic Waves With COMSOL Multiphysics Module", ASME International Mechanical Engineering Congress and Exposition.

doi:org/10.1115/IMECE2014-38619

76- Birks, A.S., Green R.E. Jr., Mc. Intire, P. 1991.*Nondestructive Testing Handbook*. Columbus, 2nd Ed., American Society for Nondestructive Testing.

77- Javadi ,Y., M. A. Najafabadi, and M. Akhlaghi.2012." Residual Stress Evaluation in Dissimilar Welded Joints Using Finite Element Simulation and the LCR Ultrasonic Wave." *Russian Journal of Nondestructive Testing*, Vol.48,No.9,pp.541-552.

doi.org/10.1134/S1061830912090033

78- Withers, P. J., and H. K. D. H. Bhadeshia.2001." Residual Stress Part 1 – Measurement Techniques." *Journal of Materials Science and Technology*, Vol.17, ISSN 0267 – 0836.

79-Ye, Chong, I. Charles Ume, Yuanlai Zhou, and Vishnu V.B. Reddy.2019." Inspection of The Residual Stress on Welds Using Laser Ultrasonic Supported with Finite Element Analysis." *EDP Sciences, Journal of Manufacturing Review*, Vol.6, No.3.

doi.org/10.1051/mfreview/2019001

80- Schneider, E.1997."Ultrasonic Techniques". In *Structural and Residual Stress Analysis by Non-destructive Methods*. Edited Victor Hauk, Elsevier.

81- Javadi, Y., M. Hasani, and S. Sadeghi.2015." Investigation of Clamping Effect on The Welding Sub-Surface Residual Stress and Deformation by Using the Ultrasonic Stress Measurement and Finite Element Method." *Journal of Nondestructive Evaluation*, Vol.34.

doi.org/10.1007/s10921-015-0277-9

82-Wei, Zhi, Xiaojun Zhou, and Yaodong Cheng.2000."Acoustoelastic Determination of Local Surface Stresses in Polymethyl Methacrylate." *Journal of Applied Acoustics*, Elsevier, Vol.6, pp.477-485.

83- Ye, Chong, I. Charles Ume, Yuanlai Zhou "Inspection of the Residual Stress on Welds Using Laser Ultrasonic Supported with Finite Element Analysis." *Munfaechung Review*, Vol, 6,No. 3. doi.org/10.1051/mfreview/2019001.

84- Pan,Qinxue Chang Shao, Dingguo Xiao, Ruipeng Pan, Xiaohao Liu, and Wei Song.2019." Robotic Ultrasonic Measurement of Residual Stress in Complex Curved Surface Components." *Journal of Applied Bionics and Biomechanics*, Hindawi.,Vol.2019.

doi.org/10.1155/2019/2797896

85- Tanala E, Bourse G, Fremiot M, and De Belleval JF. 1995. "Determination of Near Surface Residual Stresses on Welded Joints Using Ultrasonic Methods." *Journal of NDT & E International* , Vol. 28, No. 2, pp. 83–88.

86- Garbacz, Andrzej ,and Edward J. Garboczi.2003."Ultrasonic Evaluation Methods Applicable to Polymer Concrete Composites.", National Institute of Standards and Technology.

87- Sharma, J., S. Ahuja, and R.K. Arya. 2019."Effect of Molecular Weight on Morphology and Thermal Properties of Poly (Styrene)-Poly Methyl Meth Acrylate-Ethyl Benzene Coatings." *Progress in Organic Coatings*, Vol.132 ,pp.468-474.

88- Namazi, Hassan. 2017."Polymers in Our Daily Life." *BioImpacts*, Vol. 7, No. 2, pp.73-74.

89- Razavi, Masoud, Shiwang Cheng, Da Huang, Shufan Zhang and Shi-Qing.2020."Crazing and Yielding in Glassy Polymers of High Molecular Weight." Elsevier,*Polymer*,Vol.197.

90- Strong, A.B. 2005.*Plastics: Materials and Processing*. Prentice Hall PTR, Paramus, IL, 3rd Ed,ISBN-13:978-0131145580.

91-Sasmita, Firmansyah, Tania Zefanya S. Tarigan, Hermawan Judawisastra, Toni Agung Priambodo.2019." Study of Elastic Modulus Determination of Polymers

with Ultrasonic Method." International Journal on Advanced Science Engineering and Information Technology, Vol.9, No.3.

92- Engqvist, Jonas.2016." Mechanical Behavior of Glassy Polymers: Experiments and Modelling." PhD Diss. Division of Solid Mechanics, Lund University, ISBN: 978-91-7623-817-2.

93- Robeson, L.M., Q. Liu, B.D. Freeman, and D.R. Paul.2015." Comparison of Transport Properties of Rubbery and Glassy Polymers and The Relevance to The Upper Bound Relationship." Journal of Membrane Science, Vol.476, pp. 421-431.

94- Huang, Y., and D.R. Paul.2004." Experimental Methods for Tracking Physical Aging of Thin Glassy Polymer Films by Gas Permeation." Journal of Membrane Science, Vol.244, pp. 167-178.

95- Valerio, Ing. Loianno. 2018."Thermodynamics of Thermoplastic Polymers and Their Solutions." PhD Diss.

96- Kumar, Raj Arya¹, Devyani Thapliyal, Jyoti Sharma, and G. D. Verros.2021."Review, Glassy Polymers – Diffusion, Sorption, Aging, and Applications." MDPI, Vol.11, No.9.

doi:10.20944/preprints202107.0576.v1

97- Cichosz, Stefan, et al.2018. "Polymer-Based Sensors: A review." *Polymer Testing*, Vol. 67, pp. 342-348.

98- Arfin, Tanvir , Faruq Mohammad, and Nor Azah Yusof.2014."Applications of Polystyrene and Its Role as a Base in Industrial Chemistry." *In Polystyrene Synthesis ,Characteristics, and Applications*. Ed. Cole Lynwood, NOVA Publishers, New York.

99- Wankasi,D., and E.D.Dikio.2014." Comparative Study of Polystyrene and Poly Methyl Methacrylate Wastes as Adsorbents for Sorption of Pb⁺² from Aqueous Solution." Asian Journal of Chemistry; Vol. 26, No. 24 ,pp. 8295-8302.

doi.org/10.14233/ajchem.2014.16809

100- Basavaraju, K. C., Darshan Jayanna, et al. 2021. "A New Composition of High Heat General purpose polystyrene (High Heat GBBS) Resin."

101- Sastri, Vinny R. 2010. *Plastics in Medical Devices – Properties, Requirements, and Applications*. Elsevier, ISBN 978-0-8155-2027-6.

102- Franklin . 2022. "Cradle –to-Gate Life Cycle Analysis of General Purpose Polystyrene (GPPS) Resin." American Chemistry Council (ACC) Resin.

103- Prasittisopin, Lapyote, Pipat Termkhajornkit, and Young Hoon Kim. 2022. "Review of Concrete with Expanded Polystyrene (EPS): Performance and Environmental Aspects." *Journal of Cleaner Production*, Vol. 366, doi.org/10.1016/j.jclepro.2022.132919.

104- Sun, Yi, Chenxi Li, Junjie You, Changming Bu, et al. 2022. "An Investigation of The Properties of Expanded Polystyrene Concrete with Fibers Based on an orthogonal Experimental Design." *MDPI, Materials*, Vol. 15, No. 3, doi.org/10.3390/ma15031228.

105- Maghfouri, Mehdi, Vahid Alimohammadi , Rishi Gupta, Mohammad Saberian, Pejman Azarsa, Mohammad Hashemi, Iman Asadi, and Rajeev Roychand. 2022. "Drying Shrinkage Properties of Expanded Polystyrene (EPS) Light Weight Aggregate Concrete: A Review." *Case Studies in Construction Materials*, Vol. 16.

doi.org/10.1016/j.cscm.2022.e00919

106- Lin ,Tina ,Kuan Ting ,and Wu Wisdom Huang. 2021. "Electronics Parts with Polystyrene Plastic." *Technical Disclosure Commons, HP Inc Defensive Publications Series, Art. 4025*.

107- Huang, Wenyan, Weikai Gu, Hongjun Yang, et al.2017. "Preparation and Properties of Branched Polystyrene through Radical Suspension Polymerization." *Polymers*, MDPI, Vol. 9,No.1.

doi: 10.3390/polym9010014

108- Petrukhina, N. N. , O. N. Tsvetkov, and A. L. Maksimov,2019." Hydrogenated Styrene–Diene Copolymers as Thickening Additives to Lubricating Oils." *Russian Journal of Applied Chemistry*, Vol. 92, pp.1179–1189.

109- Guazzotti,Valeria, Anita Gruner, Mladen Juric,Vernika Hendrich,and Frank Welle.2022."Migration Testing of GPPS and HIPS Polymers: Swelling Effect Caused by Food Simulants Compared to Real Foods." *Molecules*, Vol.27,No.3.

doi:10.3390/molecules27030823

110- Aruova , L., A. Utkelbaeva, A. Budikova, N. Saktaganova, G. Karshyga, U. Sarabekova and U. Abdikerova.2021."Heat Treatment of Polystyrene Solar Energy." *Polytechnic Institute, Kyzylorda State University, Kyzylorda, Khstanazak*, Medwell Publications, Research Journal of Medical Sciences, Vol. 15, No.1, pp.26-40, ISSN: 1815-9346.

111- Gajevic, Sandra, Blaza Stojanovic, Lozica Ivanovic, et al.2019. "Application of Nanocomposites in the Automotive Industry." *Mobility& Vehicle Mechanics*, Vol.45,No.3,pp.51-64.

doi: 10.24874/mvm.2019.45.03.05

112- Nashrah, Nisa, Rosy Amalia Kurnia Putri, Early Zahwa Alharissa, et al.2021."Hybrid Organic-Inorganic Materials on Metallic Surfaces: Fabrication and Electrochemical Performance." *MDPI, Metals*, Vol.11,No.7,doi.org/10.3390/met11071043.

- 113- Andrady, Anthony L., and Mike A. Neal. 2009. "Applications and Societal Benefits of Plastics." *Philosophical Transactions of the Royal Society B Biological Science*, Vol. 364, No. 1526, doi:10.1098/rstb.2008.0304.
- 114- Castle, L. 2007. "Chemical Migration into Food: an Overview." *In Chemical Migration and Food Contact Materials*. Edited: Karen A. Barnes, C. Richard Sinclair, and D. H. Watson, Woodhead Publishing Limited, ISBN: 978-1-84569-029-8.
- 115- Cruz, Rui M.S., Bruna P.M. Rico, and Margaride C. Vieira. 2019. "Food Packaging and Migration." *Food Quality and Shelf Life*, pp. 281-301, doi.org/10.1016/B978-0-12-817190-5.00009-4.
- 116- Acevedo-Morantes, María Teresa, María Brieva-Sarmiento, and Alvaro Realpe-Jiménez. 2014. "Effect of The Molding Temperature and Cooling Time on the Residual Stresses of Crystal Polystyrene." *DYNA*, Vol. 81, No. 187, pp. 73-80.
- 117- Kadhim, Raheem G. 2014. "Effect of Nanosilver Particles on the Mechanical Properties of (PVA-PVP) Films." *Advances in Physics Theories and Applications*, Vol. 30.
- 118- Abd-Ali, Karrar Obeid, Abdul-Kareem J. Al-Bermany, and Majeed Ali Habeeb. 2015. "Enhancement of Some Mechanical Properties of Polyethylene Glycol by Adding Carboxymethyl Cellulose as a Blends and Applied in Wood Glue." *World Scientific Research*, Vol. 21, pp. 12-23.
- 119- Judawisastra Hermawan, Claudia, Firmansyah Sasmita, Toni Agung P. 2019. "Elastic Modulus Determination of Thermoplastic Polymers with Pulse-Echo Method Ultrasonic Testing." *IOP Conference Series: Materials Science and Engineering*, Vol. 547.
- 120- Sasmita, Firmansyah, Tania Zefanya S. Tarigan, Hermawan Judawisastra, Toni Agung Priambodo. 2019. "Study of Elastic Modulus Determination of

Polymers with Ultrasonic Method." International Journal on Advanced Science Engineering and Information Technology, Vol.9, No.3.

121- Yang, Shunmin, Mingquan Wang, LU Yang.2019."Investigation of Uncertain Factors on Measuring Residual stress with Critically Refracted Longitudinal Waves." Applied Science, MDPI, Vol.9, No.485.

doi: 10.3390/app9030485

122- Yang, Yang.2020."Development of a Method to measure residual Stresses in cast components with complex Geometry." School of industrial Engineering and Management.

123- Zou, Zhouyiao , Yanpeng Hao, Fangyuan Tian, et al.2020."An Ultrasonic Longitudinal Through-Transmission Method to Measure the Compressive Internal Stress in Epoxy Composite Specimens of Gas-Insulated Metal-Enclosed Switchgear." MDPI energies, Vol.13, No.1248.

124- Najm, Sanaa S.2021."Study of Some Physical Properties for Polyvinyl Alcohol-Polyethylene Glycol Blends." NeuroQuantology , Vol.19, No.1, pp 49-56.

125- In Hwang, Geonwoo Kim, and Young-II Kim, et al. 2021."Experimental Measurement of Residual Stress Distribution in Rail Specimens Using Ultrasonic L_{CR} Waves." Applied Science, MDPI, Vol. 11, No. 9306.

doi: org/10.3390/app11199306

126- Zhu ,Qimeng, Jia Chen, Guoqing Gou¹, et al. "Residual Stress Measurement of A7N01 Aluminum Alloy Welded Joints Using Longitudinal Critically Refracted (LCR) Wave Transmission Method."

127- Zamil, M. F., K.O Chan, M.A Hussain.2019."Algorithm in the Fluidized-Bed Reactor for the Polymerization of Propylene." International Journal of Innovative Technology and Exploring Engineering (IJITEE), Vol.-8, No.4S.

128- Guo, Xiaohui, Xiaojing Yuan, Genliang Hou,etal.2022"Natural Aging Life Prediction of Rubber Products Using Artificial Bee Colony Algorithm to Identify Acceleration Factor." MDPI, Polymers, Vol.14,No.3439.

129- Chepurmenko Anton.2022." Determining the Rheological Parameters of Polymers Using Artificial Neural Networks, MIDP Polymers, Vol. 14, No.3977.

130- Parkinson, R., Richard J. Balling, John D. Hedengren. 2018. *Optimization Methods for Engineering Design Applications and Theory*, Brigham Young University,2nd ed.

131- Sharma, Tushar. 2016. "Bat Algorithm : an Optimization Technique." MSc Diss. in Power Systems, *Thapar University*, Patiala, Electrical & Instrumentation Engineering Department.

132- Habib, Shah.2021." Using New Artificial Bee Colony as Probabilistic Neural Network for Breast Cancer Data Classification." Frontiers in Engineering and Built Environment,Vol.1, No. 2,pp.133-145.

DOI [10.1108/FEBE-03-2021-0015](https://doi.org/10.1108/FEBE-03-2021-0015).

133- Soori, Mohsen, and Mohammed Asmael.2022." A Review of the Recent Development in Machining Parameter Optimization." Jordan Journal of Mechanical and Industrial Engineering,Vol.16,No.2,pp.205-223.

134- Nandy, Sudarshan, Pratim Sarkar, Partha and Das, Achintya.2012." Training a Feed-Forward Neural Network with Artificial Bee Colony Back propagation Method." International Journal of Computer Science & Information Technology (IJCSIT), Vol.4, No.4.

135- Kaya, Ebubekir.2022." A New Neural Network Training Algorithm Based on Artificial Bee Colony Algorithm for Nonlinear System Identification." Mathematics,MDPI,Vol.10,No.3487.

doi.org/10.3390/math10193487

136- Mahmood, S. Mahmood.2016." Hybrid Fuzzy Logic and Artificial Bee Colony Algorithm for Intrusion Detection and Classification." Iraqi Journal of Science, Vol. 57, No.1A, pp: 241-252.

137- Bullinaria, John A., and Khulood AlYahya, Khulood.2015."Artificial Bee Colony Training of Neural Networks: Comparison with Back-Propagation." Mimetic Computing, Vol. 6, No. 3, pp.171-182.

doi: 10.1007/s12293-014-0137-7

138- Ashiqin, Nur Azlin, Siti Hafawati Jamaluddin, Nur Syuhada Muhammat Pazil, etal. 2021"Minimizing Power Loss Using Modified Artificial Bee Colony Algorithm." Journal of Computing Research and Innovation (JCRINN) ,Vol. 6, No. 2 ,pp111-118.

139- Wang, Meng, Chen, Bingrui and Zhao, Hongbo .2022."Data-Driven Rock Strength Parameter Identification Using Artificial Bee Colony Algorithm." Buildings, MDPI,Vol.12,No.725.

doi.org/10.3390/buildings12060725.

140- Cheng, Guo.2015."Investigation of Modified Bee Colony Algorithm with Particle and Chaos Theory." International Journal of Control and Automation. Vol. 8, No. 2 ,pp. 311-322.

141- Sazli, Murath H.2006" A Brief Review of Feed-Forward Neural Networks." Communications Faculty Of Science, University of Ankara, Series A2-A3, V.50,No.1, pp 11-17.

- 142- Noor Aldeen, Mahmood Al Nuaimi, Zakaria and Abdullah, Rosni .2017." Neural Network Training Using Hybrid Particle-Move Artificial Bee Colony Algorithm for Pattern Classification." *Journal of Information and Communication Technology*, Vol. 16, No. 2 , pp: 314–334.
- 143- Reimer, Andreas, and Xichun Luo.2018."Prediction of Residual Stress in Precision Milling of AISI H13 Steel." 4th CIRP Conference of Surface Integrity, *Procedia*,Vol.71,pp.329-334.
- 144- Jin ,Hongping, Yang, Wenyu and Yan, Lin .2012."Determination of Residual Stresses and Material Properties by an Energy-Based Method using Artificial Neural Networks." *Proceedings of the Estonian Academy of Sciences, Materials Science*, Vol. 61, No.4, pp.296–305.
- 145- Raeva, Elista, Vesela Mihova, and Ivaylo Nikolaev.2019."Using SPSS for Solving Engineering Problems." *European Union Conference*.
- 146- Okagbue, Hilary I., Pelumi E. Oguntunde, Emmanuela C.M. Obasi,etal.2021." Trends and Usage Pattern of SPSS and Minitab Software in Scientific Research" *Journal of Physics: Conference Series*,1734.
- 147- Wang, Zheliang.2022."The Toughness and Residual Stresses of Polymers Produced by Melt Extrusion Process." PhD Diss., The Johns Hopkins University.
- 148- Jarzynki, Jacek, Edward Balizer, Jeffry J. Fedderl Y., and Gilbert Lee. 2003."Acoustic Properties." *In Encyclopedia of Polymer Science and Technology*, Edited :Herman F. Mark, John Wiley & Sons, Inc., 3rd Ed., Vol. 5, ISBN:9780471275091.
- 149- Sim, Wei-Ming. 2005."Challenges of Residual Stress and Part Distortion in the Civil Airframe Industry." COMPACT (AST4-CT-516078).

الخلاصة

تنشأ الاجهادات المتبقية نتيجة لعمليات التصنيع المختلفة وتؤثر بشكل كبير على انجاز المواد وتؤدي الى حدوث فشل مفاجئ من دون سابق انذار. لقد اصبح من المهم تطوير طرق دقيقة وموثوقة لقياس الاجهادات المتبقية في المركبات الهندسية. تعتبر البوليمرات مواد ضعيفة تجاه تمدد الشقوق، لذا فان وجود الاجهادات المتبقية يؤثر بشكل حتمي على انجاز المواد البوليميرية. يعتبر تطوير تقنيات القياس اللا تدميرية مهم جدا من وجهة نظر علمية واقتصادية. تطبق تقنية الموجات فوق الصوتية بشكل واسع على تقييم الاجهادات المتبقية في المعادن. في الاطروحة الحالية يتم تطبيق تقنية الموجات فوق الصوتية من نوع (النبضة-الصدى) لأول مرة في قياس الاجهادات المتبقية لمنتجات البولي ستيرين.

تختلف المركبات البوليميرية فيما بينها من ناحية المورفولوجيا، لذا فقد تم حساب الاجهادات المتبقية خلال السمك مرتين في هذه الأطروحة من خلال قياس الاجهادات المتبقية بدلالة الثابت فوق السمعي مرة وبالاعتماد على قيمة للثابت فوق السمعي محسوبة مسبقاً لألواح البولي ستيرين مرة أخرى. لقد تم تقييم الاجهادات المتبقية تبعاً للتبريد من درجتي (١٨٠، ٢٠٠) درجة مئوية بواسطة الهواء والماء تحت تأثير ضغوط مختلفة (٤٥.٧١٤ ، ٧٦.١٩ ، ١٠٦.٦٦٧ ، ١٥٢.٣٨١) ميكا باسكال. تم اعتماد سرعة عينة التخمير القياسية الخالية من الاجهادات (٢٢٦٠) م/ثانية في تقييم الاجهادات المتبقية بالاعتماد على تقنية الموجات فوق الصوتية. فيما يخص الاجهادات المتبقية المحسوبة بدلالة الثابت فوق السمعي فان التبريد بالهواء والماء من درجتي (١٨٠، ٢٠٠) درجة سيليزية يعطي نتائج مطابقة لقاعدة ان الاجهادات الانضغاطية تقابل الزيادة في سرعة الموجات فوق الصوتية بينما اجهادات الشد تقابل نقصانها.

بخصوص البرنامج الاحصائي SPSS تظهر قيمة (p) ان التبريد بالماء والهواء من (١٨٠، ٢٠٠) درجة مئوية ينتج اجهادات شد في عينات البولي ستيرين في حالة الضغط الصفري وهذا يتطابق مع القياسات العملية من خلال تقنية الموجات فوق الصوتية. كانت القيم المثلى للضغوط من خلال البرنامج الهجين من خلايا النحل الاصطناعية مع الخلايا العصبية ذات التغذية الأمامية (HABCFFNN) متمثلة ب (١٠٦.٦٦٧، ٧٦.١٩) ميكا باسكال عند الدرجات الحرارية (١٨٠، ٢٠٠) درجة مئوية، أما القيم المثلى المقابلة للإجهادات المتبقية فقد كانت مساوية الى (٣-٧٠.٠٠٣، ١٠.٥٩٧) ميكا باسكال.

لقد تم استنتاج ان الدرجة الحرارية الافضل لتصنيع عينات البولي ستيرين هي ٢٠٠ درجة مئوية لأنها تؤدي الى توليد اجهادات متبقية مفيدة من نوع الانضغاط والتي تكون نافعة في مقاومة اجهادات الكلال والزحف. لقد تم التوصل الى ان نشوء الاجهادات المتبقية يعود الى (الاجهادات الحرارية حسب نوع التبريد، الاحمال العالية نتيجة الضغوط المسلطة، تقييد الالواح البوليميرية داخل القوالب المعدنية). كانت سرعة الموجات فوق الصوتية بين (٢٠٠٠-٢٥٠٠) م/ثانية نتيجة التبريد بالماء والهواء من الدرجتين (١٨٠، ٢٠٠) درجة مئوية. طبقاً لنتائج SPSS فان قيمة الضغط المؤثرة على الاجهادات المتبقية في حالة التبريد بالماء من درجة ٢٠٠ درجة مئوية هو الضغط (١٥٢.٣٨١) ميكا باسكال.



جمهورية العراق

وزارة التعليم العالي والبحث العلمي

جامعة بابل

كلية هندسة المواد

قسم هندسة البوليمرات و الصناعات

البتروكيمياوية

التحقق من الاجهادات المتبقية في منتج من البولي ستيرين باستخدام تقنية الموجات فوق الصوتية

أطروحة

مقدمة الى قسم البوليمرات و الصناعات البتروكيمياوية في كلية هندسة
المواد / جامعة بابل كجزء من متطلبات نيل درجة الدكتوراه فلسفة في
هندسة المواد / بوليمر

من قبل

لينا فاضل كاظم

بكالوريوس هندسة مواد (٢٠٠١)

ماجستير هندسة مواد (٢٠٠٦)

اشراف

أ. د. هناء جواد كاظم

أ. د. علي عبد الامير الزبيدي

٢٠٢٣ م

١٤٤٥ هـ